# Non-Fermi-liquid behavior in *d*- and *f*-electron metals

G. R. Stewart

*Department of Physics, University of Florida, Gainesville, Florida 32611-8440*

(Published 31 October 2001)

A relatively new class of materials has been found in which the basic assumption of Landau Fermi-liquid theory—that at low energies the electrons in a metal should behave essentially as a collection of weakly interacting particles—is violated. These "non-Fermi-liquid" systems exhibit unusual temperature dependences in their low-temperature properties, including several examples in which the specific heat divided by temperature shows a singular log $T$ temperature dependence over more than two orders of magnitude, from the lowest measured temperatures in the milliKelvin regime to temperatures over 10 K. These anomalous properties, with their often pure power-law or logarithmic temperature dependences over broad temperature ranges and inherent low characteristic energies, have attracted active theoretical interest from the first experimental report in 1991. This article first describes the various theoretical approaches to trying to understand the source of strong temperature- and frequency-dependent electron-electron interactions in non-Fermi-liquid systems. It then discusses the current experimental body of knowledge, including a compilation of data on non-Fermi-liquid behavior in over 50 systems. The disparate data reveal some interesting correlations and trends and serve to point up a number of areas where further theoretical and experimental work is needed.

## CONTENTS



 

## I. INTRODUCTION

At the March 1991 American Physical Society meeting, Seaman, Ghamaty, Lee, Maple, Torikachvili, Kang, Liu, and Allen presented measurements of specific heat, magnetic susceptibility, and electrical resistivity on the $Y_{1-x}U_xPd_3$ system. This generated a great deal of interest, including significant theoretical input at the meeting from D. L. Cox, based on his development (the quadrupolar Kondo model) of the multichannel Kondo model. The measurements of Seaman *et al.* strongly disagreed with the Fermi-liquid model of Landau and launched the intense experimental and theoretical efforts to understand such "non-Fermi-liquid" behavior in bulk *d*- and *f*-electron metals. (Due to length restrictions, the work on marginal Fermi-liquid behavior in high-$T_c$ superconductors, although related, is not discussed herein. For an overview of this work, see the recent proceedings of the 6th International Conference on Materials and Mechanisms of Superconductivity and High $T_c$ Superconductors, Physica C, **341-348**, November, 2000.)

Just as the study of "heavy-fermion" materials after the discovery by Steglich *et al.* (1979) of superconductivity in $CeCu_2Si_2$ had roots in earlier work on, for example, $CeAl_3$ (Andres, Graebner, and Ott, 1975) and $UBe_{13}$ (Bucher *et al.*, 1975), so also was the study of non-Fermi-liquid behavior in bulk *d*- and *f*-electron metals preceded by work that had shown clear violation of Fermi-liquid behavior at low temperatures. [See, for example, Mydosh and Ford (1973), who showed $\rho=\rho_0+AT^{1.5}$ in the spin glass AuFe, and Rivier and Adkins (1975), who offered the theoretical explanation.] In addition, the current theory of non-Fermi-liquid behavior in general has important early predecessors, including, e.g., the work by Hertz (1976) and Nozières and Blandin (1980).

The Fermi-liquid model of Landau predicts certain temperature dependences at sufficiently low temperatures (often $\leqslant 1$ K) for physically observable quantities. For example, the specific heat $C$, divided by temperature $T$, follows $C/T \sim$ const, the magnetic susceptibility $\chi$ also becomes independent of temperature, and the electrical resistivity $\rho$ behaves as $\rho_0+AT^2$. The Fermi-liquid model is the correct description of the low-temperature measurable parameters of a metal provided that the electron interactions as $T \rightarrow 0$ become temperature independent and are short ranged in both space and time. What Seaman *et al.* discovered in $Y_{1-x}U_xPd_3$ was, with the perspective gained from the intervening years of work, a system with electron-electron interactions that are too strong to permit entry into the Fermi-liquid ground state at low temperatures. Possible theoretical explanations for this behavior in $Y_{1-x}U_xPd_3$ that have been put forward include nearness to a magnetic instability in the phase diagram, disorder causing incomplete screening of local moments, or overcompensation of local moments.

The fascination of researchers with this new, non-Fermi-liquid physics is a combination of factors. "Nearness to magnetism" in a phase diagram is not an unusual condition for many *d*- and *f*-electron systems, e.g., high-$T_c$ superconductors and heavy-fermion compounds, and may in fact—provided that the system is "near" enough—be tuned via doping or application of such external parameters as pressure ($P$) or magnetic field ($B$). (Doping, or even imperfect annealing, is of course associated with disorder.) At the point where the magnetism is suppressed to $T=0$, the experimentally measurable parameters—responding to the long-range electron-electron interactions that inhibit Fermi liquid behavior—often have a constant temperature dependence over at least a decade of temperature. Such a situation is a natural invitation to theorists, with the strong advantage that at low temperatures the characteristic energy is manageably small. In fact, theorists have been extremely active in trying to understand non-Fermi-liquid behavior and have often worked in close collaboration with experimentalists to help explain and focus their research. A number of different models have been proposed, all of which have strong predictive capability. The possibility that one or more of the theoretical models could succeed in even partially unifying the many hundreds of widely diverse experiments on the more than 50 known systems still lies in the future. The purpose of this review is to aid in that effort, as well as to organize the rather massive literature on non-Fermi-liquid behavior and highlight perhaps as yet unnoticed correlations therein. This work begins with a discussion of the theory, as is both historically and didactically proper. Then follows a discussion of the experiments organized partly by system (e.g., $Y_{1-x}U_xPd_3$) and partly by tuning parameter (e.g., doping, $P$, or $B$). The external perturbation is usually necessary to achieve non-Fermi-

liquid behavior, but there are a few systems such as $CeNi_2Ge_2$ in which the critical point in the phase diagram occurs in the pure system under normal conditions. In order to correlate as far as possible currently known results, while keeping the review of manageable length, a comprehensive table will be extensively used to organize the data. This review makes liberal use of a scanner and the associated software to replot data to check for possible temperature dependences other than were considered in the original publications. Such scanned results are listed in bold print in the table. The review ends with a summary of insights, conclusions, and suggestions for further work.

## II. THEORY

Current theories to explain non-Fermi-liquid behavior have played an important role in experimental efforts. These theories can be divided into three general categories: multichannel Kondo models, models based on nearness to a magnetic transition that has an ordering temperature near 0 K (the quantum critical point), and models based on a disorder that can, for example, induce a spread of Kondo temperatures, $T_K$, which includes a finite weight in the distribution for $T_K=0$. A general overview of the theories will be presented here. More in-depth discussions are contained in the references.

### A. The single-impurity multichannel Kondo model and non-Fermi liquids

The multichannel Kondo model for a single impurity first developed by Nozières and Blandin (1980) is described by the following Hamiltonian:

$$H_K=\sum_{k,m,\sigma} \varepsilon_k a^t_{km\sigma}a_{km\sigma} + J\sum_{k,k',m,\sigma,\sigma'} \mathbf{S}\cdot a^t_{km\sigma}\sigma_{\sigma\sigma'}a_{k'm\sigma'}, \quad (1)$$

where $\mathbf{S}$ are the spin operators describing the (dilute) magnetic, spin-bearing impurity (e.g., Fe in Cu), $J$ is the antiferromagnetic coupling constant, the $\sigma$ are the Pauli matrices, and $m$ labels the orbital "channels" or degrees of freedom. The spins of the conduction electrons near the impurity (for a review, see Schlottmann and Sacramento, 1993) are bound together to partially or totally compensate the impurity spin. In general, the number $n$ of orbital degrees of freedom, or channels, of the conduction electrons and the impurity spin $S$ fall into three cases.

(1) If $n=2S$, the number of conduction-electron channels (or bands) is just sufficient to compensate the impurity spin into a singlet. This gives rise to normal Fermi-liquid behavior. For $S=\frac{1}{2}$ and $n=1$ (one electron band), this is just the normal Kondo problem (Kondo, 1964), where $C_{\text{impurity}}/T\sim 1/T_K$ and the Kondo temperature $T_K$ is the temperature below which the conduction electrons fully screen the local impurity spin.

(2) If $n<2S$, the impurity spin is not fully compensated, since there are not enough conduction-electron degrees of freedom to yield a singlet ground state.

(3) If $n>2S$, the impurity spin is overcompensated and critical behavior (divergence of the length $\xi$ over which the spins affect the conduction electrons, power-law, or logarithmic behavior in measured quantities like magnetization, resistivity, or specific heat) sets in as the temperature and external field$\rightarrow$0.

The multichannel Kondo model for dilute impurities has been solved exactly (Andrei and Destri, 1984; Tsvelik and Wiegmann, 1984; Affleck and Ludwig, 1991) and generates non-Fermi-liquid behavior for case 3 (the overcompensated $n>2S$ situation), namely, $\chi$ and $C/T$ both vary as $T^{[4/(n+2)]-1}$. For the case of $n=2$, $S=\frac{1}{2}$ the critical power-law behavior (Schlottmann and Sacramento, 1993) near the critical point at $H=T=0$ becomes simply logarithmic and the low-$T$, zero-field magnetic susceptibility $\chi$ and specific heat divided by temperature, $C/T$, are $\sim\log(T/T_K)$. This "two-channel" model further predicts that, as $T\rightarrow 0$ at zero field, the resistivity $\rho-\rho_0\propto A\sqrt{T}$ (Ludwig and Affleck, 1991) and there is a residual ground-state entropy of 0.5 ln2 per impurity that is removed (causes a peak in $C$ plotted vs $T$) by applying a magnetic field. (In fact, for all $n>2S$ a residual entropy is predicted.) These theoretical predictions clearly conflict with simple Fermi-liquid behavior and, although valid only in the dilute limit, should be experimentally verifiable. To date, the experimental examples that exhibit non-Fermi-liquid behavior have been generally more in the concentrated, or "lattice," limit—a more challenging regime for theory.

Cox and co-workers (Cox, 1987; Cox and Zawadowski, 1998 and references therein) have utilized a special case of the two-channel Kondo model, valid in the dilute limit, to address the lattice case, while Jarrell and co-workers (1996, 1997) have extended the two-channel model to the lattice, or concentrated, limit, using the theoretical limit of infinite dimension. Coleman *et al.* (1998) have discussed how the single-channel Kondo lattice model is affected by additional screening degrees of freedom (channels).

The special case of the multichannel Kondo model as first proposed by Cox (1987) was intended to explain the unusually small change (Stewart, Fisk, and Willis, 1983) of the specific heat with applied magnetic field of the highly correlated electron (so-called heavy-fermion) superconductor $UBe_{13}$ in its normal state. Additionally, the magnetic neutron-scattering cross section for $CeCu_2Si_2$ showed a quasielastic peak around 1 meV (Horn *et al.*, 1981), while that for $UBe_{13}$ was thought to occur first at 15 meV (Shapiro *et al.*, 1985). The basic features of Cox's initial model were as follows.

- The U ion in $UBe_{13}$ is tetravalent, leaving a $5f^2$ configuration.

- The crystalline electric field in $UBe_{13}$, which is cubic, splits these outer *f* electrons such that the ground state is the (nonmagnetic) $\Gamma_3$ doublet with the first excited state being the $\Gamma_4$ triplet.
- The nonmagnetic ground state does have an electric crystalline field quadrupolar moment (hence the name "quadrupolar Kondo model") and the magnetic susceptibility comes solely from $\Gamma_3$-$\Gamma_4$ transitions (Van Vleck paramagnetism.) The quasielastic neutron-scattering peak would then be due as well to $\Gamma_3$-$\Gamma_4$ transitions, with a spacing $\Delta$ of ~15 meV, and the field dependence of $C$ would be small "below $(0.2–0.3)\Delta/\mu_B$, which could be of order 30–50 T" (Cox 1987).

The Kondo effect is incorporated into this model (Cox, 1987) by hybridizing the $5f$ electrons with the conduction states and by considering virtual excitations into the $5f^1$ configuration.

This model for tetravalent U impurities in cubic symmetry was later extended to include tetragonal and hexagonal symmetry, as well as trivalent Ce impurities in cubic and hexagonal symmetry (Cox, 1993); see also references in Cox and Zawadowski, 1998. Trivalent Yb impurities were ruled out for two-channel Kondo behavior by Cox (1993). Considering, for comparison to the above discussion, trivalent Ce in cubic symmetry, for certain (not *a priori* unlikely) values of the crystalline electric-field-splitting parameter, in contrast to the U case a magnetic ground-state doublet ($\Gamma_7$) separated by $\Delta$ from a $\Gamma_8$ quartet is predicted. Thus the Ce case corresponds in the work of Cox to a two-channel magnetic Kondo effect, with associated larger magnetic-field effects expected on, for example, the specific heat.

These $n=2$ models, restricted to specific symmetries, building on the exact, Bethe ansatz results for the general multichannel Kondo model (Andrei and Destri, 1984; Tsvelik and Wiegmann, 1984), predict various quantities, including the temperature dependences of the resistivity, for the uranium case the Van Vleck magnetic susceptibility as well as the quadrupolar electric susceptibility ($\chi_Q$), and the specific heat. These predicted quantities (except for $\chi_Q$) perforce agree with the temperature dependences mentioned above for the general multichannel Kondo model. Thus the contribution of this particular version of the more general (dilute impurity) theory launched by Nozières and Blandin is the concerted attempt to relate other specific predictions, based on the proposed multiplet scheme and involving such parameters as $\Delta$ (the multiplet splitting), to known measured quantities including the field behavior of the specific heat. Despite several experimental results in various systems, including nonlinear susceptibility measurements in $UBe_{13}$ (Ramirez *et al.*, 1994), which appear not to follow[1] this quadrupolar Kondo model of the general multichannel model, the impact and utility of these theories must be also measured by their ease of applicability and predictive ability, which has led to invaluable discussion and inspiration for further work, both theoretical and experimental.

For a more thorough discussion of multichannel Kondo models, see the reviews by Schlottmann and Sacramento (1993), Cox and Jarrell (1996), and Cox and Zawadowski (1998).

### B. Quantum critical point theories

Non-Fermi-liquid behavior is often found experimentally near a magnetically ordered phase in the phase diagram, indicating that the non-Fermi-liquid state in those systems may be linked to a magnetic instability that arises at $T=0$. A number of investigators (Continentino, 1993; Millis *et al.*, 1993; Tsvelik *et al.*, 1993; Moriya and Takomoto, 1995; Lonzarich, 1997; Sondhi, 1997; Coleman, 1999) have considered the thermodynamic and transport properties in theoretical models in the special case of a quantum phase transition. [For an overview of quantum phase transitions, see the recent book by Sachdev (1999). For work in this area in the field of high-temperature superconductivity, see, for example, Pines (2000) and the recent proceedings of $M^2S$-HTSC-VI, Houston, Feb. 2000, in *Physica C* **341-348**.] In contrast to a classical phase transition at nonzero temperatures, driven by temperature as a control parameter with thermal fluctuations, a quantum phase transition is driven by a control parameter other than temperature, e.g., external pressure, doping, or magnetic field, at absolute zero, with quantum-mechanical fluctuations. Such a control parameter tunes a system at the zero-temperature boundary from an ordered ground state towards a non-ordered state crossing a quantum critical point. Although this definition of a quantum phase transition is strictly valid only for $T=0$, sufficiently close in temperature to this critical point the system's behavior is still determined by the quantum critical point (Sondhi *et al.*, 1997). The nature of a classical transition at some finite temperature $T_c$ is characterized by a diverging correlation length and correlation time approaching the transition. Such fluctuations of the order parameter are associated with a frequency $\omega^*$ that vanishes at the transition. A quantum system at finite temperatures behaves in a classical way, if the temperature exceeds the fluctuation frequencies.

In the methodology of the path-integral formulation of quantum mechanics, a $d$-dimensional quantum system $(T=0)$ can be viewed as a $(d+z)$-dimensional classical system, where $z$ is the scaling exponent for the dynamics. (Note that, in contrast to the classical problem, for a quantum phase transition the dynamics and thermodynamics are not separable.) This allows the application of general ideas of finite-temperature critical points to quantum critical phenomena. Since in experiment only the behavior for $T\neq 0$ can be studied, the identification of the underlying quantum critical point in the phase diagram relies on the findings of scaling behavior, e.g.,

[1]See Cox and Jarrell (1996) for a review of these conflicting results. A more thorough comparison between theory and experiment will follow the discussion of the experiments below.

for temperature or frequency (see Sondhi *et al.*, 1997 and Sachdev, 1999 for a more thorough discussion). Below, several different models are reviewed, in which the influence of a quantum critical point on finite-temperature properties is considered and therefore predictions accessible to experimental verification arise. Within these models the starting point is rather different, and they can be assigned to two groups as done by Coleman (1999), as shown in Fig. 1. In the first group, the "weak-coupling" approach, the instability is approached from the Fermi-liquid side, and the quantum critical point is treated as a magnetic instability, i.e., a weakly coupled fixed point in a mean-field picture. In the second group, the "strong-coupling" approach, the instability is approached from the magnetic side, where local magnetic moments exist. During the approach to the instability from this side, the magnetic order disappears and an underlying Kondo lattice is revealed.

### 1. Scaling analysis at a quantum critical point

After the discovery of non-Fermi-liquid behavior in $U_{0.2}Y_{0.8}Pd_3$, induced by a critical concentration, Andraka and Tsvelik proposed in 1991 for the first time that a quantum critical point was responsible for the unusual low-temperature behavior. They performed a scaling analysis for the special case of a quantum phase transition. (As mentioned above, this is a method at finite temperatures to investigate a quantum critical point at $T=0$.) A theoretical model, including precise predictions for the magnetic-field-dependent specific heat and the magnetization, was established in 1993 by Tsvelik and Reizer.

In general, this scaling analysis is an extension of the scaling formalism in the Landau model, which describes critical behavior near a (finite-temperature) second-order phase transition at $T_c$. The scaling analysis carried out by Andraka and Tsvelik and theoretically discussed by Tsvelik and Reizer assumed the existence of hyperscaling, which (a) imposes a very strong restriction upon the possible type of theoretical model and (b) holds only below the upper critical dimension. (The upper critical dimension $d_c^+$ is, in most cases, equal to $4-z$, where $z$ is the dynamical exponent $z$, discussed more fully below; see also Table I(a). Above the upper critical dimension, Landau theory is correct and spin fluctuations are weak—the Gaussian regime.)

Hyperscaling (see also Goldenfeld, 1992, p. 207, and Continentino, 1994) suggests that the singular part of the free energy is given as in the Landau model by

$$F=-T^{1+d/z}g\left(\frac{h_i}{t^{\beta_i}}\right), \tag{2}$$

where $g$ is some function of the $h_i$ (the generalized magnetic fields) and the scaling exponents $\beta_i$, but with the reduced temperature $t$ $[=(T-T_c)/T_c]$ replaced by $T$, since the finite-temperature, second-order phase transition in the Landau model is replaced by a quantum phase transition with $T_c=0$ (see, for example, Fisher *et al.*, 1989; Andraka and Tsvelik, 1991; Tsvelik and Reizer, 1993; ). From Eq. (2), with $t\rightarrow T$, one can derive the following expressions for the magnetic-field dependence of the specific heat $C$ and the magnetization $M$:

$$\frac{C(H,T)}{T}-\frac{C(0,T)}{T}=f_1\left(\frac{H}{T^{gb}}\right), \tag{3}$$

$$M=\frac{H}{T^{\eta}}f_2\left(\frac{H}{T^{\beta}}\right), \tag{4}$$

where $f_1$ and $f_2$ are related to $g$.

In order to experimentally investigate such a scaling analysis, which is based on the assumption of hyperscaling and the singular form of the free energy given in Eq. (2), for non-Fermi-liquid systems, measurements at several temperatures and in different magnetic fields of measurable quantities, i.e., specific heat and magnetization, must be available. An analysis of the $C/T$ and $M$ data is used to determine if the predicted [Eqs. (3) and (4)] scaling behavior obtains, including whether the dc magnetic susceptibility at low temperatures has the divergent form $\chi\propto T^{-\eta}$. If this scaling behavior and the divergent behavior of the low-temperature $\chi$ obtain, then the two critical exponents $\beta$ and $\eta$ can be consistently extracted. A minimal requirement of self-consistency (Tsvelik, 2000) for checking whether hyperscaling (the underlying assumption to this whole scaling analysis) is indeed taking place is fulfillment of the Maxwell relations, which require, in systems that obey Eqs. (3) and (4) and have a divergent $\chi$ at low temperatures, that $1+\eta/2=\beta$. The fact that scaling behavior exists in a broad temperature range (e.g., the range in which $C/T$ $\propto -\log T$ is observed) shows that one relevant energy scale, which is not the Fermi energy as in the Fermi-liquid model, dominates the thermodynamic properties. For a Fermi liquid no such scaling behavior should be observable.

Using the resulting exponents, conclusions can be drawn about the nature of the spin fluctuations that underlie the non-Fermi-liquid state. For $\beta>1$ a single-ion effect's being responsible for the non-Fermi-liquid behavior can be ruled out (Andraka and Tsvelik, 1991), whereas for $\beta\leqslant 1$ either single-ion or correlation behavior can be the cause for the fluctuations.

From the experimental view, as will be discussed below in the experimental sections, scaling behavior is observed when the specific heat $C/T$ diverges logarithmically. Thus, for the cases known to date, the above-described scaling (known as hyperscaling, or "non-Gaussian" behavior) is always observed where a $\log T$ divergence is present in the specific heat. The converse question of whether scaling of $C/T$ and $M$ with field [Eqs. (3) and (4)] functions when the data show weak-coupling Gaussian behavior (where $C/T$, as discussed below, equals $\gamma_0-a\sqrt{T}$) is at present at least experimentally varied, since there are conflicting results (see Secs. III.B.3 and III.D.1.a below).

A problem with scaling $M$ in a system that displays non-Fermi-liquid behavior in its specific heat and resistivity appears if the susceptibility at low temperatures does not fit a power law of the expected form $\chi\propto T^{-\eta}$

over some appreciable temperature range to allow the determination of $\eta$, which is needed to perform the scaling [Eq. (4)]. Experimentally $\chi$ is sometimes found to go to a finite value rather than diverging at low temperature. Possible physical reasons for this behavior are discussed by Coleman (1999) and Si *et al.* (1999). A constant limit is found, e.g., in the experimental results below for doped $UPt_3$ and $CeCu_{6-x}(Au,Ag)_x$, whose susceptibilities show a modified Curie-Weiss law: $1/\chi = 1/\chi_0 + aT^\eta$. In these cases, the divergent quantity is $\tilde{\chi} = (1/\chi - 1/\chi_0)^{-1} \propto T^{-\eta}$. Thus the scaling behavior of the magnetization has to be modified (see, for example, Heuser *et al.*, 1998b) in the same way by

$$\left[\frac{H}{M} - \frac{1}{\chi_0}\right]^{-1} = \frac{1}{T^\eta} f\left(\frac{H}{T^\beta}\right). \tag{5}$$

In conclusion, a scaling analysis of measured thermodynamic or dynamic properties at finite temperatures is a method to infer the existence of a quantum critical point at $T=0$. Such a scaling analysis yields in addition, in the case of $\beta>1$, the result that the fluctuations at the quantum critical point, i.e., at $T=0$, are correlated in nature—ruling out single-ion theories.

### 2. Spin-fluctuation theory of non-Fermi-liquid behavior

#### *a. Millis and Hertz*

Quantum critical phenomena have been investigated using renormalization-group theory by a number of authors, including Hertz (1976), Millis (1993), Zülike and Millis (1995), and, in the special case of $CeCu_{6-x}Au_x$, Rosch *et al.* (1997). This treatment assumes that, within the renormalization-group methodology, it is acceptable to integrate out the conduction electrons (see, however, Altshuler, Ioffe, and Millis, 1995) where $d$ is the physical dimension and $z$ is the dynamical critical exponent with $z=2$ for the antiferromagnetic and $z=3$ for the ferromagnetic case (Hertz, 1976; Millis, 1993). Systems are above their upper critical dimension, $d_c^+$ [i.e., hyperscaling does not apply; see Brezin (1982) and Privman and Fisher (1983)], when this effective dimension $d+z>4$. The treatment of Millis assumes that all the systems considered arise from an underlying Fermi-liquid state and, except for the two-dimensional antiferromagnet (i.e., $d=z=2$), are above $d_c^+$. While approaching the quantum critical point the correlation time $\tau$ diverges more rapidly than the correlation length $\xi$, $\tau \propto \xi^z$. The results of the various models depend on the dimension $d$, the critical exponent $z$, the reduced temperature ($t=T/T^*$ with $T^*$ as a characteristic temperature), and a control parameter $\delta$, which is related to a Hamiltonian parameter such as pressure, doping, or magnetic field (Zülicke and Millis, 1995). In the case of a Gaussian fixed point, the interaction scales to a negligibly small value (Millis, 1993). A qualitative phase diagram (Millis, 1993) can be drawn for the different cases; such a diagram for the three-dimensional antiferromagnetic scenario of a quantum critical point is given in Fig. 2. [A similar diagram for the case of heavy-fermion systems above a zero-temperature instability to describe observed universal behavior in the low-temperature renormalized Fermi-liquid state was given by Continentino (1989, 1993). See also later work (Continentino, 1996) in which non-Fermi-liquid behavior is discussed.] The results (for the calculation of the susceptibility, see Ioffe and Millis, 1995) for the other cases can be viewed in Table I(a). Different regions, indicated in Fig. 2 as I–III, appear, where $T_{\rm I}$ and $T_{\rm II}$ mark the crossover temperatures between these regions. In region I, fluctuations on the scale of $\xi$ have energies much greater than $k_B T$ and are therefore of quantum nature and Fermi-liquid behavior appears in the specific heat with $C/T = \gamma + a_1 T^2 \log T + a_2 T^2 + \cdots$. The crossover line to region II, varies as $T_I \propto (\delta - \delta_c)^{z/2}$, which means a linear behavior in the case of the antiferromagnet. Region II is a *quantum-classical crossover* regime, where the energy of the modes becomes less than $k_B T$. For $T_{\rm II} > (\delta - \delta_c)^{z/d+z-2}$, in the classical region III, the correlation length is controlled by $T$ rather than $(\delta - \delta_c)$. From an experimental point of view a distinction between regions II and III is not possible, since the predictions for the specific heat and the resistivity are equal for both. The reason that classical Gaussian behavior is found in such a large range of the phase diagram is that, due to the transformation of the quantum problem into an effective classical problem, interactions are neglected (Millis, 1993; Rosch *et al.*, 1997).

In three dimensions, in the case of antiferromagnetism, $C/T = \gamma_0 - a\sqrt{T}$, $\chi \sim T^{3/2}$, and $\rho = \rho_0 + cT^{3/2}$ and in the case of ferromagnetism $C/T = a \log(T_0/T)$ and $\rho = \rho_0 + cT$ [see Table I(a)]. (For a different treatment with comparable results, see Continentino, 1996.)

#### *b. Self-consistent renormalization model*

A self-consistent renormalization study of the spin fluctuations near magnetic phase transitions, by Moriya and Takimoto (1995) especially to explain the critical behavior in itinerant magnetic systems, gives several theoretical predictions about non-Fermi-liquid behavior. Weakly interacting spin fluctuations above a $T=0$ phase transition are the basis in the theory for this behavior. The self-consistent renormalization model gives a more systematic treatment of mode-mode coupling between spin fluctuations at zero wave vector, $q=0$, and spin fluctuations at the wave vector for antiferromagnetic ordering, $q=Q$, than the theory of Millis and Hertz. Application of this model to systems with local moments, e.g., several of the heavy-fermion systems, leads in only a few cases to a satisfactory description of the low-temperature properties. Mainly itinerant *d*-electron systems are explainable within this model; in addition, some heavy-fermion systems near a quantum critical point, like results for $Ce_{1-x}La_xRu_2Si_2$ by Kambe *et al.* (1996), described in the experimental section, can be well explained. Any kind of microscopic disorder, which exists in at least all doped systems, is not included in this theory and leaves open the question of the interplay of the disorder with the spin fluctuations. The self-

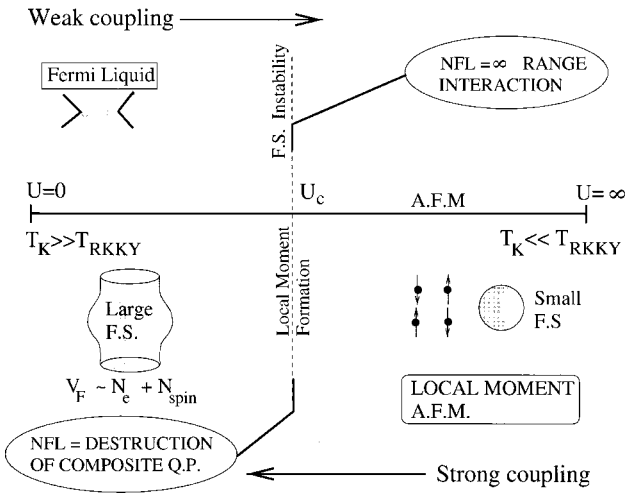


FIG. 1. The two types of models—weak vs strong coupling—for treating the quantum critical point, after Coleman (1999), as discussed in the text: AFM, antiferromagnetism; FS, Fermi surface; NFL, non-Fermi liquid; QP, quasiparticles.

consistent renormalization model is an approximation to the Millis/Hertz model that provides results that may be compared to experiments.

The phenomenological self-consistent renormalization model is based on an assumption for the dynamical susceptibility, taking into account the couplings among different modes of spin fluctuations in a self-consistent fashion. The equation (Moriya and Takimoto, 1995) for the dynamical susceptibility for a three-dimensional antiferromagnetic metal contains two characteristic energy parameters $T_A$ and $T_0$, which are related to the spin-fluctuation energies in $\omega$ and $q$ space. The reduced inverse staggered susceptibility, $1/(2T_A\chi_Q)$, where $Q$ is the antiferromagnetic wave vector, is named $y_0$ for $T \rightarrow 0$. Due to the fact that approaching the quantum critical point by reducing the temperature leads to a divergence of $\chi_Q$, $y_0$ vanishes directly at the quantum critical point, while it stays finite away from the critical point. Thus the determination of $y_0$ gives a prediction for the proximity to the magnetic instability. To calculate the temperature-dependent specific heat and resistivity numerically, one needs the experimental values of the parameters $y_0$, $T_0$, and $y_1$ (the relation between the antiferromagnetic coupling and its dispersion) obtained by fits to the data.

In contrast to the spin-fluctuation model of Millis and Hertz described above, additional coupling between the spin-fluctuation modes is considered within the self-consistent renormalization model. The strength of this mode-mode coupling depends strongly on temperature and vanishes at lowest temperatures. This results in the fact that the predicted non-Fermi-liquid temperature dependences for the specific heat and the resistivity are equal for the low-$T$ limit to those of Millis and a Gaussian fixed point arises at $T=0$. In the specific heat $C/T_{T\rightarrow 0} = \gamma_0 - a\sqrt{T}$, while the resistivity follows $\rho = \rho_0 + cT^{\alpha}$ with $\alpha = \frac{3}{2}$ directly at the antiferromagnetic instability. With increasing temperature the mode-mode coupling increases and $C/T$ follows $-\log T$, while the resistivity obeys the above power law with $\alpha = 1$.

TABLE I. Temperature dependencies from the spin fluctuation theories of non-Fermi-liquid behavior of (a) Millis/Hertz, (b) Moriya *et al.*, and (c) Lonzarich, for the specific heat, susceptibility, and resistivity in the low-temperature limit, plus—in (a)—the dependences of the magnetic ordering temperature ($T_{\text{Néel}}$ or $T_{\text{Curie}}$) and the two crossover lines on the critical parameter $\delta_c$ from the Millis-Hertz theory, as discussed in the text.

(a)

| | AFM, $z=2$ $d=3$ | AFM, $z=2$ $d=2$ | FM, $z=3$ $d=3$ | FM, $z=3$ $d=2$ |
|---|---|---|---|---|
| $C/T$ | $\gamma - a\sqrt{T}$ | $c\log(T_0/T)$ | $c\log(T_0/T)$ | $T^{-1/3}$ |
| $\Delta\chi$ | $T^{3/2}$ | $\chi_0 - dT$ | | |
| $\Delta\rho$ | $T^{3/2}$ | $T$ | $T$ | |
| $T_{N/C}$ | $(\delta_c - \delta)^{2/3}$ | $(\delta_c - \delta)$ | $(\delta_c - \delta)^{3/4}$ | $(\delta_c - \delta)$ |
| $T_{\text{I}}$ | $(\delta - \delta_c)$ | $(\delta - \delta_c)$ | $(\delta - \delta_c)^{3/2}$ | $(\delta - \delta_c)^{3/2}$ |
| $T_{\text{II}}$ | $(\delta - \delta_c)^{2/3}$ | $(\delta - \delta_c)$ | $(\delta - \delta_c)^{3/4}$ | $(\delta - \delta_c)$ |

(b)

| | Ferro, 3-dim | Ferro, 2-dim | AFM, 3-dim | AFM, 2-dim. |
|---|---|---|---|---|
| $C_m/T$ | $-\log T$ | $T^{-1/3}$ | $\gamma_0 - aT^{1/2}$ | $-\log T$ |
| $\chi_Q$ | $T^{-4/3}$ | $-T^{-1}/\log T$ | $T^{-3/2}$ | $-(\log T)/T$ |
| $\Delta\rho$ | $T^{5/3}$ | $T^{4/3}$ | $T^{3/2}$ | $T$ |

(c)

| | Ferro, 3-$d$ ($d=z=3$) | Ferro, 2-$d$ ($d=2;z=3$) | Antiferr, 3-$d$ ($d=3;z=2$) |
|---|---|---|---|
| $C/T$ | $-\log T$ | $T^{-1/3}$ | $\gamma + \sqrt{T}$ |
| $\Delta\chi$ | $T^{-4/3}$ | $T^{-1}$ | $T^{-3/2}$ |
| $\rho$ | $T^{5/3}$ | $T^{4/3}$ | $T^{3/2}$ |

Increasing $y_0$ recovers Fermi-liquid behavior with a constant value of $C/T$ and a $T^2$ behavior of the resistivity at lowest temperatures. The temperature range for the validity of the Fermi-liquid regime scales with the value of $y_0$. For example, the $A$ coefficient in the resistivity, given by $\Delta\rho(T) \propto (\pi/8y_0^{0.5})T^2 \propto AT^2$, varies as $A \propto 1/\sqrt{y_0}$ and diverges upon approaching the magnetic instability.

Taking into account the influence of a uniform magnetic field $H$ (which is necessary for understanding the magnetic-field-induced non-Fermi-liquid behavior in the experimental section) in a phenomenological point of view, Moriya and Takimoto (1998) have stated that the same quantum critical behavior is expected at a field-induced quantum critical point. The effect of $H$ on the antiferromagnetic moment and fluctuations would be mainly to reduce them through the mode-mode coupling between the uniform magnetization induced by $H$ and the $Q+q$ component of the spin density. At the critical field $H_c$ the staggered moment and $1/\chi_Q$ vanish; in overcritical fields Moriya and Takimoto expect a proportionality between $y_0$ and $(H^2 - H_c^2)$.

In the case of a ferromagnetic instability or two-dimensional antiferromagnetic fluctuations, different

predictions are made within the self-consistent renormalization model (Ishigaki and Moriya, 1998) compared to the behavior of three-dimensional antiferromagnetic fluctuations described above. At a ferromagnetic instability, for example, the $q$ dependence of the spin-fluctuation energy differs from the antiferromagnetic case and the dynamical susceptibility has a different form. See also the work of Belitz, Kirkpatrick, and Vojta (1999) for a discussion about critical behavior in weak itinerant ferromagnets, such as MnSi, discussed below in the experimental section.

Table I(b) summarizes the results of the self-consistent renormalization theory for the different cases, where these temperature dependences are to be understood as low-temperature limits. Self-consistent renormalization theory also predicts crossover temperature dependences at higher temperatures (Moriya and Takimoto, 1995) such as $C/T \sim -\log T$ for a three-dimensional antiferromagnetism over about 60% of a decade in temperature above the $\gamma_0 - AT^{1/2}$ behavior shown for low temperatures in Table I(b).

In addition to the theories of Millis/Hertz and Moriya, a comparable theory utilizing spin fluctuations near a ferromagnetic, $T_c = 0$, critical point (with some discussion about the antiferromagnetic case) has been put forward by Lonzarich (1997). As in the other theories, as the magnetic instability is approached, the spontaneous magnetic fluctuations slow down, grow in amplitude and range, become strongly temperature dependent, and give divergent (singular) behavior as $T(T_c) \rightarrow 0$, thus producing non-Fermi-liquid behavior. The temperature dependences derived (again for the $T \rightarrow 0$ limit) via this approach for $C$, $\chi$, and $\rho$ are shown in Table I(c) and are generally in agreement with Millis/Hertz and Moriya.

In all three of these spin-fluctuation theories, the origin of the non-Fermi-liquid behavior lies in the singular dynamical spin susceptibility $\chi(q,\omega,T)$ close to the magnetic ordering vector $Q$: $\chi(q,\omega,T) = 1/[\kappa(T) + a(q-Q)^2 - i\omega]$, where $\kappa(T)$ is a smooth function of temperature.

Hlubina and Rice (1995) have pointed out that in an ordered system the resistivity $\rho$ in a system with antiferromagnetic spin fluctuations—predicted by the above theories of Millis, Hertz, Moriya, and Lonzarich for a three-dimensional system to be $\rho \sim T^{3/2}$—will be "shorted out" below a certain temperature by "cold" portions of the Fermi surface that do not have strong spin fluctuations. Thus, below a certain temperature (predicted by Hlubina and Rice, using reasonable parameters, to be well within the $^4$He temperature range), Hlubina and Rice predict that $\rho \sim T^{3/2}$ will cross over to Fermi-liquid, $\rho \sim T^2$ behavior. They further suggest that, although disorder in a system will reduce this crossover temperature, the crossover temperature is still rather high—contradicting experimental results to be discussed below. Thus the weak-coupling spin-fluctuation theories (see Fig. 1 for a schematic) discussed in this section—which have been invaluable for characterizing non-Fermi-liquid systems and for guiding further experimental efforts—have difficulty describing the observed low-temperature resistivity (see Coleman, 1999 for a discussion).

#### 3. Local deviation from Fermi-liquid behavior

Having discussed spin-fluctuation theory for non-Fermi-liquid behavior (the left side of Fig. 1) in the previous section, we now turn to how local correlations can cause quantum critical behavior (the right side of Fig. 1), as considered by Si *et al.* (1999) and Coleman (1999).

Si *et al.* (1999, 2000) and Smith and Si (2000) have shown that locally critical quantum phase transitions arise in so-called "Kondo lattice" systems, in which each unit cell in the lattice contains a moment-bearing atom, rather than the dilute case originally considered by Kondo. At a locally critical point, vestiges of local moments remain as local critical modes that coexist with long-wavelength critical fluctuations of the order parameter. In contrast to the theories in the previous section, in which the dynamical spin susceptibility $\chi(q,\omega,T)$ is singular only close to a particular ordering wave vector $Q$, the local deviation theory—because the local $\chi(q,\omega,T)$ is also singular—predicts a $\chi(q,\omega,T)$ that has anomalous frequency and temperature dependences everywhere in the Brillouin zone:

$$\chi(q,\omega,T) = 1/[f(q) + A\omega^{\alpha} M(\omega/T)], \tag{6}$$

where $M(\omega/T)$ is a scaling function and $f(q) = I(q) - I(Q)$, where $I(q)$ is the Ruderman-Kittel-Kasuya-Yosida (RKKY) interaction. The exponent $\alpha$ ($\alpha \neq 1$) is nonuniversal. The uniform, $q = 0$, spin susceptibility has a modified Curie-Weiss form, $\chi = 1/(\Theta + BT^{\alpha})$, where $\Theta$ is some constant. (As will be seen in the experimental section below, such a form—expressed as $\chi^{-1} - \chi_0^{-1} \sim T^{\alpha}$—is often seen in non-Fermi-liquid systems.) Si *et al.* (1999, 2000) discuss how the local criticality originates from a dynamical competition between the Kondo and the RKKY interactions. The critical spin fluctuations, via the RKKY interactions, produce a fluctuating magnetic field for each local moment. This fluctuating field impedes the conduction-electron screening of the local moment, rendering the Kondo physics critical. Two-dimensional spin fluctuations are found to favor this new type of quantum critical point.

For a recent review of the theory of quantum phase transitions, with several experimental examples, see Sachdev (1999).

### C. Disorder-induced non-Fermi-liquid behavior theories

As was discussed above for the multichannel Kondo model, the Kondo temperature $T_K$ is the characteristic temperature in the single-channel Kondo problem below which an impurity $S = \frac{1}{2}$ magnetic spin is compensated by the surrounding conduction electrons. This $T_K$ value may be viewed as a crossover temperature below which Fermi-liquid behavior occurs. Thus, if a process takes place in a system that depresses $T_K$ for at least some of the magnetic impurities, this will lead to non-

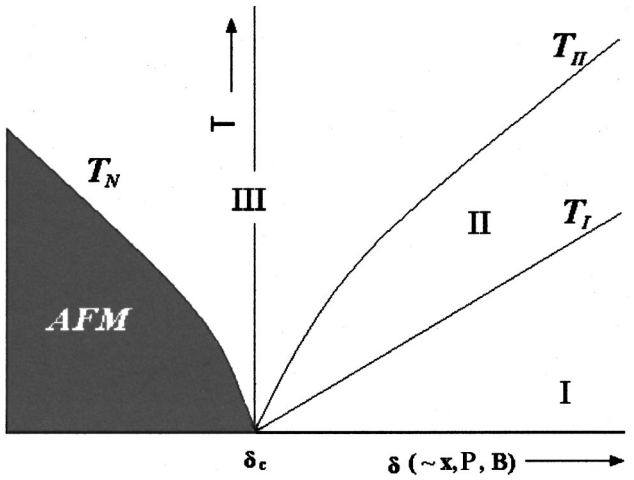


FIG. 2. A qualitative phase diagram for a quantum critical point for the case of three-dimensional antiferromagnetic interactions, after Millis (1993). The various regions, I–III, are discussed in the text, with antiferromagnetism (AFM) and the accompanying $T_N$ suppressed at a critical value of the tuning parameter $\delta_c$. The antiferromagnetism may be suppressed by either doping ($x$), pressure ($P$), or magnetic field ($B$). Note that non-Fermi-liquid behavior occurs in both regions II and III, i.e., for temperatures above the $T_I$ line and $\delta > \delta_c$ and for temperatures above the antiferromagnetism (shaded region) and $\delta < \delta_c$.

Fermi-liquid behavior (⇔ surviving long-range magnetic interactions) down to lower temperatures. One such mechanism that has been proposed and that (see the experimental sections below) appears to hold promise for providing insight into the results for a number of experimental concentrated lattice systems is that of disorder. Since the Kondo temperature may be expressed in terms of the local-moment conduction-electron exchange $J$, bandwidth of the conduction band~Fermi energy $\varepsilon_F$, and density of states at the Fermi energy $N(0)$ as

$$k_B T_K \approx \varepsilon_F \exp[-1/N(0)J], \tag{7}$$

disorder-caused width in the values of either $N(0)$ or $J$ or both would extend non-Fermi-liquid behavior to temperatures below the average $T_K$ ($\equiv T_{Ko}$).

Theoretical works by Dobrosavljevic, Kirkpatrick, and Kotliar (1992) and Bhatt and Fisher (1992) have treated the distribution in $N(0)$ or $J$ cases, respectively. In a phenomenological approach that built on these earlier rigorous theoretical treatments, Bernal *et al.* (1995) fit their strong inhomogeneous NMR line broadening and Knight-shift data on $UCu_{5-x}Pd_x$ using the assumption that disorder was causing a distribution of the values of the product $N(0)J(\equiv\lambda)$. For simplicity, this distribution was assumed to be Gaussian; the data dictated a relatively narrow distribution $P(\lambda)$, with rms width $w$. This distribution is then used to calculate a $P(T_K)$ via $T_K = (\varepsilon_F/k_B)\exp(-1/\lambda)$ and $P(T_K) = |d\lambda/dT_K| P(\lambda)$. This gives

$$P(T_K) = \frac{1}{\sqrt{2\pi}} \frac{1}{w T_K \ln^2(\varepsilon_F/k_B T_K)} \times \exp\left\{ \frac{-\frac{1}{2}}{w^2 \ln^2(\varepsilon_F/k_B T_{Ko})} \left[ \frac{\ln(T_K/T_{Ko})}{\ln(k_B T_K/\varepsilon_F)} \right]^2 \right\}. \tag{8}$$

As will be seen graphically below when the data are discussed, the exponential behavior of $T_K$ with λ broadens $P(T_K)$ and skews it to higher values of $T_K$. An important aspect of this model is that $P(T_K)$ is also finite for $T_K = 0$.

Using this distribution of Kondo temperatures, the average magnetization of a sample at field $H$ and temperature $T$, $\langle M(H,T)\rangle$, can be calculated via the following integral:

$$\langle M(H,T)\rangle = \int_0^\infty M(H,T;T_K) P(T_K) dT_K, \tag{9}$$

where Bernal *et al.* simply use the Brillouin function for the magnetic response of an atom with angular momentum quantum number $J$:

$$M(H,T;T_k) = \frac{2J+1}{2J} \coth\left\{ \left( \frac{2J+1}{2J} \right) \Upsilon(T_K) \right\} - \frac{1}{2J} \coth\left\{ \left( \frac{1}{2J} \right) \Upsilon(T_K) \right\}, \tag{10}$$

where $\Upsilon(T_K) \equiv g\mu_B \mathbf{J} H/[k_B(T + T_K\sqrt{2})]$. Using, then, in their "Kondo disorder" model, the assumptions that (a) the Kondo impurity model provides insight into concentrated systems, and (b) disorder will create a range of Kondo temperatures (⇔ unquenched local spins remain below some average $T_{Ko}$) that may be fit to first order by a relatively narrow Gaussian distribution, Bernal *et al.* vary the four fit parameters involved in Eq. (9) (distribution width $w$, average Kondo temperature $T_{Ko}$, Fermi energy $\varepsilon_F$, and angular momentum **J**) to achieve the best fit to their measured $M$ vs $H$ data at low temperature. They then proceed to use the fitted parameters in this formalism to examine their NMR linewidth and Knight-shift results for $UCu_{5-x}Pd_x$ as discussed below in the experimental section. It is worth noting that the divergence of $P(T_K)$ for low $T_K$ [see Eq. (8)] (below ~2.4 K for $UCu_4Pd$) may be physical or may be subject to a low-energy ("infrared") cutoff when spin-spin RKKY interactions would be included in the theory (Miranda *et al.*, 1996).

Miranda *et al.* (1996, 1997a, 1997b) focused on the Cu NMR study of Bernal *et al.* and used dynamical mean-field theory (neglecting the RKKY interactions) to address how non-Fermi-liquid behavior can arise from the interplay of disorder and strong electron-electron correlations. The core of their theory is based on a relatively small amount of disorder, as suggested by the experimental results of Bernal *et al.*, having a disproportionate influence on low-temperature thermodynamic and transport properties due to strong local correlations between

the unquenched moments and the conduction electrons. Their results agree rather well with the more phenomenolgical work of Bernal *et al.* A major focus of the Miranda *et al.* work is to predict the linear in temperature resistance behavior observed in several non-Fermi-liquid systems. The distribution of $T_K$'s model has an advantage over the normal incalculable concentrated ordered lattice case because, at low temperatures, the unquenched moments from the limited $P(T_K)$ distribution weight remaining are few in number and therefore treatable in the dilute limit.

In a recent work (Rosch, 1999), the interplay of disorder and spin fluctuations near a quantum critical point, where magnetism has just been suppressed to $T \rightarrow 0$ (see below for a discussion), has been found to give $\rho \sim \rho_0 + A T^{\alpha}$, with $1 \leqslant \alpha \leqslant 1.5$ depending on the amount of disorder. Rosch indexed disorder in his theory by the parameter $x$ (a measure of the relative strength of impurity scattering), with $x=0$ being a perfectly ordered sample and $x \geqslant 0.1$ being rather disordered. As shown in Fig. 3, a crossover regime for $\alpha$ is predicted to exist as a function of temperature and disorder, with even very small disorder shifting $\alpha$ from the clean-limit, Fermi-liquid value of 2 to 1.0 at lowest temperatures, followed by a rise at higher temperatures up to almost 2, followed by a monotonic fall at still higher temperatures; i.e., this theory predicts a "bump" in plots of $\alpha$ vs $T$ except in the dirty, $x \geqslant 1$, limit, where $\alpha$ grows monotonically with decreasing temperature to approach 1.5 as $T \rightarrow 0$. [One way to relate $x$ to an experimentally accessible parameter is to simply consider $1/x$ as approximated by the residual resistivity ratio, or $R(300\,\mathrm{K})/R(T \rightarrow 0)$ of the sample; e.g., $x = 10^{-2}$ corresponds roughly to a sample with RRR=100 (Rosch, 2000).]

In the model of Miranda *et al.* (1996), it was pointed out that the thermodynamic behavior at low temperature of a disordered system containing unquenched spins and strong correlations is dominated by the tail of $P(T_K)$ rather than $T_{Ko}$, a situation commonly known as a *Griffiths phase* (Griffiths, 1969). In the work by Castro Neto *et al.* (1998), non-Fermi-liquid behavior in disordered (e.g., alloyed) systems is described as arising from disorder and the competition between the RKKY spin-spin interaction and the Kondo moment-compensation effect leading to Griffiths-phase (rare strongly coupled magnetic clusters) behavior. Due to postulated strong anisotropy, results from Ising-model calculations are deemed as being appropriate to Griffiths phases—averaged over disorder—at very low temperatures, leading Castro Neto *et al.* to predict power-law behavior for a number of measurable quantities (see Table I) in non-Fermi-liquid systems when disorder is present, including $C/T \propto T^{\lambda - 1}$, with $\lambda < 1$. Experimental comparisons to this theory have been made and will be discussed below.

Links between these disorder models and the earlier work that (a) showed $\rho = \rho_0 + A T^{1.5}$ in spin glasses [e.g., the work on AuFe by Mydosh and Ford (1973)], and (b) theoretically explained (Rivier and Adkins, 1975) such behavior based on scattering by diffusive excitations have apparently not been addressed in the literature.

For theoretical work that links disorder and the quantum criticality of a zero-temperature phase transition, see Sachdev and Ye (1992) and Sachdev and Read (1996). The work of Boyanovsky and Cardy (1983) discussed the effect of disorder (quenched time-independent random fields) on the dynamical critical behavior of spin systems. Recent work by Motrunich *et al.* (2000) on the effect of disorder on criticality contains further references on this subject.

## III. EXPERIMENT

One goal of this review is, via organization of the results to date into appropriate sorting categories as well as by summarizing the measured properties (Table II), to reveal correlations and insights previously hidden in the mass of data. One caveat is that the nature of the magnetic order remains either uncertain in some incompletely studied systems [e.g., in the early work (Andraka, 1994b) on $Ce_{1-x}Th_xRhSb$, where broadened antiferromagnetism vs spin glass for $x \geqslant 0.5$ was not differentiated] or rather complex (e.g., antiferromagnetism in $URu_{1.9}Re_{0.1}Si_2$ followed by ferromagnetism in $URu_{1.6}Re_{0.4}Si_2$), so that any sorting scheme will necessarily be inexact. Table II attempts to summarize the disparate results of as many as possible of the non-Fermi-liquid systems known to date: doped, undoped, pressure induced, and field induced. Measured properties, such as far-infrared absorption or Hall effect, that have been measured for only a few systems are discussed for the systems in which the measurements exist but are not tabulated.

Since doping perforce introduces disorder, and since that amount of disorder may—depending on which theoretical model is applicable—play a crucial role in the non-Fermi-liquid behavior, a second caveat is that sample quality may be important for drawing conclusions about intrinsic behavior. (This is also true for undoped systems; see Sec. III.B below.) However, except for a few prototype non-Fermi-liquid systems such as $U_{0.2}Y_{0.8}Pd_3$, $UCu_{5-x}Pd_x$ ($x=1.0$ and 1.5), and $CeNi_2Ge_2$, very few of the non-Fermi-liquid systems listed in Table II have been subjected to intensive study by more than one group. As we shall see, sample quality issues in the prototype systems have been investigated; the results do indeed suggest caution when drawing conclusions from less thoroughly researched sample systems. An early example of the difficulties of characterizing doped systems away from the dilute limit is the study of the onset of ferromagnetism in PdNi at only the 2% doping level, where even the most careful work (Murani, Tari, and Coles, 1974) found it difficult to determine the precise critical concentration (see also the theoretical work on PdNi by Kato and Mathon, 1976). Unless stated otherwise, all samples discussed below are unannealed.

Further, for a given system to be classified as exhibiting Fermi-liquid behavior or not is stringently dependent on measurements of physical properties down to low temperatures. One of the classic examples of en-

hanced Fermi-liquid-behavior in a highly correlated, heavy-fermion system—$CeAl_3$—only shows $C/T \rightarrow$const below 0.3 K (Andres *et al.*, 1975). In addition, to distinguish between competing theoretically predicted temperature dependences, as will be seen particularly herein for the magnetic susceptibility, precise data are needed.

If a system shows characteristic non-Fermi-liquid behavior in the specific heat (e.g., $C/T \sim \log T$ or $T^{\alpha}$, $\alpha \neq 0$) in one or more measured quantities down to 0.3 K over at least a decade of temperature, this may be taken as indicative of non-Fermi-liquid behavior. However, an example ($Ce_7Ni_3$) will be shown in the "pressure-induced" section below in which even a decade of non-Fermi-liquid behavior down to 0.45 K evolved, when further measurements were taken, into Fermi-liquid behavior at lower temperatures, effectively ruling out a quantum critical point at $T=0$ at that point in the phase diagram. That said, systems that display non-Fermi-liquid behavior over a more limited temperature range may provide valuable information (see Fig. 2) that a quantum critical point is nearby in the phase diagram, and they are therefore included here. One example in which early work on a doped system not exactly at a quantum critical point led to researchers' later finding the correct composition is the work on $Ce(Ru_{0.5}Rh_{0.5})_2Si_2$, which led to finding non-Fermi-liquid behavior down to 0.15 K in $Ce(Ru_{0.6}Rh_{0.4})_2Si_2$.

For the nonspecialist reader, the discussion below of more than 50 non-Fermi-liquid systems may be somewhat lengthy. A reading of the introduction to each section, plus the first system in each section, should suffice to allow the reader—with reference to Table II, in which all the data are summarized—to follow the discussion and conclusions at the end and to gain an overview of the current status of the experimental and theoretical study of non-Fermi-liquid behavior.

### A. Doped systems

Although several undoped non-Fermi-liquid systems are now known (see Sec. III.B), it is appropriate to start the discussion of experiment with doped systems. Not only are doped systems more numerous, but historically the experimental investigation of non-Fermi-liquid behavior began with the discovery of Seaman *et al.* (1991) of non-Fermi-liquid behavior in $UPd_3$ doped with 80% Y on the U sites while following up on earlier work of Kang *et al.* (1989) in which photoemission spectroscopy had shown "Fermi-level tuning" of the Fermi energy upon substitution of $Y^{3+}$ for $U^{4+}$. Since that early experimental discovery of non-Fermi-liquid behavior ($\rho=\rho_0+AT^{1.0\pm0.1}$, $\chi=\chi_0-cT^{1/2}$, $C/T\sim-\log T$), quite a large number of non-Fermi-liquid systems have been found—using the early hint that such behavior occurred when a second-order magnetic phase transition was suppressed by doping in $UNi_2Al_3$ (Kim *et al.*, 1993)—by doping either to suppress or to approach magnetic behavior in a phase diagram (see, for example, Fig. 2). As we now understand, strong, long-range electron correlations that remain temperature and frequency dependent as $T\rightarrow0$ (one route to which might be via suppressing a magnetic transition to $T=0$) are necessary to prevent entry into the Fermi-liquid ground state. However, at the start of the experimental search for additional systems besides $U_{0.2}Y_{0.8}Pd_3$, the idea of suppressing an antiferromagnetic $T_N\rightarrow0$ was not so obvious, as the only nearby magnetic behavior in the $Y_{1-x}U_xPd_3$ phase diagram (see Fig. 4) is spin-glass behavior for $0.3\leqslant x\leqslant0.75$. Furthermore, the next non-Fermi-liquid system to be discovered, $UCu_{3.5}Pd_{1.5}$ (Andraka and Stewart, 1993), seemed at the time (later results changed this perception) relatively far away in the $UCu_{5-x}Pd_x$ phase diagram from any magnetic behavior, the nearest being also spin-glass behavior thought to occur only for $x\geqslant2$, with the long-range antiferromagnetism, $T_N=16.5$ K, in $UCu_5$ being suppressed for Pd concentrations above $x=0.5$.

At the time of writing this review, over 30 systems are known in which non-Fermi-liquid behavior is achieved via doping, including systems in which doping (1) induces non-Fermi-liquid behavior relatively far from antiferromagnetism; (2) has just suppressed $T_N\rightarrow0$ or is just about to induce antiferromagnetism; (3) has not yet suppressed antiferromagnetism (i.e., non-Fermi-liquid behavior is observed coexistent with antiferromagnetism); (4) just suppresses a ferromagnetic ordering temperature, $T_c\rightarrow0$, or induces ferromagnetic ordering at a slightly higher doping concentration.

#### 1. Antiferromagnetism "distant" in the phase diagram

A number of systems have been reported in which antiferromagnetism is suppressed with doping and non-Fermi-liquid behavior is found in the phase diagram far from this critical point. Some of the systems in this subclass of doped non-Fermi-liquid materials exhibit spin-glass behavior (designated herein as type **I**), some have been checked for spin-glass behavior and do not exhibit it, at least down to the lowest temperature measured (type **II**), and some (primarily those systems researched for non-Fermi-liquid behavior prior to the Griffiths-phase scenario of Castro Neto *et al.*) were not studied for possible spin-glass behavior (type **III**). These require further work, as they may, due to the rare magnetic clusters, exhibit spin-freezing phenomena if the characteristic temperature for such freezing is high enough. At present, there remain open questions concerning the correct underlying reason(s) for the non-Fermi-liquid behavior in this subclass of doped systems. Thus, rather than the spin-glass behavior's being the cause of the non-Fermi-liquid behavior, spin-glass behavior might be only an effect of the underlying low-temperature electron-interaction-producing mechanism plus the disorder inherent in doped systems, i.e., non-Fermi-liquid systems with spin-glass behavior may not be above a spin-glass transition with $T_{\text{freezing}}=0$. [For a theory on non-Fermi-liquid behavior near a $T=0$ spin-glass transition see Sengupta and Georges, (1995).] There could still be a quantum phase transition at $T=0$, which through disor-

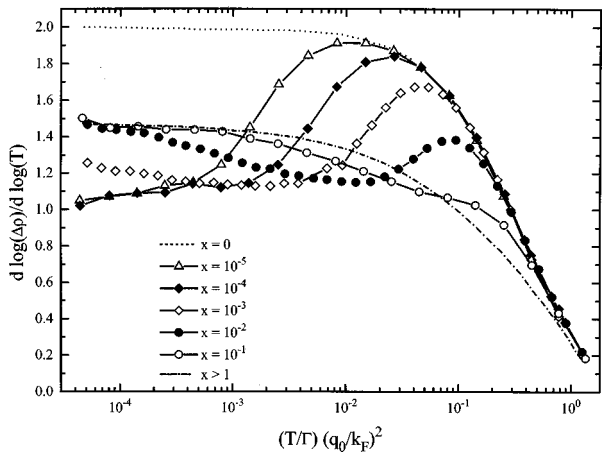


FIG. 3. The exponent $\alpha(=d\log\Delta\rho/d\log T)$ in $\rho=\rho_0+AT^{\alpha}$ for a system with disorder near a quantum critical point, as a function of disorder $(\sim x)$, plotted vs the logarithm of the temperature divided by a characteristic energy scale $\Gamma$, after Rosch (1999), as discussed in the text.

der leaves spin-glass behavior at finite temperatures as evidence for the underlying phase transition.

#### a. $U_xY_{1-x}Pd_3$ (I)

$UPd_3$ occurs in the $DO24$, hexagonal $Ni_3Ti$ structure and is one of only a few known U systems in which neutron scattering shows clearly the crystalline electric-field levels (Shamir *et al.*, 1978). The photoemission work of Kang *et al.* (1989) showed a decrease in the energy separation between the localized $5f$ level and $\varepsilon_F$, the Fermi energy, as U is replaced with Y, which the authors identified as a way to "tune" $\varepsilon_F$ via the change in the conduction-electron density effected by the substitution of $Y^{3+}$ for $U^{4+}$.

In a thermodynamic and transport study of $U_xY_{1-x}Pd_3$ to further investigate the evolution of the localized $5f$ behavior in the U-dilute side of the phase diagram, Seaman *et al.* (1991) discovered the non-Fermi-liquid behavior already mentioned above and listed in Table II. Note that in their study (see Table II), the resistivity followed $\rho\sim\rho_0+aT^{1.1}$ (not $\sqrt{T}$ as predicted by the multichannel Kondo model) down to 0.2 K, $C/T\sim-\log T$ down to only 0.6 K, and $\chi\sim A-BT^{1/2}$ down to only 1.6 K. A later study (Maple *et al.*, 1994), with the assumption of an impurity contribution, also extended the $\chi\sim A-BT^{1/2}$ region down to 0.6 K. A phase diagram of the magnetic behavior as a function of $x$ is shown in Fig. 4.

In the theoretical discussion in their discovery paper, Seaman *et al.* present the quadrupolar Kondo model of Cox as explaining their data, including a purported "missing" entropy of $0.5R\ln 2$/U mole at low temperatures. The electronic entropy $S(T)=\int(C_{\text{measured}}-C_{\text{lattice}})/T\,dT$ as measured (one of many experiments in the study of non-Fermi-liquid behavior that was inspired by theory) by Seaman *et al.* for $U_{0.2}Y_{0.8}Pd_3$ is shown in Fig. 5 and is, compared to the $x\geqslant 0.3$ data, clearly smaller above 10 K. However, such calculated electronic entropies for dilute systems—due to the large lattice background subtraction (in this case their estimate for the lattice contribution to $C$ is $\frac{2}{3}$ of the measured $C$ at 20 K)—normally have large error bars associated with them. In addition, other workers report larger specific heats for $U_{0.2}Y_{0.8}Pd_3$ than those reported by Seaman *et al.*—Ott *et al.* (1993), in agreement with Andraka and Tsvelik (1991), observe $C$ at 1 K to be 50% larger in their low-temperature data for $U_{0.2}Y_{0.8}Pd_3$, while Andraka and Tsvelik, whose data extend to somewhat higher temperature than that of Ott *et al.*, report a 30% larger $C$ at 3.2 K than Seaman *et al.* An electron microprobe study of $U_xY_{1-x}Pd_3$, $0\leqslant x\leqslant 0.2$, by Süllow *et al.* (1994) has revealed at least one possible reason for sample dependence in $C$: local variations on a 10-$\mu$m scale of up to 30% in the uranium concentration $x$ for arc-melted and unannealed (i.e., typical) samples.

In their paper (published simultaneously with Seaman *et al.*), Andraka and Tsvelik (1991), based on further data (including specific heat $C$ and magnetization data as a function of field), argue against the two-channel Kondo model based on (a) their observed decrease in $C$ with $H$ at low temperatures, whereas the missing entropy in the Cox model should lead to an increase in $C$ with $H$, and (b) scaling results for both $C(H)$ and $M(H)$ that give scaling with $H/T^{\beta}$ with $\beta=1.3$, i.e., inconsistent with a single-ion picture as discussed above in the theory section. Later ultrasonic velocity studies, sensitive to quadrupolar moment distortions of the lattice (Amara *et al.*, 1995), also disputed the quadrupolar model as being applicable to $U_xY_{1-x}Pd_3$. Possible explanations for these seeming discrepancies have been put forward by Cox and Zawadowski (1998). Andraka and Tsvelik, based on their scaling results, argue for a second-order phase transition at $T=0$, i.e., a quantum phase transition, without specifying the nature of the proposed transition. Certainly, the phase diagram (Fig. 4) now known argues against any other possibility for a $T=0$ phase transition than a spin glass.

Central to this discussion of a possible spin-glass quantum critical point is the thorough work of Gajewski *et al.* (1996) on the spin-glass behavior in $U_xY_{1-x}Pd_3$, clearing up conflicting reports from muon spin relaxation (Wu *et al.*, 1994) and neutron-diffraction (Dai *et al.*, 1995) measurements, as well as adding points to the phase diagram (see Fig. 4) originally published by Maple *et al.* (1995). In this work, partially inspired by the neutron-diffraction-based report of antiferromagnetism for $x=0.45$, which contradicted the phase diagram of Maple *et al.* (1995), Gajewski *et al.* reported field-cooled vs zero-field-cooled $\chi_{\text{dc}}$ data for 11 samples of $U_xY_{1-x}Pd_3$, $0.25\leqslant x\leqslant 0.55$, showing that the two field history sets of data deviate from one another below a certain $T_{\text{irreversible}}$. However, using careful measurements of the time behavior of the magnetization of samples cooled in zero field below $T_{\text{irr}}$ before application of a field, they were able to show that, at $x=0.4$, the magnetization grows vs time (characteristic of a spin glass, i.e., $T_{\text{irr}}=T_{\text{freezing}}$), while for $x=0.45$, the magnetization remains constant (characteristic of long-range or-

der). As $x \to 0.2$, the question of where $T_f \to 0$ is made uncertain by the fact that the deviation between the field-cooled and the zero-field-cooled curves essentially goes to zero as $x$ decreases below 0.3, making it difficult to verify experimentally whether $T_f$ ever goes to zero. However, the extrapolation of the data of Gajewski *et al.* for $x \geqslant 0.25$ would give $x \approx 0.2$ as the point in the phase diagram where the spin-glass transition is suppressed to $T=0$, approximately consistent with the earlier, less complete data of Maple *et al.* (1995) shown in Fig. 4.

One phenomenological tool available in general for scanning a phase diagram, $T$ vs doping parameter $x$ (or $P$ or $B$: see Fig. 2) in order to check whether a quantum critical point at $T=0$ is the explanation for non-Fermi-liquid behavior in a given system, is to investigate how far down in temperature the power laws in $\rho$ or $\chi$/the $\log T$ in $C/T$ extend. As one can see qualitatively in the phase diagram in Fig. 2, these temperature dependences should disappear as temperature is decreased at finite temperatures below crossover lines (which disorder may smear into regions) except at a single critical concentration, $x_{\rm crit}(P_c, B_c)$. The further a sample is away from $x_{\rm crit}$, the higher the temperature below which deviations from the pure non-Fermi-liquid dependence should first occur. Although a thorough set of data to allow such a phenomenological check for a quantum critical point exists for relatively few non-Fermi-liquid systems, $U_xY_{1-x}Pd_3$ has been rather intensively studied. Resistivity, susceptibility, and specific-heat data are summarized here (see also Table II). [Hall-effect measurements (Sato *et al.*, 1999) on $U_{0.2}Y_{0.8}Pd_3$ indicate that the Hall coefficient $R_H$ behaves as $-\log T$ over the whole temperature range (2–300 K) of measurement, while optical reflectivity measurements find a far-infrared absorption that seems to be characteristic of the several non-Fermi-liquid systems in which such measurements exist (Degiorgi, 1999).]

Resistivity data down to 0.1 K (Maple *et al.*, 1996) for $x=0.2$, 0.15, 0.1 show $\rho \sim \rho_0 + A T^{\alpha}$ with $\alpha = 1.1$, 1.1, and 1.4, respectively, over a broad temperature range, 0.1–40 K. [Resistivity data for $x=0.2$ down to 0.02 K (Ott *et al.*, 1993) show $\rho = \rho_0 - T^1/T_0$ with $\rho_0 = 210.5\,\mu\Omega$ cm and $T_0 = 284$ K, with sufficient scatter in their data below 0.1 K to prevent any statement about small deviations.] Resistivity data between 1.5 and 30 K for $x=0.086$ and 0.049 (Aoki *et al.*, 1995) show Fermi-liquid behavior ($\rho \sim \rho_0 + a T^2$).

Susceptibility data (Maple *et al.*, 1996), corrected for an impurity contribution, for $x=0.1$ and 0.2 are shown in Fig. 6. Whereas $(\chi - \chi_{\rm impurity}) \sim A - B T^{1/2}$ down to 0.6 K for $x=0.2$, $\chi - \chi_{\rm imp}$ for $x=0.1$ shows a tendency to saturate ($\Leftrightarrow$ Fermi-liquid behavior) below 5 K.

Specific heat data (Maple *et al.*, 1996) for $x=0.1$ and 0.2 measured down to ~0.1 K are shown in Fig. 7. There is a positive (i.e., more divergent) deviation to the $C/T \sim -\log T$ behavior proportional to $T^{-2}$ below ~0.25 K in both samples (see also Ott *et al.*, 1993). Thus both the resistivity and the specific heat seem to indicate a region, rather than a point, in the phase diagram, $0.1 \leqslant x \leqslant 0.2$, where non-Fermi-liquid behavior occurs, with Fermi-liquid behavior observed in the resistivity for $x<0.1$, whereas the susceptibility data appear to indicate non-Fermi-liquid behavior only for $x=0.2$.

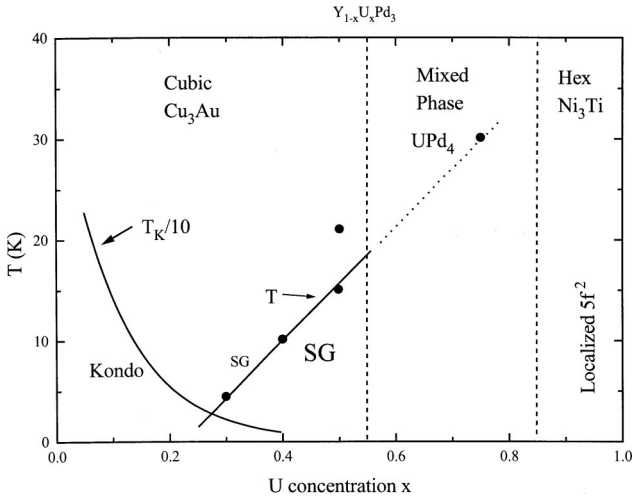


FIG. 4. Structural and magnetic phase diagram for $Y_{1-x}U_xPd_3$, where the Kondo temperature $T_K$ and the temperature below which spin-glass (SG) behavior is observed are plotted vs U concentration, after Maple (1995). The cubic, $Cu_3Au$-type structure is stable only until $x \approx 0.55$.

MacLaughlin *et al.* (1996), based on $^{89}Y$ NMR linewidths, do not believe that the Kondo disorder model can be applied to $U_{0.2}Y_{0.8}Pd_3$.

Left with the situation in $U_xY_{1-x}Pd_3$ that there are experimental indications contradicting both the original theoretical interpretations (quadrupolar Kondo/quantum critical point) and the Kondo disorder model, deAndrade *et al.* (1998) have proposed that the power-law behavior of the Griffiths-phase model of Castro Neto *et al.* (1998) could describe the $C$ and $\chi$ data for, among other systems, $U_{0.2}Y_{0.8}Pd_3$, i.e., that $C/T$ and $\chi \propto T^{-1+\lambda}$; work is in progress to address the resistivity. The values of $\lambda = 0.76$ and 0.70 shown in Table II for $C/T$ and $\chi$, respectively, that deAndrade *et al.* obtain, though not equal as required by the theory, are rather close. For $\chi$ the power law fits the data between 0.6 and 100 K, a larger regime than shown in Fig. 6 for the $1 - \sqrt{T}$ temperature dependence. The power-law functional form fits the $C/T$ data from 3.6 K down to where the upturn (see Fig. 7) starts at 0.25 K, which, although over a decade in temperature, is a significantly smaller region than that over which the $\log T$ shown in Fig. 7 appears to fit the data. deAndrade *et al.* argue that a smaller deviation from the power-law fit in this reduced-temperature regime argues for the Griffiths-phase scenario.

Thus, qualitatively, it is fair to say that the data for the perhaps most often studied non-Fermi-liquid system, $U_xY_{1-x}Pd_3$, are not yet describable in their entirety by any one theory. Certainly none of the theories address the upturns in $C/T$ in $U_{0.1}Y_{0.9}Pd_3$ and $U_{0.2}Y_{0.8}Pd_3$ at the lowest temperatures, leaving this possible interaction-caused effect to future calculations. Considering now in more detail this upturn in $C/T$ below 0.25 K (Fig. 7), this

TABLE II. Compilation of resistivity, susceptibility, and specific heat data for non-Fermi-liquid systems. †=unannealed unless otherwise noted; $A$ is in the appropriate units, i.e., $\mu\Omega$ cm/K$^{\alpha}$. *⇔ not lowest temperature of measurement; results in **bold** print are reanalyzed published data that have been scanned and fit to a different temperature dependence for this review than used in the original publication; values for the residual resisitivity ratio [$\equiv R(300\text{ K})/R(T\rightarrow 0)$], or RRR, are given where known.

| System† | $\rho=\rho_0+AT^{\alpha}$ ($A\equiv\rho_0/T_0^{\alpha}$) | | | | | | $\chi=f(T)$ (e. g. $\chi_0(1-aT^{1/2})$ / $T^{-1+\lambda}$ / -logT) | | |
|---|---|---|---|---|---|---|---|---|---|
| | $\rho_0$ ($\mu\Omega$-cm) | $A$# | $T_0$ (K) | $\alpha$ | T range (K) | | $\chi_0$(memu/molU,Ce) | a($K^{-1/2}$) or $\lambda$ | T range(K) |
| **I. Doped Systems** | | | | | | | | | |
| **1. Antiferromagnetism 'Distant' in the Phase Diagram:** | | | | | | | | | |
| $U_{0.2}Y_{0.8}Pd_3$ | 240 | -0.95 | 250 | 1 | 0.36-20[1] | | $\chi=\chi_0(1-aT^{1/2})$ 5.9 | a=0.06 | 0.6-40[4] |
| | 358 | -1.01 | 180 | 1.13[2] | 0.2-20[2] | | or $\chi\sim T^{-1+\lambda}$ | $\lambda$=0.70 | 0.6-100[5] |
| | 210 | -0.74 | 284 | 1 | 0.02-5[3] | | | | |
| $U_{0.1}Y_{0.9}Pd_3$ | 60 | -0.013 | 142 | 1.4 | 0.2-40[6] | | $\chi=\chi_0(1-aT^{1/2})$ 3.9[7] | a=0.025 | 5(*)-300[6] |
| | | | | | | RRR | | | |
| $UCu_4Pd$ | 375 | -6.3 | 60 | 1 | 0.3-10[8] | 0.5 | $\chi\sim T^{-1+\lambda}$ | $\lambda$=0.7 | 1.8-10[8] |
| | 258 | -4.1 | 63 | 1 | 2-9.3[9] | | $\chi\sim$-logT $\chi$(2K)=18.3 | | 2-10[9] |
| | | | | | | RRR | | | |
| $UCu_4Pd$ (annealed) | 50 | -0.6 | 580 | ~1 | 1(*)-4[10] | 2.5 | $\chi\sim T^{-1+\lambda}$ | $\lambda$=0.8 | 1.8-4 |
| | | | | | | | or $\chi^{-1}-\chi_0^{-1}=aT^{+0.3}$ | | 1.8-10 |
| $UCu_{3.5}Pd_{1.5}$ | 235 | -0.9 | 260 | 1 | 1.3-10[8] | | $\chi\sim T^{-1+\lambda}$ / $\lambda$=0.7 / 1.8-10[8] or $\chi^{-1}-\chi_0^{-1}=aT^{0.63}$/a=5.47/1.8-200 | | |
| | 183 | -0.6 | 286 | 1 | 1-10[9] | | $\chi\sim$-logT | | 2-10[9] |
| $UCu_{4.5}Pt_{0.5}$ | 183 | -0.83 | 221 | 1 | 1.4-20[11] | | still has cusp in $\chi$ at 5 K | | |
| $UCu_{4.25}Pt_{0.75}$ | 266 | -1.27 | 210 | 1 | 1.4-20[11] | | $\chi=\chi_0\log(T_0/T)$ $\chi_0$=7.4 / $T_0$=220K / 2.7-10[11] or $\chi\sim T^{-0.3}$ | | |
| $UCu_4Pt$ | 141 | -0.19 | 742 | 1 | 1.4-10[11] | | $\chi=\chi_0\log(T_0/T)$ $\chi_0$=4.6 / $T_0$=1009K/ 2-10K[11] or $\chi\sim T^{-0.2}$/2-10[11] | | |
| | 114 | -0.21 | 555 | 1 | 1.4-13[9] | | $\chi\sim$-logT | | 1.8-300[9] |
| | Annealed;Unannealed | | | | | | | | |
| $UCu_4Ni$ | 446;467 | -1.22;-1.89 | 370;250[12] | 1 | 0.4-40 | | $\chi=\chi_0(1-aT^{1/2})$ 8.9 | a=0.20 | 0.4-2.5 |
| | | | | | | RRR | | | |
| $UCu_{3.5}Al_{1.5}$ | ?-cracks | +? | 490 | 0.67 | 0.3-10[13] | 0.85 | $\chi=a+bT^{-1/3}$ $\chi_0$=12.3 | | 1.4-17 |
| $Ce_{0.1}La_{0.9}Cu_2Si_2$ | ? | -? | 42 | 1 | 1-5[14] | | $\chi=\chi_0$-alogT $\chi_0$=23.8 | a=10 | 1.8-20 |
| $(U_{0.5}La_{0.5})_2Zn_{17}$[15] | | | | | | | $\chi=\chi_0(1-aT^{1/2})$ 40 | a=0.125 | 1.8-40 |
| $(U_{0.3}La_{0.7})_2Zn_{17}$[15] | | | | | | | $\chi\sim$ -logT $\chi$(1.8 K)=38 | | 1.8-40 |
| $U_2Cu_{12}Al_5$ | 88 | -0.29 | 300 | 1 | 0.3-20[16] | | $\chi\sim T^{-1+\lambda}$ $\chi$(1.8 K)=38 | $\lambda$=0.7 | 1.9-15 |
| | | | | | | RRR | | | |
| $U_{0.1}Y_{0.9}Al_2$ | 95 | -0.39 | 240 | 1 | 0.8-10[17] | 0.91 | $\chi=aT^{-1+\lambda}$ | $\chi$(1.7K)=55 a=80,$\lambda$=0.5 | 3*-400 |
| $U_{0.05}Y_{0.95}Al_2$ | | | | | | | $\chi=aT^{-1+\lambda}$ | $\chi$(1.7K)=24 a=28,$\lambda$=0.7 | 5*-170 |
| $U_{0.125}Y_{0.875}Al_2$ | | | | | | | $\chi=a/T^{0.6}$ | $\chi$(1.7K)=50 a=96,$\lambda$=0.4 | 4*-400 |
| | | | | | | RRR | | | |
| $U_{0.07}Th_{0.93}Ru_2Si_2$ | $\rho=3.5+0.42\log T$ | | | | 1.3-8[18] | 8 | $\chi\sim$ - logT $\chi_0$=77 (B$\|\|$c) | | 0.4-10 |

| $C/T = -R[(0.25/T_0)\ln(T/0.41T_0)]$ | | | $C/T \sim T^{-1+\lambda}$ | | $S_{elec}$(10 K)/mol U/Ce |
|---|---|---|---|---|---|
| $T_0$ (K) | C/T at 1 K/ (mJ/molU/Ce $K^2$) | T range/ scaling β (K) | λ | T range (K) | (fraction of Rln2) ($S_{elec}=S_{measured}-S_{lattice}$) |
| 24 | 280 | 0.3-3.2[1] | 0.76 | 0.2(*)-3.5[5] | 0.29[5] |
| 42 | 200 | 0.8(*)-18[2] | | | |
| 45 | 300 | 0.17(*)-1[3] | | | |
| 224 | 115 | 0.3(*)-10[6] | | | 0.19[6] |
| *$C/T \sim T^{-1+\lambda}$* | *450* | | 0.68 | *1(*)-10[8]* | 0.54[8] |
| | | | 0.71 | 0.2-7[5] | |
| 27 | 375 | 0.07-5[10] / β=1.1[93] | | | 0.50[10] |
| 28 | 400 | 0.3-10[8] | 0.81 | 0.6-7[5] | |
| 323 | 235 | 0.6-2.8 | 0.81 | 0.6-4[11] | 0.32 |
| 53 | 310 | 0.6(*)-6 | | | 0.46 |
| 8.8 | 700 | 1-10 | | | 0.62 |
| 5.6 | 1100 | 0.3(*)-5 | | | 1.1 |
| 3.5 | 1250 | 0.3(*)-3 | | | 1.2 |
| 10 | 600 | 0.45(*)-3.5 | | | 0.72 |
| 13.4 | 550 | 0.3-20 | | | 0.62 |
| 28 | 420 | 0.4-20 | | | 0.58 |
| 14.5 | 530 | 0.35-20 | | | 0.55 |
| 9.7 | 320 | 0.3-1 | **0.33** | **0.35-3 (Fig. 13)** | 0.08 |

TABLE II. (*Continued*).

| System† | $\rho=\rho_0+AT^\alpha$ ($A\equiv\rho_0/T_0^\alpha$) | | | | | $\chi=f(T)$ (e. g. $\chi_0(1-aT^{1/2})$ / $T^{-1+\lambda}$ / -logT) | | |
|---|---|---|---|---|---|---|---|---|
| | $\rho_0$ ($\mu\Omega$-cm) | A# | $T_0$ (K) | $\alpha$ | T range (K) | $\chi_0$(memu/molU,Ce) | a($K^{-1/2}$) or $\lambda$ | T range(K) |
| $U_{0.03}Y_{0.97}Ru_2Si_2$ | 1.6 | + | | 1.27 | 0.1-8[19] | $\chi\sim$ - logT $\chi_0$=52 (B‖c) | | 0.1-8 |
| $U_{0.07}Th_{0.93}Pt_2Si_2$ | 40 (I‖a), 124 (I‖c)[20] RRR=1.3 , 1.3 | | | | | $\chi\sim T^{-1+\lambda}$ $\chi$(1 K)=38,160 | $\lambda$=0.5 | 1.8-10 (B‖a,c) |
| $U_{0.03}Th_{0.97}Pd_2Si_2$ | 29 (I‖a)[21] | - | | | | $\chi\sim$ logT $\chi$(1 K)=250 | | 0.2-6 (B‖c) |
| $U_{0.85}Hf_{0.15}Pt_3$ | | | | | | **$\chi^{-1}-\chi_0^{-1}=aT^{0.82}$ $\chi_0^{-1}$=0.11 U-mol/memu/a=0.0027/1.8-30[22]** | | |
| $U_{0.75}Zr_{0.25}Pt_3$ | | | | | | **$\chi^{-1}-\chi_0^{-1}=aT^{0.87}$ $\chi_0^{-1}$=0.097Umol/memu/a=0.0026/1.8-30[22]** | | |
| $U_{0.7}Zr_{0.3}Pt_3$ | | +? | 20.7 | 1.5 | 0.1-1.5 RRR 1.7[22] | **$\chi^{-1}-\chi_0^{-1}=aT^{0.62}$ $\chi_0^{-1}$=0.075Umol/memu/a=0.0096/1.8-30[22]** | | |
| $Ce_{1-x}Th_xRhSb$ x=0.2-0.4 | | | | | | $\chi$(1.8 K) ~ 13 for x=0.3[23] | | |
| $URu_{2-x}Re_xSi_2$ | | | | 1.6,1.1 x=0.15,0.35 | 1.8-15[24] | $\chi\sim T^{-1+\lambda}$ x=0.2 and 0.35 | $\lambda$=0.9 | 1.8-6 |
| $U_2Pd_{1-x}Si_{3+x}$ | | | | | | $\chi\sim T^{-1+\lambda}$ | $\lambda$=0.61 (x=0.4),0.62 (x=0.5) | 1.8-17[25] |
| $Ce_{0.1}La_{0.9}Pd_2Al_3$ | | -? | 200 | 0.5 | 1.7-9[26] | $\chi\sim$ -logT $\chi$(1.9 K)=95 | | 1.9-7 |
| $U_{0.1}Y_{0.9}In_3$ | | | | | | $\chi\sim$ -log T $\chi$(1.7 K)=49 | | 1.7-7K[27] |
| $U_{0.1}Y_{0.9}In_{2.5}Sn_{0.5}$ | | | | | | $\chi\sim$ -log T $\chi$(1.7 K)=75 | | 1.7-7K[27] |
| $CePt_{0.96}Si_{1.04}$ | | | | | | | | |

**2. $T_N$ just suppressed to 0 or just about to be induced via doping:**

| | | | | | | | | |
|---|---|---|---|---|---|---|---|---|
| $U_{0.9}Th_{0.1}Ni_2Al_3$ | | +? | 46 | 1 | 1.2-20[28] | $\chi=\chi_0(1-aT^{1/2})$ 12.1 | a=0.18 | 1.8-9 |
| $U_{0.9}Pr_{0.1}Ni_2Al_3$ | | +? | 53 | 1.34 | 1.2-10[28] | $\chi=\chi_0(1-aT^{1/2})$ 9.8 | a=0.04 | 1.8-9 |
| $U_{0.6}Th_{0.4}Pd_2Al_3$ | peak in $\rho$ at ~ 7 K[29] | | | | | $\chi\sim T^{-1+\lambda}$ $\chi$(1.8 K) ~ 75 | $\lambda$=0.6 | 0.5-9[5] |
| | | | | | | or **$\chi^{-1}-\chi_0^{-1}=aT^{0.62}$** | | **0.5-50** |
| $U_{0.4}Th_{0.6}Pd_2Al_3$ | | -? | 190 | 1 | 3-30 RRR=0.56 | $\chi=\chi_0(1-aT^{1/2})$ 130 or $\chi\sim T^{-1+\lambda}$ or **$\chi^{-1}-\chi_0^{-1}=aT^{0.66}$** | a=0.25 $\lambda$=0.6[5] | 1.8-4.8[4] ? **1.8-25** |
| $U_{0.2}Y_{0.8}Pd_2Al_3$ | 76.3 | +0.42 | 180 | 1 | 0.1-7/RRR=1.25[30] | $\chi=\chi_0(1-aT^{1/2})$ 57 | a=0.15 | 0.4-7[30] |
| $CeCu_{5.9}Au_{0.1}$ | 39 (I‖b) | +28 | 1.4 | 1 | 0.02-0.5[31] | $\chi=\chi_0(1-aT^{1/2})$ 132 (B‖c) | a=0.26 | 0.08-3[31] |
| | 31 (I‖b) | +23 | 1.3 | 1 | 0.015-0.3[32] | or $\chi^{-1}-\chi_0^{-1}\sim T^{0.8}$ | | 0.08-7[33] |
| | 31.5 (I‖c) | +23 | 1.3 | 1 | 0.015-0.3[32] | | | |
| | 61 (I‖a) | +53 | 1.2 | 1 | 0.015-0.2[32] | | | |
| $CeCu_{5.95}Pd_{0.05}$ | $\rho$ not reported[34] | | | | | $\chi(T\rightarrow 0)_{polyxtal}\sim 53$ | | |
| $CeCu_{5.9}Pt_{0.1}$ | $\rho$ not reported[34] | | | | | $\chi=\chi_0(1-aT^{1/2})$ 75(poly) | a=0.37 | 0.08-0.8 |
| $CeCu_{5.8}Ag_{0.2}$ | | | 0.82 | 1.3 | 0.03-0.3[35] | $\chi^{-1}-\chi_0^{-1}\sim T^{0.8}$ $\chi$(1.8 K)=39 (poly) | | |

| $C/T = -R[(0.25/T_0)\ln(T/0.41T_0)]$ | | | $C/T \sim T^{-1+\lambda}$ | | $S_{elec}$(10 K)/mol U/Ce |
|---|---|---|---|---|---|
| $T_0$ (K) | C/T at 1 K/ (mJ/molU/Ce $K^2$) | T range/ scaling β (K) | λ | T range (K) | (fraction of Rln2) ($S_{elec}=S_{measured}-S_{lattice}$) |
| 160 | 110 | 0.65(*)-7.5 | | | 0.16 |
| ***$C_{elec}/T \sim \gamma_0 - AT^{0.5}$* (1.7(*)-12 K, see Fig. 15)** | | | | | |
| **17.6(from $C/T=\gamma_0-(\gamma_0/T_0^{0.5})T^{0.5}$)** | C/T (1K)=650 | | | | 0.7 |
| 8.8 | 670 | 1.6-10 | | | 0.57 |
| 34 | 410 | 0.1-20 | | | 0.56 |
| 27 | 410 | 0.4-20 | | | 0.57 |
| 25 | 400 | 0.4-20 | | | 0.53 |
| | 275, 425, 625 x=0.2, 0.3, 0.4 | | **0.6,0.5,0.3 x=0.2,0.3,0.4** | **1.4-8,0.6(*)-8,1.2-10 x=0.2, 0.3 , 0.4** | 0.30,0.40,0.53 |
| | | 0.6(*)-2.5 x=0.2 and 0.35 | 0.9 | 0.6(*)-2.5 K | |
| $C/T \sim T^{-1+\lambda}$ | x=0.4,0.5 C/T (2 K)=200,275 | 1.8-7.5 | x=0.4,0.5 0.82,0.85 | | 0.21, 0.15 |
| 8.7 | 720 | 1.5-7 | | | 0.75 |
| 15 | 590 | 0.07-2 | | | 0.74 |
| 11 | 750 | 0.07-3 | | | 0.92 |
| 12 | 650 | 0.07-9 | | | 0.77 |
| 140 | 30 | 0.7*-7.6 | | | 0.02 |
| 160 | 28 | 0.3-5.4 | | | 0.02 |
| 28 | 500 | 0.15*-$10^{29}$ | | 0.6/1.4-$8^{28}$ ; 0.8/0.5*-$10^5$ | 0.71 |
| 23 | 550 | 0.13-$10^{29}$ | 0.8 | $?^5$ | 0.76 |
| 32 | 400 | 0.6-$5^{30}$ | 0.8 | 0.6-$5^{30}$ | 0.56 |
| 3.3 | 1100 | 0.06-2 | | | 0.9 |
| | | | | For pure $CeCu_6$, | 0.8 |
| 3.8 | 1100 | 0.2(*)-2.5 | | | 0.9 |
| 3.5 | 1100 | 0.05-1.8 | | | 0.9 |
| 3.1 | 1250 | 0.06-2.2 | | | 0.9 |

TABLE II. (*Continued*).

| System† | $\rho=\rho_0+AT^\alpha$ ($A\equiv\rho_0/T_0^\alpha$) | | | | | $\chi=f(T)$ (e. g. $\chi_0(1-aT^{1/2})$ / $T^{-1+\lambda}$ / -logT) | | |
|---|---|---|---|---|---|---|---|---|
| | $\rho_0$ ($\mu\Omega$-cm) | A# | $T_0$ (K) | $\alpha$ | T range (K) | $\chi_0$(memu/molU,Ce) | a($K^{-1/2}$) or $\lambda$ | T range(K) |
| $Ce_{0.95}La_{0.05}Ru_2Si_2$ | ? | +0.3 | 12 | 2 | 0.2-1.5 | | | |
| $YbCu_{3.5}Al_{1.5}$ | ? | +? | 11 | 1.3 | 0.03-0.25[36] | $\chi$(1.8 K) ~ 225 memu/Ybmol[37] | | |
| | x=0.35 | | | | | | | |
| $Ce(Ru_{1-x}Rh_x)_2Si_2$ | 15 | 1.1 | 6.6 | 1.4 | 0.3-3[38] | $\chi=\chi_0(1-aT^{1/2})$ 40 | a=0.095 | 1.8-20[38] |
| | | | | | | x=0.4 $\chi^{-1}-\chi_0^{-1}=aT^{1.00}$ | **a=0.72**[39] | **1.8-100** |
| | | | | | | x=0.5 $\chi^{-1}-\chi_0^{-1}=aT^{0.63}$ | **a=0.013**[40] | **1.8-33** |
| $CePtSi_{0.9}Ge_{0.1}$ | | | | | | | | |
| $UCu_{5.6}Al_{6.4}$ | | | | | | | | |
| | x=0.5 | | | | | | | |
| $CePd_{2-x}Ni_xAl_3$ | 39 | 2.2 | 17 | 1 | 0.8-5[42] | $\chi$(1.8 K) = 57 | | |
| $CeCoGe_{1.5}Si_{1.5}$ | 36 | +0.75 | 48 | 1 | 0.03-6[43] | | | |
| $CeCo_{1.2}Cu_{0.8}Ge_2$ | ? | -? | 1160 | **0.6** | **0.5-15**[44] | | | |
| | $x=x_c=0.007$ / x=0.004 | | | | | | | |
| $U(Pt_{1-x}Pd_x)_3$ | ?/3.7 | +?/+2 | ?/1.4 | 1.6/1.77 | ?[45]/0.28-0.85 K(sample superconducts T<0.2K) | | | |

**3. nFl behavior coexistent with long range magnetic order:**

$U(Pt_{0.94}Pd_{0.06})_3$

**4. doping just suppresses or just induces ferromagnetism:**

| | | | | | | | | |
|---|---|---|---|---|---|---|---|---|
| | x=0.1 | | | | | x=0.03,0.07,0.1 | | |
| $U_xTh_{1-x}Cu_2Si_2$ | 230 | +2.16/ | 109 | 1.13[48] | 0.35-3.5 | $\chi\sim T^{-1+\lambda}$ | $\chi$(1.8 K)=7,10,13 $\lambda$=0.55,0.39,0.31 | 1.8-250 |
| $Ni_{0.026}Pd_{0.974}$ | 1.4 | +0.0014 | 63 | 1.671 | 0.05-20[49] | $\chi\sim\chi_0-aT^{3/4}$ | $\chi$(1.8 K)=22 memu/formula unit | 5.5-20 |
| | | | | | | or $\chi^{-1}-\chi_0^{-1}\sim T^{1.8}$ ($T^{1.35}$, $T^{1.06}$ for x=0.024,0.022) | | **1.8–20** |
| $CePd_{0.05}Ni_{0.95}$ | 16 | +0.38 | 30 | 1.1 | 3-30[50] | | | |
| $URh_{1/3}Ni_{2/3}Al$ | ? | ? | 420 | 0.96 | 0.3-7[51] | $\chi_{FC}$(1.7 K) = 12.5 | | |

**II. Undoped Systems:**

| | | | | | | | | | |
|---|---|---|---|---|---|---|---|---|---|
| | | | | | | RRR | | | |
| $U_2Pt_2In$ | 110 | +8.5 | 10 | 1.1 | 0.3-2.6[52](I \|\| a) | 1.9 | $\chi\sim\chi_0-bT^{0.7}$ | $\chi_0$=10.7 (B \|\| a) b=0.24 | 2-10 |
| | 200 | +8.5 | 24? | 0.3 | 0.3-2.3[52](I \|\| c) | 1.05 | | | |
| | 220 | +1.84 | 120 | 1 | 1.5-10[53] | 1.2 (polyxtal) | | | |
| $CeNi_2Ge_2$ | 2.08 | +0.17 | 5.2 | 1.4 | 0.2(*)-2[54] | | | | |
| | 2.7 | +0.21 | 5.5 | 1.5 | 0.02-3[55] (in 1T field) | | | | 5-20[56] |
| | 0.8 | +0.28 | 2.2 | 1.3 | 0.2(*)-2.5[57] | RRR=75 | $\chi\sim T^{-1+\lambda}$ | $\chi$(2 K)=8.3 $\lambda$=0.87 | 1.8-10[57] |
| | 0.43 | +0.27 | 1.4 | 1.40 | 0.02-2[58] (in 0.1 T) | | | | |
| | 0.34 | +0.29 | 1.1 | 1.37 | 0.02-2.5[58] (in 0.1 T) | RRR=200[56] | | | |
| $U_2Co_2Sn$ | 795 | +13 | 10 | 1.76 | 0.3-2[59] | | $\chi\sim$- logT | $\chi$(2K)=15 | 4(*)-40[59] |
| | 59.8 | +3.1 | 8 | 1.40 | 0.3-3[60] | RRR=9.6 | or $\chi\sim T^{-1+\lambda}$ | $\lambda$=0.83 | 1.8–5 |

| $C/T = -R[(0.25/T_0)\ln(T/0.41T_0)]$ | | | $C/T \sim T^{-1+\lambda}$ | | $S_{elec}$(10 K)/mol U/Ce |
|---|---|---|---|---|---|
| $T_0$ (K) | C/T at 1 K/ (mJ/molU/Ce $K^2$) | T range/ scaling β (K) | λ | T range (K) | (fraction of Rln2) ($S_{elec}=S_{measured}-S_{lattice}$) |
| ? | 580 | | | | 0.73 |
| 2.7 | 850 | 0.2-1.2[36] / β=1.5 ; $C/T=\gamma_0-a\sqrt{T}$ 0.1-0.3 K, $y_0$=0.05 | | | 0.8 |
| x=0.4 | | | | | |
| 12.4 | 630 | 0.15-10[39] | | | 0.72 |
| 5.3 | 1000 | 0.8-5[41] | | | 0.9 |
| 18 | 500 | 0.4-4[41] | | | 0.55 |
| x=0.4 | | | | | |
| 13.5 | 570 | 1.5-6 | | | 0.64 |
| 39 | 190 | 0.3-2 | | | 0.22 |
| 12 | 450 | 0.35-7[44] | | | 0.48 |
| 16 | 620 (ΔC/T=190) | 0.3-4.3[46-47] | using ΔC/T in the inset, Fig. 23 ⇒ | | S ~0.1 |
| x=0.03,0.07,0.10 | | | | | |
| 5,5.5,3.5 | 2000,1700,1000 | 1-10,0.35-3.5,0.35-7.5 / β=1.6 | | | 0.76 |
| 37 | 615 (per mole Ni) | 0.4(*)-10 | | | 0.95 |
| 48 | 210 | 0.9-4 | | | 0.27 |
| 200 | 230 | 0.5-5 | 0.94 | 0.5-5 | 0.42 |
| 23 | 415 | 0.1-5 / β=0.5 | | | 0.18 |
| 39 | 320[55] | 1-3 ($C/T=\gamma-A\sqrt{T}$, 0.4-1 K) | | | |
| 38 | 330[57] | 0.4-10 / β=1.05±0.05 | | | 0.45 |
| 39 | 320[58] | 0.4-5 | | | |
| $C_{electronic}/T=\gamma_0-AT^{0.5}$ | | (0.3-10 K)/β=1.6/$T_0$=16 K (from $C/T=\gamma_0-(\gamma_0/T_0^{0.5})T^{0.5}$)/C/T (1K)=145 | | | 0.17 |

TABLE II. (*Continued*).

| System† | $\rho=\rho_0+AT^\alpha$ ($A\equiv\rho_0/T_0^\alpha$) | | | | | $\chi=f(T)$ (e. g. $\chi_0(1-aT^{1/2})$ / $T^{-1+\lambda}$ / -logT) | | |
|---|---|---|---|---|---|---|---|---|
| | $\rho_0$ ($\mu\Omega$-cm) | A# | $T_0$ (K) | $\alpha$ | T range (K) | $\chi_0$(memu/molU,Ce) | a($K^{-1/2}$) or $\lambda$ | T range(K) |
| $YbRh_2Si_2$ | 2.4 | +1.8 | 1.3 | 1 | 0.02-10/35[61] | $\chi_{ac}$ ~ -logT $\chi$(2 K)=140 | | 0.09-0.6 |
| $Yb_2Ni_2Al$ | 120 | | | | RRR ~1.3[62] | | | |
| $CeRu_4Sb_{12}$ | 19.2 | +.25 | 15 | 1.6 | 0.1-5 RRR 5[63] | | | |
| $CeCu_2Si_2$ (S-type, 2 T) | 36 | +14.9 | 1.8 | 1.5 | 0.02-1.7[55-56] | | | |
| $UBe_{13}$ | 26 | + 69 | 0.5 | 1.5 | 0.4-1[56] | | | |
| $CeIrIn_5$ | ~0.2 | +1 | 6 | 1.3 | 0.06-5[64] RRR 50 | B in basal plane $\chi^{-1}-\chi_0^{-1}=aT^{0.84}$, $\chi_0^{-1}$=0.11 molCe/memu, a=0.0041 | | 1.8-300[92] |
| | | | | | | B⊥basal plane: $\chi^{-1}-\chi_0^{-1}=aT^{0.33}$, $\chi_0^{-1}$=0.03 molCe/memu, a=0.019 | | 1.8-15[92] |
| $CeCoIn_5$ | | | ~1 | | 2.3-20[65] | B in bas. plane: $\chi^{-1}-\chi_0^{-1}=aT^{0.10}$, $\chi_0^{-1}$=-0.11 molCe/memu, a=0.21 | | 1.8-20[92] |
| | | | | | | B⊥basal plane: $\chi=aT^{-0.4}$ | | 1.8-15[92] |
| $CeRhIn_5$ (21 kbar) I ∥ c, I ∥ a | | | ~1 | | 2.3-6[66] | | | |
| UCoAl | 7.9,22 | +0.08,0.43 | 15.6,10.6 | 1.67 | 1.8-17,1.8-12[67-68] | | | |
| $CaRuO_3$ | ~80 | +? | ? | 1.5 | 1.8-10[69] RRR 6 | | | |
| $U_3Ni_3Sn_4$ | | | | | | $\chi=\chi_0-bT^{-0.3}$ 6.7, b=1 | | 1.8-10[70] |

**III. Pressure Induced nFl Behavior**

**Superconductivity induced by pressure:**

| | | | | | | | | |
|---|---|---|---|---|---|---|---|---|
| $CePd_2Si_2$ | | | | | | | | |
| at $P_c$=28 kbar: | 4 | +0.93 | 3.4 | 1.2 | 0.43(=$T_c$)-40 K[71] | ($H_{c2}'$= -5 T/K) | | |
| at 27 kbar: | 22,33 | ? | ? | 1.5 | 0.03-1[72] | (no $T_c$) | | |
| at 39 kbar($P_c$=34 kbar) | 2.8 | ? | ? | 1.2 | 0.52 (=$T_c$)-35 K[73] | ($H_{c2}'$= - 10 T/K) | | |
| "A-type" $CeCu_2Si_2$ 6.7 kbar, 2 T | | | | | | | | |
| $CeCu_2Ge_2$ at 101 kbar ($P_c$=75 kbar) | ~1.4 | +6 | 0.2 | 1 | 0.7(~$T_c$) - 4 | ($H_{c2}'$= - 11 T/K)[74] | | |
| $CeIn_3$ at 29 kbar ($P_c$=26 kbar) | ~0.6 | ~+0.25 | 1.7 | 1.6-0.8 | 3-25[75] | | | |
| $UGe_2$ | 0.2 (2.4 at 13.5 kbar) | ? | ? | <2 | ? | ($H_{c2}'$ "anomalously large"[76], $H_{c2}$(T=0)>3 T at 12 kbar) | | |

**Non-superconducting systems under pressure:**

| | | | | | | |
|---|---|---|---|---|---|---|
| $CeRu_2Ge_2$ at $P_c$=84 kbar | | | | | | |
| 2.5(0.3 at P=0) | ~0.1 | ~7 | 1.58 | 0.03-1.5[77] | RRR | |
| at P=91.5 kbar: **2.2** | **+0.23** | **6** | **1.26** | **0.03-11** | **116**[78] | |
| $CeCu_{5.8}Au_{0.2}$ at $P_c$=4.1 kbar | | | | | | |
| $CeCu_{5.7}Au_{0.3}$ at $P_c$=8.2 kbar | | | | | | |

| $C/T = -R[(0.25/T_0)\ln(T/0.41T_0)]$ | | | $C/T \sim T^{-1+\lambda}$ | | $S_{elec}$(10 K)/mol U/Ce |
|---|---|---|---|---|---|
| $T_0$ (K) | C/T at 1 K/ (mJ/molU/Ce $K^2$) | T range/ scaling β (K) | λ | T range (K) | (fraction of Rln2) ($S_{elec}=S_{measured}-S_{lattice}$) |
| 12 | 530[61] | 0.35(*)-10 / 1.05±0.05 | | | 0.45 |
| 13 | 600 | 0.5-4 | | | 0.56 |
| 24 | 180 | 0.25-0.7 | | | 0.14 |
| *$C/T = \gamma_0 - A\sqrt{T}$, $\gamma_0$=1120 , A=420 mJ/mole$K^{2.5}$* | | *0.7-3* | | | 0.6 |
| 8 | 750 (12 T) | 0.2(*)-3 | | | 0.68 |
| *$C/T = \gamma_0 - A\sqrt{T}$, $\gamma_0$=780, A=170 mJ/mole$K^{2.5}$* | | *0.3 – 6 for B⊥basal plane*[92] | | | |
| 11 | 500 | 0.3 – 8 for B in both field directions[92] | | | |
| ? | 110 | | 0.5 | 0.4-2 K[70] | |
| 10 | 600[55] | 1.2-5 | | | 0.6 |
| | *$C/T = \gamma_0 - A\sqrt{T}$ between 0.4-1.2 K, $\gamma_0$=990 , A=380 mJ/mole$K^{2.5}$* | | | | |
| 3.5 | 1100[79] | 0.07-3 | | | 0.9 |
| 3.1 | 1000[80] | 0.1-2 | | | 0.9 |

TABLE II. (*Continued*).

| System† | $\rho=\rho_0+AT^\alpha$ ($A\equiv\rho_0/T_0^\alpha$) | | | | | $\chi=f(T)$ (e. g. $\chi_0(1-aT^{1/2})$ / $T^{-1+\lambda}$ / -logT) | | |
|---|---|---|---|---|---|---|---|---|
| | $\rho_0$ ($\mu\Omega$-cm) | $A^\#$ | $T_0$ (K) | $\alpha$ | T range (K) | $\chi_0$(memu/molU,Ce) | a($K^{-1/2}$) or $\lambda$ | T range(K) |
| $Ce_7Ni_3$ | | | | | | at 4.7 kbar ($\chi_{ac}$ arb. units) $\chi_{ac}=\chi_0(1-aT^{1/2})$ | | 0.3-5[81] |
| | | | | | | (B \| a) at 3.9 kbar, $\chi\sim T^{-1+\lambda}$ $\chi$(0.5 K)=30[82] | $\lambda$=0.8 | |
| | | | | | | **(B \| c) at 3.9 kbar, $\chi^{-1}-\chi_0^{-1}\sim T^{1.0}$** $\chi$(0.5 K)=500[82] | | **0.5-4** |
| MnSi | at $P_c$=15 kbar | | | | | RRR | | |
| | ~0.3 | ~0.18 | 1.4 | 1.6 | 0.02-10[83] | ~1000[84] | $\chi_{ac}\sim$ const. | |
| $ZrZn_2$ | at $P_c$=7.5 kbar | | | | | | | |
| | 2 | ~0.009 | 25 | 1.67(lower below 10 K) | | 1-20[85] | | |
| $CeNiGa_2$ | at $P_c$=4 kbar | | | | | | | |
| | 5 | 3.7 | 1.2 | 1.5 | 0.3-1.9[86] | | - | |
| **IV. Field Induced nFl Behavior:** | | | | | | | | |
| $CeCu_{5.2}Ag_{0.8}$ | at $B_c$=2.3 T, B \| c | | | | | | | |
| | 82.3 | +37 | 1.8 | 1.4 | 0.03-0.17[87] | $\chi^{-1}-\chi_0^{-1}=aT$ | $\chi$(1.8 K)=100, a=1.44[35] | 1.8-40 |
| $CeCu_{5.7}Ag_{0.3}$ | at $B_c$=0.7 T, B \| c | | | | | | | |
| | 56.3 | +59 | 1.0 | 1.5 | 0.03-0.16[35] | $\chi^{-1}-\chi_0^{-1}=aT$ | $\chi$(1.8 K)=93, a=1.44[35] | 1.8-30 |
| $YbCu_{3.4}Al_{1.6}$ | at $B_c$=2.0 T (polyxtal) | | | | | | | |
| | | | | 1.5 | 0.03-0.32 | | | |
| $YbCu_{3.3}Al_{1.7}$ | at $B_c$=2.5 T (polyxtal) | | | | | | | |
| | | +0.30 | | 1.5 | 0.03-0.32 | $\chi=\chi_0(1-aT^{1/2})$ 285 | a=69[37] | 1.8-6 |
| $CeCu_{5.8}Au_{0.2}$ | 86.5 | +6.8 | 5.4 | 1.5 | 0.015-0.2[95] | (at $B_c$=0.4 T \| c) | | |
| $CeRu_2Si_2$ at $B_{metamag}$=8 T | | | | | | | | |
| | | | | | | RRR | | |
| $UPt_3$ | 7.7(22 T) | | | 1.2(22T) | 0.5-3 | 100[91] | at $B_{metamag}$=20.5 T: $\chi=\chi_0$-aT 12, a=0.13 | 0.5-20 |
| $Sr_3Ru_2O_7$ | 2-4 | | | ~1($B_{meta}$=5.5T) | | ≥2.5 K[94] | | |

**References for Table 2** (Note: If a reference is cited for one property for a given system, e. g. for $\rho$, and no reference is cited for the other properties listed, this reference also applies to the other data.)


1. Andraka and Tsvelik (1991).
2. Seaman, et al. (1991).
3. Ott, et al. (1993).
4. Maple, et al. (1994).
5. deAndrade, et al. (1998).
6. Maple, et al. (1996).
7. Gajewski, et al. (1996).
8. Andraka and Stewart (1993).
9. Chau and Maple (1996).
10. Weber, et al. (2001).
11. Chau, et al. to be published.
12. Lopez de la Torre, et al. (1998).
13. Nakotte, et al. (1996).
14. Andraka (1994a).
15. von Blanckenhagen, et al. (2001).
16. Pietri, et al. (1997).
17. Mayr, et al. (1997); Mayr (1997).
18. Amitsuka, et al. (1994).
19. Amitsuka, et al. (2000).
20. Amitsuka, et al. (1995a).
21. Amitsuka, et al. (1995b).
22. Trinkl, et al. (1996); Trinkl (1996).
23. Andraka (1994b).
24. Bauer, et al. to be published.
25. Homma, et al. (2000).
26. Nishigori, et al. (1999).
27. Hirsch, et al. to be published.
28. Kim, et al. (1993).
29. Maple, et al. (1995).
30. Freeman, et al. (1998).
31. von Löhneysen, et al. (1994).
32. Neubert, et al. (1997).
33. Schroeder, et al. (1998).
34. Sieck, et al. (1996).
35. Heuser (1999).
36. Seuring, et al. (2001).
37. Seuring to be published.
38. Nakano, et al. (2000).
39. Taniguchi, et al. (1998).
40. Graf, et al. (1997).
41. Steglich, et al. (1994).
42. Galatanu, et al. (2000).
43. Eom, et al. (2000).
44. Maeda, et al. (1999).
45. Graf, et al. (2000).
46. Stewart, et al. (1986).
47. Kim, et al. (1992).
48. Lenkewitz, et al. (1997).
49. Nicklas, et al. (1999).
50. Kappler, et al. (1997).
51. Prokes, et al. (2000).
52. Estrela, et al. (1998).
53. Strydom and du Plessis (1996).
54. Julian, et al. (1996).

| $C/T = -R[(0.25/T_0)\ln(T/0.41T_0)]$ | | | $C/T \sim T^{-1+\lambda}$ | | $S_{elec}$(10 K)/mol U/Ce |
|---|---|---|---|---|---|
| $T_0$ (K) | C/T at 1 K/ (mJ/molU/Ce $K^2$) | T range/ scaling β (K) | λ | T range (K) | (fraction of Rln2) ($S_{elec}=S_{measured}-S_{lattice}$) |
| 7.9 | 750[81] | 0.45-5 (3.7 kbar) | | | 0.6 |
| | *C/T ~ const. for P≥$P_c$ for T<0.5 K*[82] | | | | |
| 1.9 | 1450[88] | 0.2-1.2 | | | 0.9 |
| and *C/T=$\gamma_0$-$aT^{0.5}$ 0.07-0.20 K, $y_0$=0.02/scaling β=1.6* | | | | | |
| 2.2 | 1250[35] | 0.13-1.3 | | | |
| and *C/T=$\gamma_0$-$atT^{0.5}$ 0.07-0.13 K, $y_0$=0.015, scaling β=0.9* | | | | | |
| 3 | 1250 | 0.3-3[89] / 1.5 | | | |
| 3.5 | 1250 | 0.3-5[36] / 1.5 | | | 0.8 |
| *at B=0.5 T, C/T=$\gamma_0 - aT^{0.5}$, 0.05-0.36 K, $y_0$=0.01* | | | | | |
| *C/T ~ $\gamma_0$ - bT, $\gamma_0$=563 mJ/mol-$K^2$ 0.06-1.8*[90] | | | | | 0.57 |
| 14 | 560 | 0.5-10[91] | | | 0.68 |
| 51 | 150 (/molRu at 1.7 K) | 1.7-15[94] | | | 0.17 |


55. Steglich, et al. (1996).
56. Steglich, et al. (1997).
57. Koerner, et al. (2000).
58. Gegenwart, et al. (1999).
59. Kim, et al. (2000a).
60. Kim, Alwood, Stewart to be pub.
61. Trovarelli, et al. (2000a).
62. Geibel, et al. (1996).
63. Takeda and Ishikawa (1999).
64. Petrovic, Movshovich, et al. (2001).
65. Petrovic, Pagliuso, et al. (2001).
66. Hegger, et al. (2000).
67. Havela, et al. (2000a).
68. Havela, et al. (2000b).
69. Klein, et al. (1999).
70. Shlyk, et al. (1999).
71. Grosche, et al. (1996).
72. Link, et al. (1996).
73. Raymond and Jaccard (2000).
74. Jaccard, et al. (1992).
75. Walker, et al. (1997).
76. Saxena, et al. (2000).
77. Wilhelm and Jaccard (1999).
78. Wilhelm and Jaccard (1998).
79. Sieck, et al. (1997).
80. Bogenberger and von Löhneysen (1995).
81. Umeo, et al. (1996b).
82. Umeo, et al. (1999).
83. Julian, et al. (1998).
84. Pfleiderer, et al. (1994).
85. Grosche, et al. (1995).
86. Hauser, et al. (1998).
87. Scheidt, et al. (1999).
88. Heuser, et al. (1998b).
89. Bauer, et al. (2000).
90. Heuser, et al. (2000).
91. Kim, et al. (2000b).
92. Kim, et al. (2001).
93. Weber, et al. (2001).
94. Perry, et al. (2001).
95. von Löhneysen, et al. (2001).

has been further investigated for $x=0.2$ down to 0.05 K (Ott *et al.*, 1993), and is much too large to be explained by any stray internal magnetic fields from the moments involved in the weak spin-glass behavior or by disorder-producing electric-field gradients that might split the nuclear quadrupole moments of the $^{105}$Pd nuclei. Although Maple *et al.* (1996) have taken this upturn in $C/T$ at low temperatures in $U_xY_{1-x}Pd_3$ as consistent with removal of the residual $0.5R\ln 2$ entropy of the quadrupolar Kondo model, the observed $T^{-2}$ divergence would have to continue unchanged down to a factor of 2500 lower temperature than the current lowest-measured temperature of 0.05 K in order to produce the "missing" (modulo error bar and sample dependence) $0.5R\ln 2$ of entropy. At present, the cause of this upturn, which shows sample dependence in both its starting temperature (~0.17 K in the data of Ott *et al.*, 1993) and magnitude, remains open but, as will be seen in the discussion of other systems below, is not unique and may be indicative of some common, as yet not understood, underlying physics.

### b. $UCu_{5-x}Pd_x$ (I)

In the first non-Fermi-liquid system discovered (Andraka and Stewart, 1993) with no dilution of the active *f*-atom site, non-Fermi-liquid behavior was reported for doping Pd on the Cu sites in $UCu_5$, which has a Néel temperature of 16.5 K. [Doping of Au(Ag) for Cu increases $T_N$ up to $x=2$ (does not suppress $T_N$) and thus does not lead to non-Fermi-liquid properties (Chau *et al.*, 2001). Doping with Pt is discussed below.] The results for $UCu_{3.5}Pd_{1.5}$ and $UCu_4Pd$, which both occur in the cubic, $cF24$ $AuBe_5$ structure, are $\rho=\rho_0-AT$ between 0.3 and 10 K (with, however, a much steeper slope for $UCu_4Pd$), $\chi=\chi_0T^{-1+\lambda}$ with $\lambda\sim 0.7$ between 1.8 and 10 K (for both), and $C/T\sim-\log T(T^{-1+\lambda})$ for $UCu_{3.5}Pd_{1.5}$ ($UCu_4Pd$) between 0.3 and 10 K (1 and 10 K)—see Table II. Below 1 K, $C/T$ for $UCu_4Pd$ rises less rapidly than the power law given (see Fig. 8), but still remains more divergent than $C/T\sim-\log T$ (Andraka, 1994c). Later work on $\chi$ by Maple *et al.* (1994) was able to find the same behavior, $\chi=\chi_0[1-a(T/T_K)^{1/2}]$, as for $U_xY_{1-x}Pd_3$ in $UCu_{3.5}Pd_{1.5}$ in a limited temperature range, 0.4–2 K. Still later, Chau and Maple (1996) showed that $\chi$ for both $UCu_{3.5}Pd_{1.5}$ and $UCu_4Pd$ can be plotted linearly vs $\log T$ between 2 and 10 K, illustrating the difficulty in distinguishing between a weak power law and $\log T$ behavior in a limited temperature range. In writing this review, it was noticed that a plot of $(1/\chi-1/\chi_0)$ vs $T^{\eta}$ (see discussion at the end of Secs. II.B.1 and II.B.3 above) for $UCu_{3.5}Pd_{1.5}$ (but not $UCu_4Pd$) gives a straight line between 1.8 and 200 K—an enormous temperature range compared to either the $\chi\sim T^{-1+\lambda}$ or $\log T$ fit ranges just discussed. Further, the exponent $\eta$ (0.63) would, if we identify $(1/\chi-1/\chi_0)$ with a "$1/\chi_{\text{effective}}$," correspond to a $\chi_{\text{eff}}\sim T^{-0.6}$, which is not far from the $\chi=\chi_0T^{-1+\lambda}$, $\lambda=0.7$, found in Table II from the unadjusted $T<10$ K data. The significance of this non-Curie-Weiss power law (where $\chi^{-1}\sim T$) for $UCu_{3.5}Pd_{1.5}$ is, as discussed by Coleman (1999) and Si *et al.* (1999, 2000), an indication of a fundamental local deviation from Fermi-liquid behavior.

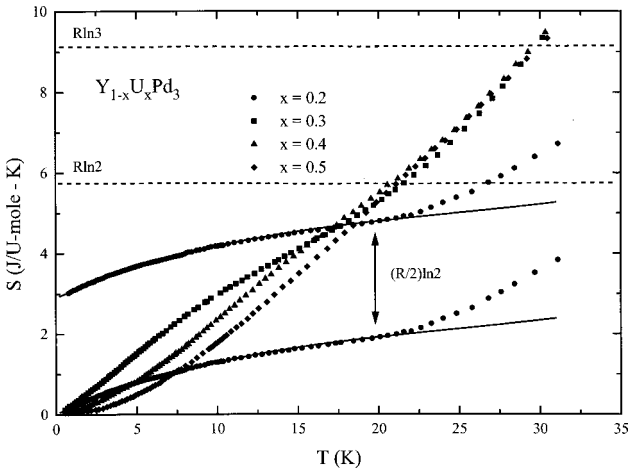


FIG. 5. Measured electronic entropy (the lattice contribution has been subtracted) as a function of temperature in $Y_{1-x}U_xPd_3$ for various U concentrations $x$, after Seaman *et al.* (1991). The entropy data for $x=0.2$ are considerably lower than for the other compositions; the $x=0.2$ data are also shown shifted upwards by $(R/2)\ln 2$ to make the point (see the discussion in the text) that the ground state for $U_{0.2}Y_{0.8}Pd_3$ may have a "missing" entropy down to low temperatures that would be restored by the application of a magnetic field. The line through the $x=0.2$ data is from a fit of the $C/T$ data to $-\log T$.

A recent work of Weber *et al.* (2001) has shown that sample dependence (specifically annealing) can play a large role in measurements of $\rho$, $\chi$, and $C$ in $UCu_{5-x}Pd_x$ such that some samples show entirely different, even on a qualitative basis, low-temperature behaviors than previously reported. For example, annealed $UCu_4Pd$—despite the convincing result of Andraka and Stewart that their $C/T$ data for this composition diverge more rapidly than $\log T$ down to 0.3 K—appears to display $C/T\sim-\log T$ down to 0.1 K, with any deviation at lower temperatures being less divergent. Also, annealed $UCu_4Pd$ shows a resistivity sharply in contrast to the unannealed specimen. As may be seen in Table II, $\rho$ of unannealed $UCu_4Pd$ has the largest (negative) linear temperature coefficient $A$ of any non-Fermi-liquid system—a factor of 6 larger than most systems. The sample of $UCu_4Pd$ annealed for 14 days has a much smaller negative slope, which is only (approximately) linear in a narrow temperature range. This annealed sample has a resistivity ratio $[\rho(300\,\text{K})/\rho(T\to 0)]$ that is $\approx$2.5 vs the 0.5 value for the unannealed samples. In addition (see Table II), the annealed $UCu_4Pd$ sample shows a susceptibility behavior more consistent with a local deviation in the Fermi-liquid behavior [i.e., $(\chi^{-1}-\chi_0^{-1})\sim T^{\alpha}$, $\alpha\neq 1$] as found for the unannealed $UCu_{3.5}Pd_{1.5}$, although not over the same large temperature range. Thus, particularly for this doped system in which the Cu sublattice possesses two inequivalent sites with therefore unavoidable issues of differing site occu-

pations, the reader is warned that the study of non-Fermi-liquid behavior is still in a developmental stage.

In terms of the rich magnetic phase diagram, the discovery work of Andraka and Stewart reported that doping the Cu sites in $UCu_5$ with Pd suppresses the antiferromagnetism monotonically, with $T_N \to 0$ at $x \approx 0.75$, while spin-glass behavior occurs for $x \geq 2$ in $UCu_{5-x}Pd_x$, as shown in the phase diagram in Fig. 9. Thus it is possible that different mechanisms may be responsible for the non-Fermi-liquid behavior observed at $x = 1.0$ and 1.5.

deAndrade *et al.* fit their $C/T$ data for unannealed $UCu_{5-x}Pd_x$ down to 0.2 K for $x = 1$ (down to only 0.6 K for $x = 1.5$) to the power-law behavior suggested by the Griffiths-phase work of Castro Neto *et al.* (1998). However, specific-heat data (Scheidt *et al.*, 1998) down to 0.06 K for unannealed $UCu_4Pd$ (see Fig. 10) reveal a $\log T$ behavior between 0.2 and 2 K followed by a deviation at lower temperatures in which $C/T$ flattens out, i.e., contradicting a power-law dependence at the lowest temperatures. Rather than an entry into Fermi-liquid behavior, $\chi_{ac}$ data (Fig. 10), including strong frequency dependence (another example of a measurement of non-Fermi-liquid behavior driven by a theory) of the observed peak at 0.25 K, imply possible spin-cluster (Griffiths-phase) behavior at this temperature in this unannealed sample. A deviation at ~0.2 K between $\chi_{FC}$ and $\chi_{ZFC}$ in unannealed $UCu_4Pd$—consistent with these $\chi_{ac}$ data—was reported by Vollmer *et al.* (1997). Scheidt *et al.* (1998) show a deviation from $C/T \sim -\log T$ behavior in $UCu_{3.5}Pd_{1.5}$ below 0.23 K that is consistent with $C/T \sim 1 - \sqrt{T}$ (this sequence of temperature dependences is consistent with the theory of Moriya and Takimoto, 1995), but data to even lower temperatures are required. In the recent work of Koerner *et al.* (2000), the low-temperature $C$ and $\chi_{ac}$ additionally for (unannealed) $x = 1.1$, 1.2, and 1.4 have been measured. Possibly due to disorder, a peak in $\chi_{ac}$ was found for all compositions (see Fig. 10) with strong shifts in the peak temperature as a function of frequency (consistent with spin-cluster behavior).

These lower-temperature data taken together clearly demonstrate the difficulty that current theories have—some (e.g., the $\chi_{ac}$ data for $UCu_4Pd$) data may agree with a particular model, but a complete explanation (e.g., of the lowest $C/T$ data for $UCu_{3.5}Pd_{1.5}$) within one model is not possible. One problem in doped systems remains the unavoidable introduction of disorder that, although visible in various measurements such as $\chi_{ac}$, may in fact not be the proximate cause of the non-Fermi-liquid behavior. This point of view was verified by the annealing work of Weber *et al.* (2001) on $UCu_4Pd$, in which they observed the vanishing of the frequency dependence of the peak in $\chi_{ac}$ after annealing.

Scaling of magnetization and specific-heat data as a function of field, in order to determine the scaling exponent $\beta$ of the theory of Tsvelik and Reizer and the nature of the excitations responsible for the observed non-Fermi-liquid behavior, has been carried out for $UCu_{3.5}Pd_{1.5}$ and $UCu_4Pd$ to very high magnetic field at the National High Magnetic Field Laboratory (NHMFL). For $UCu_{3.5}Pd_{1.5}$, scaling of the magnetization data between 1.6 and 6 K in fields to 30 T at the NHMFL gives $\beta = 0.7$ (Kim *et al.*, 1999), i.e., according to the theory of Tsvelik and Reizer (1993) the excitations, $\beta \leq 1.0$, can be either of single-ion or correlated nature. For $UCu_4Pd$, scaling of magnetization data between 1.6 and 6 K in fields to 30 T at the NHMFL gives $\beta = 0.9$ (Kim *et al.*, 1999). Due to the precision with which magnetization, in contrast to specific heat, can be measured, magnetization data for both samples were also measured between 10 and 30 K by Kim *et al.* (1999), still resulting in a lack of determination of the type of excitations for $UCu_{3.5}Pd_{1.5}$ ($\beta = 1.0$) but determining that the excitations at higher temperatures for $UCu_4Pd$ are of the correlated variety ($\beta = 1.2$).

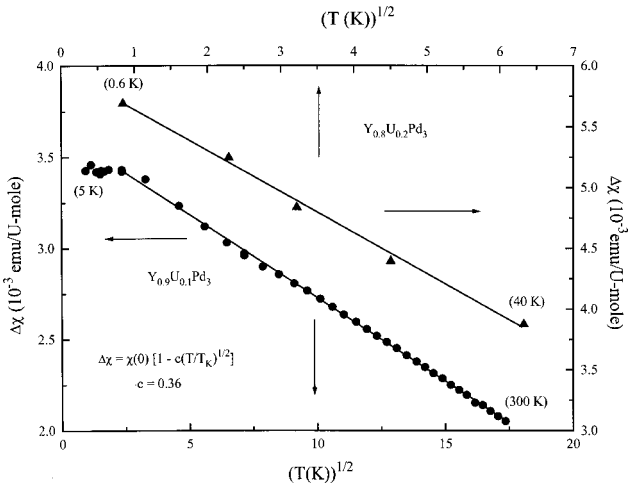


FIG. 6. Magnetic susceptibility, corrected for a magnetic impurity, of $Y_{0.8}U_{0.2}Pd_3$ and $Y_{0.9}U_{0.1}Pd_3$ vs $T^{0.5}$, after Maple *et al.* (1996). Note the saturation of the data for $Y_{0.9}U_{0.1}Pd_3$ below 5 K.

Another type of scaling has also been performed on both these systems, using inelastic neutron scattering to determine the energy dependence vs temperature ($12 \leq T \leq 300$ K) of the magnetic part of the scattering intensity, $S(\omega)$ (Aronson *et al.*, 1995). For lower energies, $\omega < 25$ meV, it was found that $S(\omega)$ is temperature independent (whereas, in a Fermi liquid, temperature is always an important scaling parameter) and the dynamical susceptibility $\chi''(\omega, T)$ was $\sim \omega^{-1/3} Z(\omega/T)$, a non-Fermi-liquid scaling. Such $\omega/T$ scaling has also been seen in high-$T_c$ materials such as $La_{1.96}Sr_{0.04}CuO_4$ (Keimer *et al.*, 1991) and $YBa_2Cu_3O_{6.6}$ (Sternlieb *et al.*, 1993). The argument of Aronson *et al.* (based on the lack of $Q$-vector dependence of the scattering intensity, the similarity of their results for both systems, and the agreement of their $\chi''$ with the measured static $\chi$ down to 30 K) that the excitations for both systems are of single-ion nature disagrees with the higher temperature scaling exponent found by Kim *et al.* (1999) for $UCu_4Pd$. The resolution of this may lie either in the limited temperature range of overlap of the two sets of data or in the precise error bar of the lack of observed $Q$ dependence.

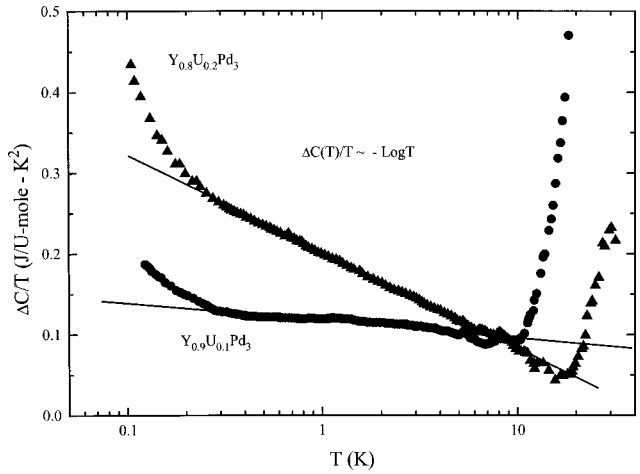


FIG. 7. 5*f* electronic specific heat, $\Delta C$, divided by temperature vs log $T$ for both $Y_{0.8}U_{0.2}Pd_3$ and $Y_{0.9}U_{0.1}Pd_3$, after Maple *et al.* (1996). Note the positive deviation from the log $T$ behavior below ~0.25 K.

As discussed in the theory section, $UCu_{5-x}Pd_x$ has been an important system for investigating the role of disorder in non-Fermi-liquid behavior. Using magnetization as a function of field curves at several low temperatures ($T \geqslant 1.8$ K) to determine the fit parameters, Bernal *et al.* (1995) determined a distribution $P(T_K)$ of Kondo temperatures for their $x=1.0$ and 1.5 samples prepared similarly to the samples of Andraka and Stewart (1993). These distributions, shown in Fig. 11, depend on the saturation observed in $M$ vs $H$ at low temperatures caused, in the disorder models, by the uncompensated, low-$T_K$ moments. Obviously a system with little or no saturation in $M$ vs $H$ at low temperatures is not a candidate for these models. Bernal *et al.* (see also MacLaughlin *et al.*, 1996) then use the determined fit parameters to see how well these describe their measured (large and strongly temperature-dependent) inhomogeneous NMR linewidths for these two compositions. They find a qualitative (factor of 2) agreement between the measured linewidths and those that would be caused by the calculated, parameter-fixed distribution of magnetic susceptibility (induced via static disorder). A similar agreement, within a factor of 2, between the measured field dependence of the specific heat for $UCu_4Pd$ and $UCu_{3.5}Pd_{1.5}$ and that calculated from their model (shown for $UCu_4Pd$ in Fig. 8) using parameters determined by fitting $M$ vs $H$ data was also obtained by Bernal *et al.*

The somewhat long-standing controversy over whether the as-prepared $UCu_4Pd$ consists of ordered sublattices or not (in the $AuBe_5$ structure there are four Be I and one Be II sites per formula unit)[2] has been recently decided by $\mu$SR relaxation measurements down to 3 K by MacLaughlin *et al.* (1998) and extended x-ray-absorption fine-structure (EXAFS) work by Booth *et al.* (1998) on unannealed $UCu_4Pd$ and by lattice parameter measurements and resistivity measurements (mentioned above) down to 0.08 K by Weber *et al.* (2001) on annealed $UCu_4Pd$. Analysis of the width of the frequency shift distribution of the $\mu$SR relaxation data led MacLaughlin *et al.* to argue for considerable magnetic susceptibility inhomogeneity in unannealed $UCu_4Pd$, in agreement with the NMR linewidth results of Bernal *et al.* On a microscopic basis, the EXAFS data of Booth *et al.* on unannealed $UCu_4Pd$ indicate that—rather than having all the Pd on the Be I site and all the Cu on the Be II site—$24 \pm 3\%$ of the Pd occupies Be II sites. Finally, as shown clearly in Fig. 12, the work of Weber *et al.* found that annealing $UCu_4Pd$ causes a decrease in the heretofore accepted lattice parameter, which, as discussed in the caption for Fig. 12, implies qualitatively that—as shown quantitatively by Booth *et al.*—a significant amount of Pd must occupy the smaller Be II sites in unannealed $UCu_4Pd$. In addition, Weber *et al.* find a strong decrease in the residual resistivity (see Table II), implying that at least some of the Pd in the unannealed sample was occupying inequivalent sites. It would be interesting to measure NMR linewidths and/or $\mu$SR relaxation in the annealed $UCu_{5-x}Pd_x$ samples.

Certainly the lack of spin-glass behavior at low temperatures for annealed $UCu_4Pd$ (Weber *et al.*, 2001) argues strongly both for close attention to sample quality, especially in systems in which disorder is thought to play an important role, and for measurements to the lowest temperatures possible. As an example of the importance of the latter, presumably the short correlation length between spins and rapid relaxation rate reported in the $T \geqslant 3$ K $\mu$SR work of MacLaughlin *et al.* (1998) is not characteristic of the sample as it approaches $T=0$, i.e., for $T < T(\chi_{\text{ac peak}})$.

### c. $UCu_{5-x}Pt_x$ (II)

Chau and Maple (1996) and Chau *et al.* (2001) investigated $UCu_{5-x}Pt_x$ (Pt is isoelectronic to Pd) and, as indicated by the subsection heading, found no spin-glass behavior, making this doped non-Fermi-liquid system one of the few examples known in which—when investigated—the disorder inherent with doping does not cause frustrated local moments (at least down to 1.8 K, the lowest temperature of measurement). One possible reason is that, unlike $UCu_{5-x}Pd_x$, the end point in the $UCu_{5-x}Pt_x$ phase diagram (i.e., $UPt_5$) occurs in the same structure ($AuBe_5$) as $UCu_5$, although Chau *et al.* (2001) report that there are impurity phases present in $UCu_{5-x}Pt_x$ for $2.5 \leqslant x \leqslant 4.0$. The electrical resistivity increases below room temperature for $x=0.5$ and 0.75, where the temperature behavior between 1.4 (lowest temperature of measurement) and 20 K follows the classic non-Fermi-liquid $\rho = \rho_0 - AT$ (see Table II) similar to $UCu_{5-x}Pd_x$ for $x=1.0$ and 1.5. (Note, however, that $T_N$ is still finite—~5 K—as determined by a cusp in the magnetic susceptibility for $x=0.5$.) Chau *et al.* (2001) note that there is a distinct minimum in the residual

[2]Bernal *et al.* argue for similar disorder present in both $x=1$ and 1.5 alloys, while Chau, Maple, and Robinson (1998), using elastic neutron-diffraction measurements, argue that Pd and Cu occupy different sublattices in $UCu_4Pd$.

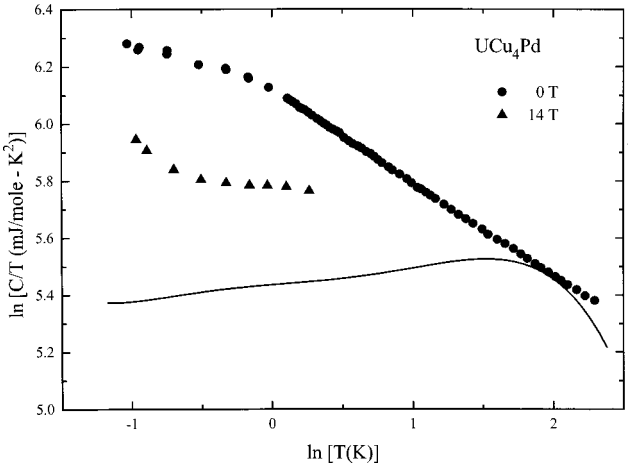


FIG. 8. ln $C/T$ vs ln $T$ for $UCu_4Pd$ in 0- and 14-T applied magnetic field, showing the power-law dependence found by Andraka and Stewart (1993). The solid line is the calculated $C/T$ in 14 T in the disorder model (Bernal *et al.*, 1995) discussed in the text.

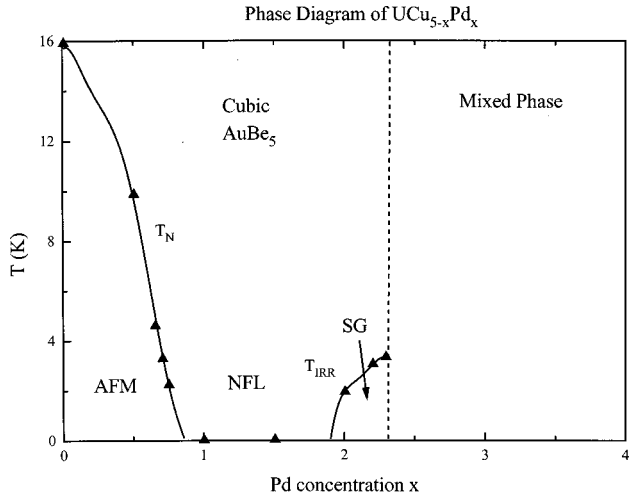


FIG. 9. Magnetic and structural phase diagram of $UCu_{5-x}Pd_x$ as a function of Pd content $x$, after Chau and Maple (1996). $T_{IRR}$ is the spin-glass freezing temperature, or where field-cooled $\chi_{FC}$ and zero-field-cooled $\chi_{ZFC}$ diverge.

resistivity ratio, $R(300\,\mathrm{K})/R(T\to 0)$, as a function of $x$ in $UCu_{5-x}Pt_x$ for $x\approx 0.75$. For $UCu_4Pt$, $\rho$ rises only slightly (~2%) at low temperatures and is essentially flat for $x=1.25$–$1.75$. The magnetic susceptibility $\chi$ behaves as $\chi_0 \log T$ between 1.8 (lowest temperature of measurement) and ~10 K for $0.75\leqslant x\leqslant 1.5$, but can be equally well fitted (Chau *et al.*, 2001) to the Griffiths-phase $T^{-1+\lambda}$ dependence; see Table II. Similarly, the specific heat for $UCu_{5-x}Pt_x$, $x=1$ and 1.25, between 0.6 and 4 K can be fitted equally well to a $-\log T$ or a $T^{-1+\lambda}$ dependence, with $C/T$ for $x=1.5$ essentially constant at low temperature. Chau *et al.* (2001) argue that in $UCu_{5-x}Pt_x$ the non-Fermi-liquid behavior is already over by $x\approx 1.5$, noting that the slight increases (~6%) in $\chi$ and $C/T$ in the lowest 5 K of measurement are more Fermi liquid like (i.e., constant) than divergent while the resistivity data already show no non-Fermi-liquid behavior by $x=1.25$. Thus $UCu_{5-x}Pt_x$ is different from $UCu_{5-x}Pd_x$ in several respects: a more rapid suppression of $T_N$ with doping, concurrent with non-Fermi-liquid behavior for lower $x$, and no spin-glass behavior (Chau and Maple, 1996), at least down to the lowest temperature of measurement, 1.8 K.

### d. $UCu_4Ni$ (II)

An annealed sample (900 °C for 1 week) of $UCu_4Ni$ (Ni is isoelectronic to Pd and Pt) showed (Lopez de la Torre *et al.*, 1998) no difference in $\chi_{FC}$ vs $\chi_{ZFC}$, i.e., no spin-glass behavior, down to 0.4 K, with $\chi=\chi_0-aT^{0.5}$ between 0.4 and 2.5 K. The resistivity was measured on both the annealed and unannealed material (see Table II) and obeyed $\rho=\rho_0-AT$ between 0.4 and 40 K, with $\rho_0$ falling 4.5% after annealing. Although Lopez de la Torre *et al.* stated that $\rho$ in $UCu_4Ni$ was not significantly changed by annealing, in light of the results of Weber *et al.* (2001) on annealed $UCu_4Pd$ it is interesting to analyze the $\rho$ data on $UCu_4Ni$ to extract the negative coefficient $A$ in $\rho=\rho_0-AT$. As shown in Table II, the magnitude of $A$ falls significantly (~35%) after one week of annealing in $UCu_4Ni$—at least qualitatively similar to the results of Weber *et al.* (2001) for two weeks of annealing in $UCu_4Pd$.

### e. $UCu_{5-x}Al_x$ (III)

This system does not form in the cubic, $AuBe_5$ structure like $UCu_{5-x}Pd_x$, but rather in the hexagonal $CaCu_5$ (cf. $UNi_2Al_3$ and $UPd_2Al_3$ in Sec. III.A.2 below). Nakotte *et al.* (1996, 1997) reported specific heat, magnetic susceptibility, and resistivity for $UCu_{5-x}Al_x$. For $x=1.5$, $C/T\sim -\log T$ between 0.6 to 6 K, with an upturn

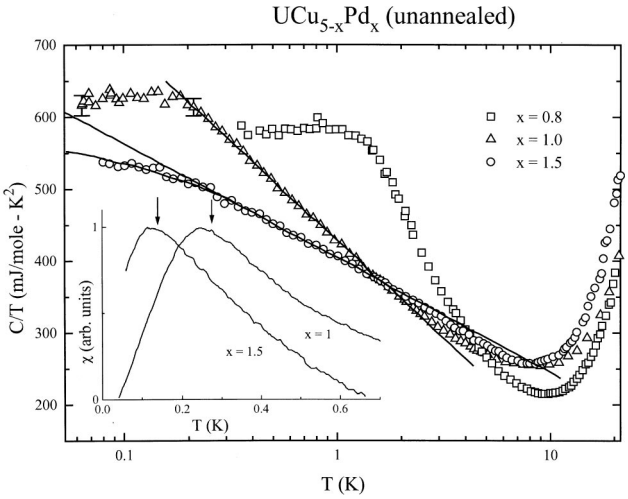


FIG. 10. $C/T$ vs $\log T$ of unannealed $UCu_{5-x}Pd_x$, after Scheidt *et al.* (1998): straight lines, $C/T\sim -\log T$ behavior; curved line through the $x=1.5$ data at lowest temperature, a fit of $C/T$ to $\gamma_0-AT^{0.5}$, as discussed in the text. $\chi_{ac}$ vs $T$ data for $UCu_4Pd$ and $UCu_{3.5}Pd_{1.5}$ are shown in the inset for an excitation frequency of 95 Hz; the arrows denote the shifted peak positions for 995 Hz.

above this behavior observed below 0.6 K down to the lowest temperature of measurement, 0.3 K, like that seen in $U_{0.2}Y_{0.8}Pd_3$. For $x=1.9$, there is an anomaly in $C/T$ at around 11 K, which moves down to 10 (4) K for $x=2$ (2.1). ($\chi$ for polycrystalline $x=2$ also shows a peak at 10 K.) At temperatures below the anomaly down to ~0.6 K, $C/T \sim -\log T$. Neutron-scattering results on a single crystal of $UCu_3Al_2$ showed no ordered magnetic moment, with an upper limit of $0.1\mu_B$, which unfortunately is still consistent—based on the small size of the anomaly in the specific heat—with the possibility of long-range magnetic order. Thus $UCu_3Al_2$ is a possible candidate for coexistent non-Fermi-liquid behavior and long-range magnetic order. The magnetic susceptibility for polycrystalline $x=1.5$ gave $\chi=a+bT^{-1/3}$ between 1.4 (lowest temperature of measurement) and ~17 K, but the authors point out that results on the single crystal of $UCu_3Al_2$ indicate strong magnetic anisotropy $[\chi(B\perp c)/\chi(B\|c)\approx 2]$ with differing temperature dependences for $\chi$ in the two directions as well, with $\chi(B\|c)$ divergent at low temperature while $\chi(B\perp c)$ decreases below a peak at 10 K. Thus the $T^{-1/3}$ behavior in $UCu_{3.5}Al_{1.5}$, although observed over a fairly wide temperature range, could be due to an averaging of anisotropic responses in the polycrystalline sample. Similarly, the results for the resistivity for polycrystalline $UCu_{3.5}Al_{1.5}$ also show an unusual temperature dependence between 0.3 (lowest temperature of measurement) and 10 K, $\rho=\rho_0+T^{2/3}$, followed by a maximum in $\rho$ at 30 K, which the authors speculate could also be due to an averaging of differing temperature dependences in the differing crystalline directions. The resistivity of polycrystalline $UCu_3Al_2$ shows a minimum at 10 K, where the anomalies in $C$ and $\chi$ are observed, followed by an unexplained drop in $\rho$ at 0.8 K, which the authors suggest might be due to a second phase. Data on high-field magnetization of the $UCu_{5-x}Al_x$ system show no apparent saturation up to 20 T, arguing against a distribution of Kondo temperatures caused by disorder as the explanation of the non-Fermi-liquid behavior. Clarification of the unusual temperature dependences in $\chi$ and $\rho$ for $UCu_{3.5}Al_{1.5}$ must await further single-crystal work.

#### f. $Ce_{1-x}La_xCu_2Si_2$ (I)

Studied for its non-Fermi-liquid behavior by only one group (Andraka, 1994a), this was the first known Ce system to show non-Fermi-liquid behavior. [Jee *et al.* (1991) had studied the strongly diluted $Ce_{0.1}La_{0.9}Cu_2Si_2$ previously to investigate the dilute-limit heavy-fermion behavior in $CeCu_2Si_2$, the prototype heavy-fermion superconductor (Steglich *et al.*, 1979).] Andraka found that just below the $x=0.9$ composition [which is the only composition in which $C/T$ and $\chi$ show $\log T$ behavior over a decade of temperature down to the lowest temperatures of measurement (~1 and 1.8 K, respectively)], $Ce_{0.15}La_{0.85}Cu_2Si_2$ shows definite spin-glass behavior—a strong difference in field-cooled and zero-field-cooled $\chi$. Since otherwise magnetic behavior seems rather distant in the phase diagram, $Ce_{0.1}La_{0.9}Cu_2Si_2$ likely also belongs to the category of doped non-Fermi-liquid systems in which the spin-glass behavior is caused by the same magnetic interactions that prevent Fermi-liquid behavior. $Ce_{0.1}La_{0.9}Cu_2Si_2$ is unusual in two respects. The electrical resistivity behaves approximately as $\rho=\rho_0-AT$ between 1 and 5 K and as $\rho=\rho_0-\log T$ (i.e., Kondo behavior) for 8–20 K. Both higher- and lower-temperature data are needed to further investigate this behavior. Second, although $C/T \sim -\log T$ first at $x=0.9$ in $Ce_{1-x}La_xCu_2Si_2$, by $x=0.975$ this logarithmic behavior is already lost whereas, as has been seen for $U_{1-x}Y_xPd_3$ and $UCu_{5-x}Pd_x$, usually the range of stoichiometry in which such relatively high-temperature measurements show non-Fermi-liquid behavior is somewhat broader.

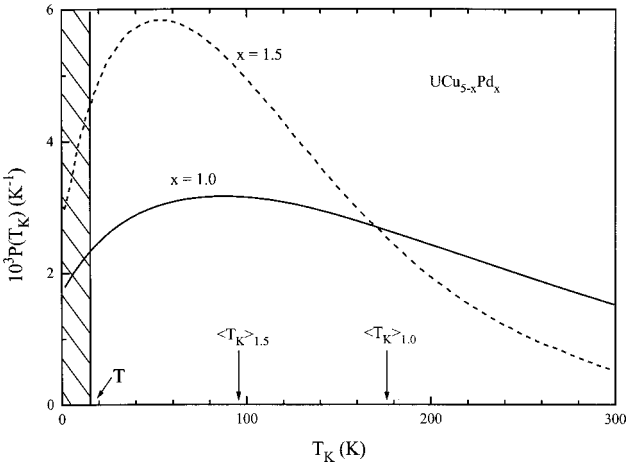


FIG. 11. Distribution of Kondo temperatures for $UCu_{5-x}Pd_x$ as calculated in the phenomenological Kondo disorder model of Bernal *et al.* (1995), after MacLaughlin *et al.* (1996), as discussed in the text. The average Kondo temperatures for both compositions are shown with arrows. The shaded area is to indicate that, at the temperature $T$, the spins with $T_K$ values that are lower than $T$ are unshielded by the Kondo compensation process and therefore retain their magnetic moments.

#### g. $(U_xLa_{1-x})_2Zn_{17}$ (I)

von Blanckenhagen *et al.* (2001) used La doping in one of the canonical heavy-fermion antiferromagnets ($U_2Zn_{17}$, $T_N=9.7$ K) to suppress antiferromagnetism and look for non-Fermi-liquid behavior at the quantum critical point. $T_N\to 0$ at $x\approx 0.8$, but although the resistivity obeys $\rho=\rho_0-AT$ fairly well from 0.1 to 3.2 K, the specific heat at this concentration still appears Fermi-liquid-like, with the inclusion of a spin-fluctuation ($C \sim T^3 \log T/T_{SF}$) term, as does $\chi$. At $x=0.5$–$0.7$, $\chi=\chi_0 - aT^{0.5}$ between 1.8 (lowest temperature of measurement) and 40 K, with, however, $C/T$ showing saturation ($\to$ constant) below 0.3 K. At $x=0.3$, i.e., far from the point in the phase diagram where the antiferromagnetism is first suppressed, the specific heat first shows non-Fermi-like behavior ($C/T$ continues to increase with decreasing temperature) over the whole temperature range of measurement—but slower than a $\log T$ divergence below 0.3 K. $\chi=\chi_0-a\log T$ between 1.8 and

40 K for $x=0.1$ and 0.3, with weak evidence ($\chi_{ZFC} \neq \chi_{FC}$, but no peak in $\chi_{ZFC}$) for spin-glass behavior below ~25 K. Further resistivity measurements and checks for spin-glass behavior need to be carried out on this system.

*h. $U_2Cu_{17-x}Al_x$ (I)*

Just as non-Fermi-liquid behavior was found in $Ce_{0.1}La_{0.9}Cu_2Si_2$ by investigation of a known highly correlated system, $U_2Cu_{17-x}Al_x$ was investigated by Pietri *et al.* (1997) due to its occurrence in the $U_2Zn_{17}$ rhombohedral structure, where $U_2Zn_{17}$ is a known heavy-fermion antiferromagnet. Pietri *et al.* report that $C/T$ was $\sim -\log T$, $\chi$ was $\sim T^{-1+\lambda}$, $\lambda=0.7$, and $\rho=\rho_0+AT^2-aT$ for $x=5$, with the quadratic term stated to be small. Perhaps a two-band picture would be appropriate to describe the presence of both a $T$ (non-Fermi-liquid) and $T^2$ (Fermi-liquid) term in the resistivity results. Pietri *et al.* remarked that if one followed the Kadowaki and Woods (1986) formula in which $A/\gamma^2 \sim 10^{-5}$, the small value of $A$ would be a factor of 3 too small for the large observed $C/T$ values. (Since $C/T$ diverges as $T \rightarrow 0$, and since $\gamma \equiv \lim_{T\rightarrow 0} C/T$, the $\gamma$ value used was just $C/T$ at 0.35 K, the lowest temperature of measurement.) Spin-glass behavior was observed by Pietri *et al.* for $x=8$ in a divergence of the field-cooled and zero-field-cooled dc susceptibility at 2.5 K. This field-cooled vs zero-field-cooled difference was also echoed in a shoulder in the $C/T$ data at a slightly higher temperature, as is typical of a spin glass. A similar feature in $C/T$ was observed at ~1 K for $x=6$, but this temperature range was not measurable in their susceptometer. At higher Al concentrations, $8 \leqslant x \leqslant 12$, Nishioka *et al.* (1998) also reported spin-glass behavior with $C/T \sim -\log T$ plus a spin-glass anomaly superimposed that was partially suppressed in a 5-T magnetic field. Pietri *et al.* did not examine their $x>5$ specific-heat data for whether a background under their spin-glass anomalies followed $C/T \sim -\log T$.

Residual resistivity values (Pietri *et al.*, 1997) suggest that the Cu and Al are disordered on the various Zn sublattice sites, implying that the disorder model should be applicable. As one last observation, the $C/T$ of Pietri *et al.* below 0.4 K in $U_2Cu_{12}Al_5$ appeared to diverge more strongly than $\log T$, similar to the behavior observed in $U_{0.2}Y_{0.8}Pd_3$.

*i. $U_{1-x}Y_xAl_2$ (I)*

$UAl_2$ was the first system in which the spin fluctuation (or "paramagnon") temperature dependence in the specific heat ($C \sim T^3 \log T/T_{SF}$)—predicted as the next term after $C \sim \gamma T$ in the Landau Fermi-liquid model—was experimentally observed (Trainor *et al.*, 1975.) Upon doping with Y, Mayr *et al.* (1997) discovered that, as the Y doping increases, the $T^3 \log T/T_{SF}$ term present in the specific heat for $x=0$ remains a good representation of the data up to $x=0.8$ (certainly a robust resistance of the spin fluctuations to destruction by doping), followed by $C/T \sim -\log T$ for the dilute $x=0.875$, 0.9, and 0.95 over almost two decades of temperature (0.3–20 K), while $\rho=\rho_0-AT$ between 0.8 and 10 K and $\chi \sim T^{-1+\lambda}$ between 3 and 400 K, with deviations in $\rho$ and $\chi$ at lower temperatures. $M$ vs $H$ for $x=0.9$ was linear up to 7 T (Mayr, 1997), inconsistent with a disorder-caused distribution of $T_K$'s being responsible for the non-Fermi-liquid behavior. It is interesting to note in Table II the relatively strong variation in, for example, $T_0$ as determined by the specific heat and the magnitude of $\chi$ (1.7 K) in this relatively narrow composition window of U concentration in which non-Fermi-liquid behavior occurs. Such strong variation is at odds with any sort of single-ion, U-ion concentration-independent universal behavior. Spin-glass behavior in the dc magnetic susceptibility (divergence of $\chi_{FC}$ and $\chi_{ZFC}$ below a certain $T_{freezing}$) was observed beginning at $x=0.2$ and was still slightly present at $x=0.9$, i.e., $U_{1-x}Y_xAl_2$ displayed concurrent non-Fermi-liquid and spin-glass behavior. This may be compared, at least as far as the resistivity is concerned, to the $\alpha=1.5$ exponent ($\rho=\rho_0+AT^{1.5}$) for the pure spin-glass case, in, for example, AuFe (Mydosh and Ford, 1973).

Spin fluctuations are weak and do not prevent entry into the Fermi-liquid ground state. There is no other magnetism observed to be present in the phase diagram

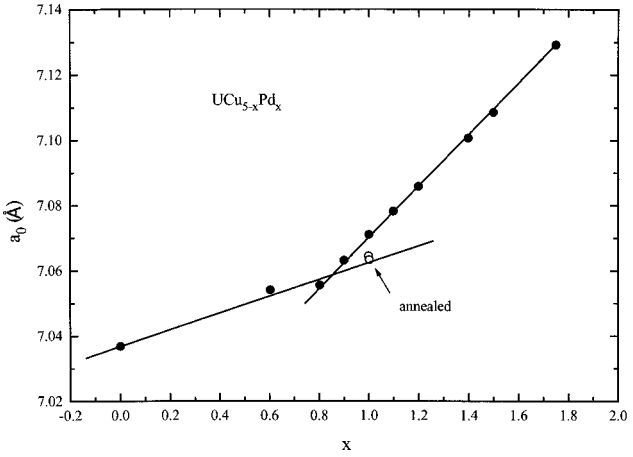


FIG. 12. Lattice parameter, $a_0$, for cubic $AuBe_5$-type $UCu_{5-x}Pd_x$ as a function of $x$, after Weber *et al.* (2001): ●, unannealed samples; ○, lattice parameter of samples of $UCu_4Pd$ annealed for 7 and 14 days at 750 °C, causing a monotonic decrease with increasing annealing, although the difference in $a_0$ between the two annealing times is small. There are two inequivalent sites in the Be sublattice of this $AuBe_5$-type structure with a ratio of $Be_I/Be_{II}=1/4$. Since the $Be_I$ lattice site has a larger volume than the $Be_{II}$ site, and since Pd is larger than Cu, the reduction of the lattice parameter with annealing in $UCu_4Pd$ implies that annealing causes Pd preferentially to occupy the larger $Be_I$ site vs the more disordered site occupation in the unannealed sample—consistent with the EXAFS site occupation results of Booth *et al.* (1998). After the $Be_I$ site is largely occupied with Pd, additionally substituted Pd must occupy the smaller $Be_{II}$ site, causing the rate of increase in $a_0$ with increasing $x$ to become larger, as can be seen in the trend of the $a_0$ data for unannealed samples for $x>0.8$.

for $U_{1-x}Y_xAl_2$ other than the spin-glass behavior, which peaks in strength at $x \sim 0.7$. However, Mayr *et al.* (1997) note that a similar (although Sc contracts the $UAl_2$ *C*-15 cubic lattice while Y expands it) doping study, on $U_{1-x}Sc_xAl_2$ (Mayr, 1997), showed similar non-Fermi-liquid behavior with no observed spin-glass behavior. Thus the source of the strong Fermi-liquid-preventing interactions in doped $UAl_2$ remains an open question.

#### *j. $U_xTh_{1-x}Ru_2Si_2$, $x \leqslant 0.07$ (I)*

$URu_2Si_2$, which is tetragonal, of the $ThCr_2Si_2$ structure type, was discovered by Schlabitz *et al.* (1986) to be a coexistent antiferromagnet ($T_N = 17.5$ K) and superconductor ($T_c \sim 1.2$ K) with a specific heat $\gamma$ just above $T_c$ of $\sim 180$ mJ/mol K$^2$. Amitsuka and co-workers (1993, 1994, 1997, 2000) discovered anisotropic non-Fermi-liquid behavior for dilute (presumably long after the antiferromagnetism is suppressed) $U_xTh_{1-x}Ru_2Si_2$: $\rho = \rho_0 + A \log T$, $1.3 \leqslant T \leqslant 8$ K, and $x \leqslant 0.07$ ($\rho$ was measured for $x = 0.03$ down to 0.1 K and $\rho = \rho_0 + A \log T$ down to 0.2 K), $\chi(B \| c) \sim \log T$ ($0.4 \leqslant T \leqslant 10$ K, $x \leqslant 0.07$). Here $\chi$ for $B \| a$ was constant vs temperature, i.e., Fermi-liquid-like, and $C/T$ was $\sim -\log T$ for $x = 0.07$ only for 0.3–1 K. Rather than stressing a $\log T$ behavior in $C/T$, Amitsuka *et al.* used the two-channel Kondo model of Sacramento and Schlottmann to fit their specific-heat data for $U_{0.07}Th_{0.93}Ru_2Si_2$ below 10 K with a positive deviation of the data vs the fit below 0.4 K.

A replotting of the data using a scanner (see Fig. 13) shows that $C/T \sim T^{-1+\lambda}$, with $\lambda \sim 0.3$, gives a reasonable fit to the $x = 0.07$ data between 0.35 and 3 K. For $x = 0.07$, Amitsuka *et al.* see a peak in $\chi$ vs $T$ at 0.25 K that is absent down to 0.1 K by $x = 0.01$—extending the $\chi = \chi_0 - B \log T$ behavior down to this lower temperature. For $x = 0.07$ Amitsuka *et al.* state that the peak in $\chi$ might be due to spin-glass behavior, but do not report either field-cooled vs zero-field-cooled $\chi_{dc}$ or frequency dependence of the peak in $\chi_{ac}$. This has since been investigated (Kim, 1995) and spin-glass behavior (divergence in $\chi_{FC}$ and $\chi_{ZFC}$ below $T \approx 10$ K) was found in polycrystalline $U_{0.07}Th_{0.93}Ru_2Si_2$. Magnetization vs field of $x = 0.03$ shows significant saturation for $T \leqslant 10$ K. Thus, in addition to the two-channel model chosen by Amitsuka *et al.* to fit their specific-heat data, either the Kondo disorder model or the Griffiths-phase scenario appears consistent with at least some of the data at this time.

#### *k. $U_xY_{1-x}Ru_2Si_2$, $x \leqslant 0.07$ (III)*

Amitsuka *et al.* (2000) report that $\chi \sim -\log T$ between 0.1 and 8 K for $U_{0.03}Y_{0.97}Ru_2Si_2$ (similar to the result found for Th doping), $C/T \sim -\log T$ between 0.65 and 7.5 K for $U_{0.07}Y_{0.93}Ru_2Si_2$ with a slightly more divergent behavior between 0.4 and 0.65 K (contrasting to the result for Th doping), and $\rho = \rho_0 + A T^{1.27}$ between 0.1 and 8 K for $U_{0.03}Y_{0.97}Ru_2Si_2$ (also in contrast to the results stated above for Th doping). In addition to the different temperature dependences for $C/T$ and $\rho$, $U_xY_{1-x}Ru_2Si_2$ has significantly smaller $C/T$ and $\chi$ values than for Th doping (see Table II).

#### *l. $U_xTh_{1-x}Pt_2Si_2$, $x \leqslant 0.07$ (III)*

Following up on their discovery of non-Fermi-liquid behavior in dilute $URu_2Si_2$, Amitsuka, Hidano, *et al.* (1995) investigated $UPt_2Si_2$, which is an antiferromagnet with $T_N = 34$ K, doped to the dilute limit with Th. The magnetic susceptibility for $x \leqslant 0.07$ in both the *c*-and *a*-axis directions ($UPt_2Si_2$ is tetragonal $CaBe_2Ge_2$ structure type) approaches $\chi \sim T^{-1+\lambda}$ between 1.8 (lowest temperature of measurement) and 10 K, while no clear temperature dependence is shown for $\rho$. The specific heat between 1.7 and 10 K for $x = 0.05$ and 0.07 was originally described as varying approximately as $\log T$ (see Fig. 14) and has been replotted here vs $T^{0.5}$ (Fig. 15). The agreement for the $x = 0.07$ sample with $C/T = \gamma_0 - A T^{0.5}$ over a rather wide temperature range (see Table II) is rather suggestive of the Millis-Hertz theoretical prediction. [The self-consistent renormalization model of Moriya and co-workers predicts $T^{0.5}$ followed by $\log T$, which is not consistent with the data shown in Fig. 15; however, the theory of Lonzarich, Table I(c), is also consistent with the data.] Further specific-heat measurements on $x = 0.07$ down to 0.3 K, inspired by Fig. 15, have recently been carried out (Kim and Stewart, 2000). Below 1.5 K these new data show that $C/T$ flattens out and is constant, i.e., Fermi-liquid behavior appears. Thus $U_{0.07}Th_{0.93}Pt_2Si_2$ is not quite at a quantum critical point but, since it is one of the few non-Fermi-liquid systems that approximately obeys $T^{0.5}$ over an appreciable temperature range, perhaps followup work on compositions nearby in the phase diagram would be of interest to see if $C/T \sim \gamma_0 - A T^{0.5}$ over a broader temperature range.

#### *m. $U_xTh_{1-x}Pd_2Si_2$ (I?)*

Amitsuka, Shimamoto, *et al.* (1995) report non-Fermi-liquid behavior in the very dilute limit, $x \leqslant 0.07$, for this compound, which occurs in the tetragonal $ThCr_2Si_2$ structure and, in the undoped state, has $T_N = 150$ K. The magnetic susceptibility for field parallel to the *c* axis for $x = 0.03$ obeys $\chi_c \sim -\log T$ between 0.2 and 6 K, while $\chi_c$ for $x = 0.05$ (0.07) has a cusp at 0.4 (1.2) K—reminiscent of the behavior seen in $U_{1-x}Th_xRu_2Si_2$ and possibly of spin-glass origin. $\chi_a$ is approximately temperature independent down to 2 K, as is the resistivity, within the data scatter, below 3.5 K (Amitsuka, Shimamoto, *et al.* 1995). The specific heat for $x = 0.05$ and 0.07 diverges below 10 K down to 1.6 K (lowest temperature of measurement) somewhat less rapidly than $-\log T$, while $C/T$ data for $x = 0.03$ obey $C/T \sim -\log T$ between 1.6 and $\sim 10$ K (see Fig. 16). Such a behavior with doping, hunting for a pure $\log T$ dependence with small changes in doping levels, is of course—so long as the sought-after non-Fermi-liquid temperature dependence is found over more than a decade of temperature (not yet the case for $U_{1-x}Th_xPd_2Si_2$)—reminiscent of critical-point behavior and is quite common in doping studies of potential non-

Fermi-liquid systems. With less than a convincing extent of the sought-after temperature dependence, however, such studies must be considered as preliminary—with experience on other systems (e.g., on $U_{0.07}Th_{0.93}Pt_2Si_2$, just discussed) dictating a high probability that deviations from the $\log T$ behavior will be found as the measurements are extended to lower temperatures.

#### n. $U_{1-x}M_xPt_3$ (I)

Trinkl, Weilnhammer, *et al.* (1996) reported that the $DO19$ hexagonal structure of $UPt_3$ was preserved with up to 30% (15%) Zr (Hf) doping on the U site, and found $C/T \sim \log T$ over more than two decades of temperature for $x=0.25$ (0.15) down to the lowest temperature (0.1 K) of measurement—i.e., without the low-temperature deviation observed in, for example, $U_{0.2}Y_{0.8}Pd_3$. Measurements of the field dependence of the specific heat of $U_{0.7}Zr_{0.3}Pt_3$ show little change in 13 T, consistent with the quadrupolar Kondo theory of Cox and co-workers. Magnetization data to 7 T show no saturation behavior for $\leqslant 25\%$ Zr, but definite saturation in the magnetization as a function of field for 30% Zr at 2 K. Where to place these results in this review is somewhat difficult, since no bulk, static evidence of antiferromagnetism exists in undoped $UPt_3$, but there are clearly tendencies towards antiferromagnetism—doping with a few percent of Pd on the Pt site or with a few percent of Th on the U site causes antiferromagnetism (see Sec. III.A.3 below), and there are results that show evidence of a dynamic antiferromagnetism at high frequencies at 5 K (Aeppli *et al.*, 1988). Also, Trinkl *et al.* speculate that the Fermi-liquid-preventing long-range magnetic correlations in $U_{1-x}M_xPt_3$ comes from antiferromagnetic correlations associated with the peak in $\chi$ in pure $UPt_3$ at 18 K being suppressed to lower temperatures with the Zr or Hf doping. In addition to the non-Fermi-liquid behavior observed in the specific heat, Trinkl *et al.* observe non-Fermi-liquid behavior for the magnetic susceptibility ($\chi$ diverges as $T \to 0$) for both $U_{0.85}Hf_{0.15}Pt_3$ (analyzed originally as a sum of $\log T$ and $T^{-\alpha}$) and $U_{1-x}Zr_xPt_3$, $x=0.25$ and 0.30. Replotting the data, $\chi$ can be fit to $(1/\chi - 1/\chi_0) = T^{1-\lambda}$, $\lambda \approx 0.1$ and 0.4, respectively, for $U_{1-x}Zr_xPt_3$, $x=0.25$ and 0.30, and, using the same form, $\lambda \approx 0.2$ for $U_{0.85}Hf_{0.1}Pt_3$, all over a large temperature range (see Table II)—convincing evidence of the correctness of such a functional form for $\chi$. This type of behavior for $\chi$ (subtracting a constant term $\chi_0^{-1}$ to give a $T^{\alpha}$, $\alpha \neq 1$, dependence; see also Secs. II.B.3 and III.A.1.b) is a sign that weak-coupling Millis-Hertz theory is inapplicable (see, for example, Coleman, 1999, Si *et al.*, 1999, and Schroeder *et al.*, 1998) and that there is a fundamental local deviation from Fermi-liquid behavior. Resistivity (Trinkl, 1996) for $U_{1-x}Zr_xPt_3$, $x=0.20$ and 0.30 behaved as $\rho = \rho_0 + A T^{1.5}$ between 0.1(*) and 1.5 K, followed by $\rho = \rho_0 + A T$ between 1.5 and 6 K, where the temperature dependence observed for the lowest-temperature resistivity would be consistent with the weak-coupling Millis-Hertz/Moriya/Lonzarich theories for three-dimensional antiferromagnetic fluctuations, while the trend in resistivity exponent with increasing temperature would, in the Rosch theory (see Fig. 3), correspond to a disorder parameter of $x \approx 0.1$.

Both the Hf- and the Zr-doped $U_{1-x}M_xPt_3$ samples show spin-glass behavior, that is, divergence in field-cooled vs zero-field-cooled $\chi$ plus a remanent magnetization after the field is turned off in the susceptometer, that decays as the log of the time over hours (Trinkl, 1996). One problem in determining the influence this has on the non-Fermi-liquid behavior is that, although the size of the difference $\chi_{FC} - \chi_{ZFC}$ grows with increasing doping, $T_{freezing}$ stays constant at about 6 K; and in fact, this work led to the discovery that pure $UPt_3$ shows spin-glass behavior (Trinkl, Corsepius, *et al.*, 1996). Note that the observed $\rho = \rho_0 + A T^{1.5}$ behavior, coupled with the spin-glass behavior, is consistent with the classic spin-glass behavior first observed down to 0.45 K by Mydosh and Ford (1973) in AuFe, almost two decades ahead of the non-Fermi-liquid behavior observed in $U_{0.2}Y_{0.8}Pd_3$ by Seaman *et al.* (1991).

#### o. $Ce_{1-x}Th_xRhSb$ (I?)

Undoped CeRhSb occurs in the orthorhombic $CeCu_2$ structure, has a specific heat $\gamma$ of 32 mJ/mol K$^2$, and has no apparent magnetic behavior. Upon doping with 10% Th, the $\gamma$ climbs to 130 mJ/Ce mol K$^2$, while further doping ($0.2 \leqslant x \leqslant 0.4$) causes $C/T$ to diverge more rapidly than $\log T$ (Andraka, 1994b; see Fig. 17). For $x=0.5$ (0.6), $C/T$ as well as ac magnetic susceptibility show broad anomalies at 0.6 K (0.8 K) which are described as "magnetic" in character and could be either broadened antiferromagnetic or spin-glass transitions. Andraka (1994b) lists as possible explanations for the non-Fermi-liquid behavior in the specific heat either disorder near a metal-insulator transition (CeRhSb is thought to have a partial gap in the electronic density of states spectrum in the theory of Dobrosavljevic *et al.*, 1992) or proximity to magnetism. Considering the rather monotonic, albeit faster than $\log T$, curvature of the $C/T$ data for $Ce_{1-x}Th_xRhSb$ shown in Fig. 17, and with the added perspective of the theory of Castro Neto *et al.* (1998), in which $C/T$ for disordered materials with Griffiths clusters should behave as $T^{-1+\lambda}$, Fig. 18 shows the $C/T$ data replotted, displaying rather good agreement with $C/T \sim T^{-1+\lambda}$, with $\lambda \approx 0.6$, 0.5, and 0.3 for $x=0.2$, 0.3, and 0.4, respectively. Note that the $x=0.3$ data fit a power law over a rather extended range.

#### p. $URu_{2-x}Re_xSi_2$ (III)

A recent report by Bauer, Freeman, *et al.* (2000) on this system reports the disappearance of small-moment antiferromagnetism, present at 17.5 K in the undoped system, by $x=0.15$ (at $x=0.1$, $T_N \approx 12$ K). Ferromagnetism, as determined by an Arrot plot analysis of $M$ vs $H$ data, appears at $T_c \approx 5$ K for $x=0.4$ with an increase in the ferromagnetic ordering temperature for further increases in $x$. For $x=0.2$ and 0.35, specific heat divided by temperature between 0.6 (lowest temperature of

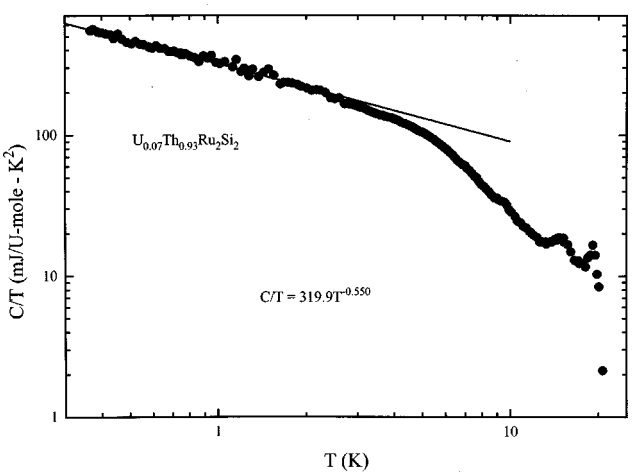


FIG. 13. log$C/T$ vs log $T$ for $U_{0.07}Th_{0.93}Ru_2Si_2$, data from Amitsuka and Sakakibara (1994). This replot of the original data, where $C/T$ was plotted vs log $T$, demonstrates a substantial temperature range of agreement for $C/T \sim T^{-1+\lambda}$, or the Griffiths-phase model, which was applied to non-Fermi-liquid systems after the data were published.

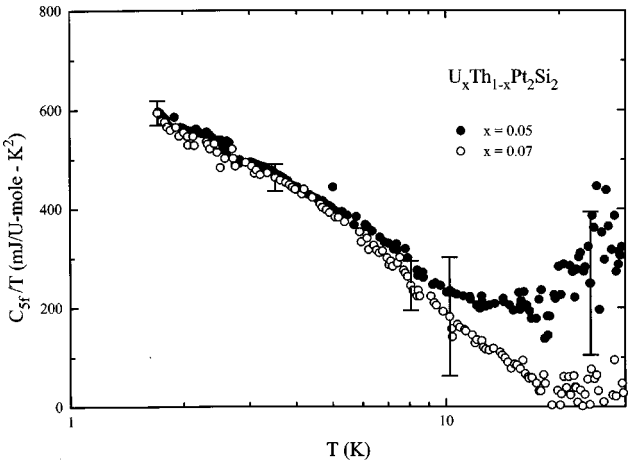


FIG. 14. $C_{5f}/T$ vs log $T$ for $U_xTh_{1-x}Pt_2Si_2$, where $C_{5f}$ equals $C_{\text{measured}} - C_{\text{lattice}}$, after Amitsuka, Hidano, *et al.* (1995). The data exhibit a concave curvature as plotted vs log $T$ over the whole temperature range up to 10 K.

measurement) and ≈2.5 K fit either a $-\log T$ or $T^{1+\lambda}$ approximately equally well, as do $\chi$ data between 1.8 and 6 K, with $\lambda \approx 0.9$. The resistivity behaves like $\rho = \rho_0 + AT^{\alpha}$ between 1.8 and 15 K, with $\alpha = 1.6, 1.2, 1.1, 1.1$ for $x = 0.15, 0.3, 0.35, 0.4$, respectively. Other than the smaller $\alpha$ exponent for the resistivity, no difference is observed in the non-Fermi-liquid behavior near the suppression of antiferromagnetism in $URu_{2-x}Re_xSi_2$ at $x = 0.15$ *vis à vis* the creation of ferromagnetic behavior at $x = 0.4$. Further work on this system is in progress.

#### q. $U_2Pd_{1-x}Si_{3+x}$ (II)

Homma *et al.* (2000) report that non-Fermi-liquid behavior occurs in this system at $x = 0.4$ and 0.5, just at the point in the phase diagram where, with increasing $x$, spin-glass behavior is suppressed. Thus this may be an ideal system in which to check the theory of Sengupta and Georges (1995) for a quantum critical point in the phase diagram where $T_{\text{freezing}} \to 0$, where $T_{\text{freezing}}$ in a spin glass is the temperature below which, for example, $\chi_{\text{FC}}$ begins to differ from $\chi_{\text{ZFC}}$. The samples of $U_2Pd_{1-x}Si_{3+x}$ were annealed for one week at 800 °C, but the difference in annealed and unannealed properties was not investigated. Both $C/T$ and $\chi$ were measured only down to 1.8 K; both were found to follow $T^{-1+\lambda}$ up to 7.5 and 17 K, respectively, with, however, differing $\lambda$ values: $\lambda_C = 0.82$ (0.85) for $x = 0.4$ (0.5), $\lambda_\chi = 0.61$ (0.62) for $x = 0.4$ (0.5).

#### r. $Ce_{0.1}La_{0.9}Pd_2Al_3$ (III)

$CePd_2Al_3$ is a hexagonal antiferromagnet, $T_N = 2.8$ K, occurring in the same structure as $UPd_2Al_3$. Polycrystalline samples of $Ce_{0.1}La_{0.9}Pd_2Al_3$ were prepared and annealed at 900 °C for five days, with no mention of the effect of annealing on the measured properties, and then characterized for non-Fermi-liquid behavior by $\rho$, $\chi$, and $C/T$ measurements (Nishigori *et al.* 1999). Although no statement was given at what composition the La doping suppressed $T_N$, presumably—based on doping results on similar systems—$T_N \to 0$ before the Ce concentration was reduced to 10%. $C/T(\chi) \sim \log T$ between 1.5 and 7 K (1.9 and 7 K), while $\rho \sim \rho_0 - AT^{0.5}$ between 1.7 and 9 K. Nishigori *et al.* pointed out that a hexagonal Ce system could be described by the quadrupolar Kondo model of Cox. As discussed above in the theory section, the multichannel Kondo model, of which the quadrupolar Kondo model is one variation, predicts $C/T$ and $\chi \sim \log T$ for $n = 2$, $S = \frac{1}{2}$ as well as $\rho - \rho_0 \sim AT^{0.5}$. An experimental finding, however, of the $T^{0.5}$ dependence in the resistivity is unusual; measurements to lower temperatures are under way.

#### s. $U_{0.1}M_{0.9}In_3$, M=Y,Pr,La (I)

Cubic $UIn_3$ is an antiferromagnet, $T_N = 95$ K. Hirsch *et al.* (2001) found that, far from where doping on the U site has already driven $T_N \to 0$, there is a maximum in the low-temperature $C/T$ values vs doping at the 10% U concentration for all the dopants tried (Y, Pr, and La). An investigation of the temperature dependence of the specific heat led to the discovery that $C/T \sim \log T$ between 0.07 and 2 K. In addition, the partial substitution of 4-valent Sn for 3-valent In led to an enhancement of the low-temperature $C/T$ values by ~30% (see Table II). Spin-glass behavior (divergence of $\chi_{\text{FC}}$ and $\chi_{\text{ZFC}}$) below ~7 K was observed.

#### t. $CePt_{0.96}Si_{1.04}$ (I?)

Götzfried *et al.* (2001) have recently tuned the heavy-fermion system CePtSi (see also work below in Sec. III.A.2 on $CePtSi_{1-x}Ge_x$) to non-Fermi-liquid behavior by varying the Pt/Si ratio. At $CePt_{0.9}Si_{1.1}$ they see an anomaly in $C/T$ at ~0.3 K that may be due to a spin-glass transition. When the Si content is decreased below this concentration to the $CePt_{0.96}Si_{1.04}$ composition, the

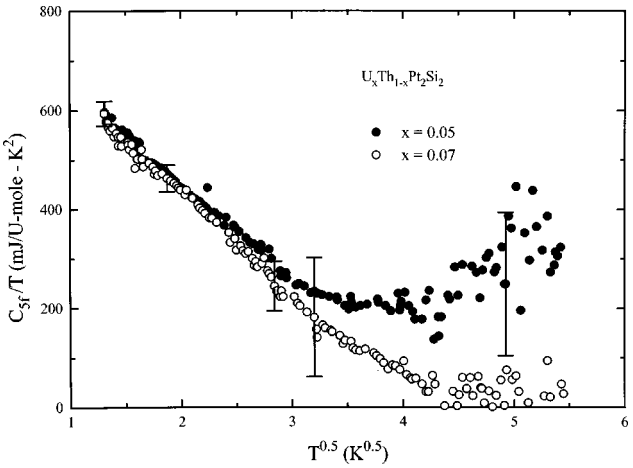


FIG. 15. The $C_{5f}/T$ data for $U_xTh_{1-x}Pt_2Si_2$ from Fig. 14 replotted vs $T^{0.5}$. Note the good agreement between 1.7 and 12 K for $x=0.07$. A slight change in the subtracted lattice-specific heat might increase the temperature range of agreement with $T^{0.5}$, since $C_{\text{measured}} \sim C_{\text{lattice}}$ above 10 K.

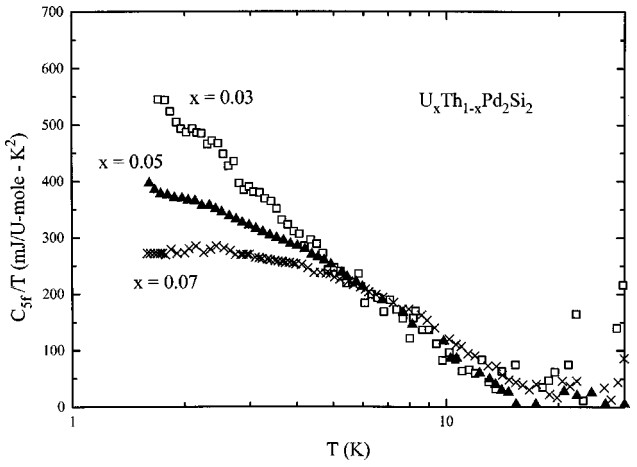


FIG. 16. $C_{5f}/T$ vs $\log T$ for $U_xTh_{1-x}Pd_2Si_2$, after Amitsuka, Shimamoto, *et al.* (1995). Possibly data for $x=0.04$ would obey $C/T$ behavior as $\sim -\log T$ over a larger temperature range than the data shown.

anomaly disappears and $C/T$ is found to obey $-\log T$ between the lowest temperatures of measurement, 0.07 K, and 9 K.

#### 2. $T_N$ just suppressed to 0 or just about to be induced via doping

In the year after the discovery of non-Fermi-liquid behavior in $U_{0.2}Y_{0.8}Pd_3$ work was already going forward on investigating the connection between magnetism and non-Fermi-liquid behavior. Kim *et al.* (1993) presented experiments in which doping-induced suppression of antiferromagnetism in two known heavy-fermion systems ($UNi_2Al_3$ and $UPd_2Al_3$) led to non-Fermi-liquid behavior in $C$, $\chi$, and $\rho$. More thorough doping investigations of $UPd_2Al_3$ were carried out in a number of successive works (Dalichaouch and Maple, 1994; Maple *et al.*, 1994, 1995). Very thorough work (see also the pressure-induced non-Fermi-liquid section below) on doping the heavy-fermion system $CeCu_6$ to the point where antiferromagnetism appears has also been carried out, as has work on $Ce_{1-x}La_xRu_2Si_2$ in which antiferromagnetism begins in the phase diagram as $x \rightarrow 0.08$. For systems near in their phase diagram to the point where doping suppresses $T_N \rightarrow 0$, the most common theoretical model used for understanding the source of the long-range magnetic interactions at low temperatures is that of the quantum critical point.

##### *a. $U_{1-x}M_xNi_2Al_3$*

This compound, together with $UPd_2Al_3$, was discovered to exhibit coexistent antiferromagnetism and superconductivity with specific-heat $\gamma$ values around 100 mJ/mol/K$^2$ (Geibel, Schank, *et al.*, 1991; Geibel, Thies, *et al.*, 1991). For studies on doped $UNi_2Al_5$ Kim *et al.* (1993) report suppression of $T_N=4.6$ K extremely rapidly, with no magnetic anomaly in the specific heat visible down to 0.3 K with 1.5% Th doping. Samples of $U_{0.9}Th_{0.1}Ni_2Al_3$ show non-Fermi-liquid behavior (see Table II), with $C/T \sim -\log T$, $\chi \sim \chi_0 - a\sqrt{T}$, and $\rho \sim \rho_0 + AT$ between 0.7 and 7.6 K, 1.8 and 9.6 K, and 1.2 and 20 K, respectively, with a positive deviation from $C/T \sim -\log T$ below 0.7 K similar to that observed in $U_{0.2}Y_{0.8}Pd_3$. $U_{0.9}Pr_{0.1}Ni_2Al_3$ shows similar behavior with, however, no deviation in $C/T \sim -\log T$ down to the lowest temperature (0.3 K) of measurement and a temperature dependence in the resistivity that is different ($\alpha = 1.34$ vs 1.0) from that seen with Th doping. Unfortunately, arbitrary units were used for the $\rho$ measurements, preventing any comment on the relative disorder using the $\rho_0$ values. Neither 10% Y or La doping results in non-Fermi-liquid behavior.

##### *b. $U_{1-x}M_xPd_2Al_3$*

In contrast to their results on the rapid suppression of $T_N$ with Th doping in $UNi_2Al_3$, Kim *et al.* (1993) found that the suppression of antiferromagnetism with Th doping in $UPd_2Al_3$ ($T_N=14$ K) is much slower, with a broadened anomaly in the specific heat still present at 6.4 K for $U_{0.6}Th_{0.4}Pd_2Al_3$ (see Fig. 19). However, with this anomaly subtracted out, Kim *et al.* found that $C/T \sim T^{-0.4}$ between 1.4 (lowest temperature of measurement) and 8 K, i.e., non-Fermi-liquid behavior was present before the suppression of $T_N \rightarrow 0$. Maple *et al.* 1995) have since studied non-Fermi-liquid behavior in $U_{1-x}Th_xPd_2Al_3$ more completely and found non-Fermi-liquid behavior in $C/T(\sim -\log T)$ and $\chi(\sim \sqrt{T})$ starting also at $x=0.4$ with $\rho=\rho_0 - AT^{-1}$ for $x \geq 0.6$ between $\sim 3$ and 30 K and a levelling off ($\rho \rightarrow$ const) at lower temperatures. (For $x=0.4$ the antiferromagnetism still present—see Fig. 19—causes a peak in $\rho$ vs $T$ and a positive slope below the peak.) In contrast, the same work finds that $\rho=\rho_0+AT$ for $U_{1-x}Y_xPd_2Al_3$, $x \geq 0.6$. For $M=$Th Maple *et al.* report $C/T \sim -\log T$ in their earlier works "already emerging with $x=0.2$" where a definite antiferromagnetic anomaly still exists, and

change their analysis to $C/T \sim T^{-1+\lambda}$, $\lambda_C \approx 0.8$, and $\chi \sim T^{-1+\lambda}$, $\lambda_\chi \approx 0.6$ (deAndrade *et al.*, 1998)—see Table II and Figs. 20 and 21—in relatively good agreement with the recent theory of Castro Neto *et al.* (1998) ($\lambda_C$ should equal $\lambda_\chi$). Liu, MacLaughlin, Lukefahr, *et al.* (2000), using NMR measurements, find no evidence for disorder being the cause of the non-Fermi-liquid behavior in $U_{1-x}Th_xPd_2Al_3$. In the $U_{0.2}Y_{0.8}Pd_2Al_3$ system, Freeman *et al.* (1998) find that $C/T$ can be fit equally well with $\log T$ or $T^{-1+\lambda}$, but that—unlike $M$=Th doping—$\chi$ is fit much better with the earlier-used $\sqrt{T}$ fit and not at all well with $\chi \sim T^{-1+\lambda}$. In $U_{0.4}Y_{0.6}Pd_2Al_3$, Freeman *et al.* find $C/T \sim -\log T$ between 0.5 and 4 K with a slight anomaly at ~1.2 K due to antiferromagnetism.

These results raise a number of questions for understanding non-Fermi-liquid behavior.

(1) According to the theoretical picture of the appearance of a quantum critical point in the phase diagram where $T_N \to 0$, non-Fermi-liquid behavior should not be present before antiferromagnetism is suppressed. However, as Kim *et al.* showed (six years in advance of the model that theoretically predicted such behavior; see Fig. 19), $C/T \sim T^{-1+\lambda}$ in $U_{0.6}Th_{0.4}Pd_2Al_3$. For comparison, Fig. 20 shows the data of Maple *et al.* for $U_{0.8}Th_{0.2}Pd_2Al_3$ and $U_{0.6}Th_{0.4}Pd_2Al_3$ plotted as $C/T$ vs $\log T$, where the anomaly seen by Kim *et al.* for $x=0.4$ is not visible but is within the noise/error bar. (The resistivity data of Maple *et al.* show an anomaly at ~7 K for $x=0.4$ which they associate with antiferromagnetism.) Rather than attempt to further discuss this coexistence of non-Fermi-liquid behavior and remanent antiferromagnetism at this point, we defer this discussion to the next section, where all the known examples of antiferromagnetism and non-Fermi-liquid behavior occurring together, including $UCu_3Al_2$ (already discussed above), will be discussed, *vis à vis* such coexistence.

(2) Another question raised by the data for $U_{1-x}Th_xPd_2Al_3$ is which temperature dependences do the $C/T$ and $\chi$ data obey? The cases for $x=0.4$ and 0.6 are discussed separately.

(i) $U_{0.6}Th_{0.4}Pd_2Al_3$. deAndrade *et al.* (1998) show data for specific heat divided by temperature down to 0.080 K for $U_{0.6}Th_{0.4}Pd_2Al_3$ with both $-\log T$ and $T^{-1+\lambda}$, $\lambda_C = 0.84$, fits (see Fig. 21) and perform an error analysis of the deviation of the data from these two temperature dependences. They conclude that, in the case of $U_{0.6}Th_{0.4}Pd_2Al_3$, the two fits for the specific heat are comparable—i.e., the question remains open until lower-temperature data can resolve this question (note the divergence between the $\log T$ and $T^{-1+\lambda}$ forms in Fig. 21). In contrast to the case of $U_{0.2}Y_{0.8}Pd_3$ discussed above, the fit of deAndrade *et al.* (see Fig. 22) of $\chi$ to $T^{-1+\lambda}$, $\lambda_\chi = 0.63$ for $U_{0.6}Th_{0.4}Pd_2Al_3$ only reproduces the data between 0.5 and 9 K. The Griffiths-phase theory says that this fit should obtain, as for $C/T$, with the same $\lambda$. If we instead fit the susceptibility data for $U_{0.6}Th_{0.4}Pd_2Al_3$ to $\chi^{-1} - \chi_0^{-1} = T^\alpha$, as was done for $U_{1-x}M_xPt_3$ above (see also the discussion in Sec. II.B.3), we find (see Fig. 22) an excellent fit to this form over the whole temperature range up to 50 K with an implied $\lambda$ of $0.38(1-\lambda = \alpha)$, which disagrees even more with the $\lambda_C$ of 0.84 derived from the specific heat in Fig. 21.

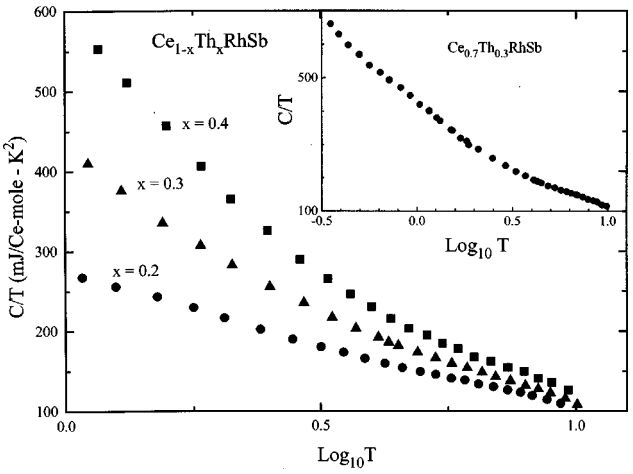


FIG. 17. $C/T$ vs $\log T$ for $Ce_{1-x}Th_xRhSb$, after Andraka (1994b). The inset shows $C/T$ vs $\log T$ down to 0.3 K for $x=0.3$. Note the faster-than-log $T$ divergence as temperature is lowered for the data.

(ii) $U_{0.4}Th_{0.6}Pd_2Al_3$. deAndrade *et al.*, without showing curves, state that $C/T$ and $\chi$ for this composition follow $T^{-1+\lambda}$, with their table listing $\lambda_C = 0.81$ and $\lambda_\chi = 0.63$. Since replotting the $\chi$ data as $(\chi^{-1} - \chi_0^{-1})$ vs $T^\alpha$ for $U_{0.6}Th_{0.4}Pd_2Al_3$ (see Fig. 22) gave such good agreement—much better than that between the data and the $T^{-1+\lambda}$ functional form—the $\chi$ data for $U_{0.4}Th_{0.6}Pd_2Al_3$ (Maple *et al.*, 1995) were also replotted (not shown) and gave the same good agreement between the data and the functional form $(\chi^{-1} - \chi_0^{-1}) \sim T^\alpha$ over the whole temperature range of measurement (see Table II). The $\lambda_\chi$ (from $1-\lambda=\alpha$) of 0.34 was in

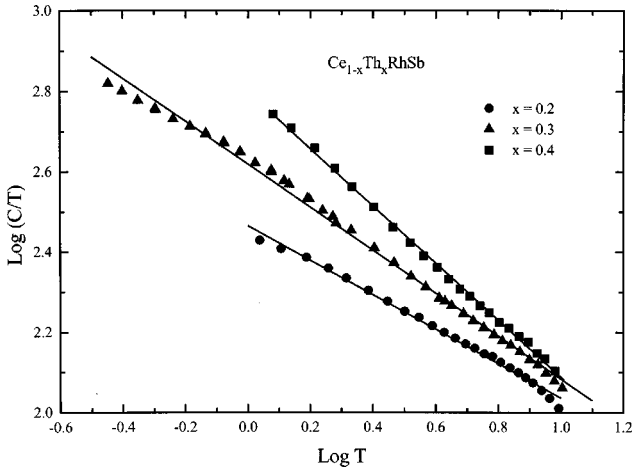


FIG. 18. The $C/T$ data for $Ce_{1-x}Th_xRhSb$ from Fig. 17 (Andraka, 1994b) replotted here as $\log C/T$ vs $\log T$ to look for power-law, $T^{-1+\lambda}$, behavior in $C/T$. Despite some waviness in the data, the agreement of $C/T$ with $T^{-1+\lambda}$, where the best fit gives $\lambda \sim 0.47$, for $x=0.3$ over an extended range suggests further work to lower temperatures on $C$ (to refine the exponent), as well as $\chi$, to check for agreement with a power-law dependence.

good agreement with that found above for $U_{0.6}Th_{0.4}Pd_2Al_3$.

### c. $CeCu_{6-x}M_x$, M=Au, Pd, Pt, Ag

Gangopadhyay *et al.* (1987, 1988) discovered, using specific heat and dc susceptibility, that $CeCu_6$ becomes antiferromagnetic with $x=0.3$ for $M=$Ag. Antiferromagnetism with $x=0.2$–$0.8$ for $M=$Au (isoelectronic to Ag) was discovered (Germann *et al.*, 1988) and specific heat under pressure on $CeCu_{5.5}Au_{0.5}$ showed the suppression of $T_N$ from 1.15 K ($P=0$) to 0.63 K at 9.4 kbar (Germann and von Löhneysen, 1989; see the pressure-induced non-Fermi-liquid section below for later work on $x=0.2$ and 0.3, $M=$Au where pressure suppresses $T_N\rightarrow 0$). Following the discovery of non-Fermi-liquid behavior where doping suppresses $T_N\rightarrow 0$ in $UNi_2Al_3$ and $UPd_2Al_3$ discussed above, work also found non-Fermi-liquid behavior at the (varying with $M$) composition of $CeCu_{6-x}M_x$ where $T_N\approx 0$ (see Table II) for $M=$Au, $x=0.1$ (von Löhneysen *et al.*, 1994), Pd ($x=0.05$), and Pt ($x=0.1$) (Sieck *et al.*, 1996), and Ag ($x=0.2$) (Heuser *et al.*, 1998a; see the field-induced non-Fermi-liquid section below for later work on $CeCu_{6-x}Ag_x$ in which field suppresses $T_N\rightarrow 0$). All the compounds $CeCu_{6-x}M_x$ at the $x$ where $T_N\approx 0$ show non-Fermi-liquid behavior in the specific heat over an extremely broad temperature range compared to most other non-Fermi-liquid systems (see Table II) and down to the lowest temperature of measurement with the exception of $M=$Pd, which shows a slight positive deviation of $C/T$ above the log $T$ behavior below 0.2 K. This broad temperature range and lack of low-temperature deviation from $C/T\sim -\log T$ for $M=$Au, Pt, and Ag is inconsistent with the crossover behavior predicted by the Moriya theory. The universality of the $C/T$ behavior shown by $CeCu_{5.9}Au_{0.1}$, $CeCu_{5.95}Pd_{0.05}$, and $CeCu_{5.9}Pt_{0.1}$ (von Löhneysen *et al.*, 1997)—all non-Fermi-liquid systems in which $T_N\rightarrow 0$ with doping—is not exhibited in $CeCu_{5.8}Ag_{0.2}$, which shows a larger (negative) slope of $C/T$ plotted vs log$T$ and a larger specific heat over the whole region 0.06–3 K (Heuser, 1999). The work on single-crystal resistivity shows non-Fermi-liquid behavior in all current directions, but with differing $\rho_0$ values and differing—and quite large—$A$ values. Variation of the temperature dependence of $\chi$ with field direction appears not to have been treated in any publication, although it is known that the magnitude of $\chi$ is strongly anisotropic in single crystals of $CeCu_{6-x}Ag_x$, e.g., $\chi_a:\chi_b:\chi_c=2.8:2:8.2$ for $x=0.3$ (Stockert *et al.*, 1997; Heuser, 1999).

Studies of $CeCu_{5.9}Au_{0.1}$ at the border of antiferromagnetism make it one of the best characterized systems for trying to understand non-Fermi-liquid behavior. Schroeder *et al.* (1998), using inelastic neutron scattering, find (a) an energy scale for the measured magnetic excitations that is not fixed, but rather scales with the temperature; (b) disagreement of their data with the Millis-Hertz theory, suggesting a local deviation from Fermi-liquid behavior; and (c) agreement between their magnetic scattering data—over apparently the whole Fermi surface—and bulk, $q=0$, susceptibility data (von Löhneysen *et al.*, 1996); if a constant term is subtracted then $\chi^{-1}-\chi_0^{-1}\sim T^{0.8}$. This is strong experimental evidence for a local deviation from Fermi-liquid behavior, as discussed theoretically by Coleman (1999) and Si *et al.* (1999).

Stockert *et al.* (1998) find rodlike features in their inelastic neutron cross-section measurements in reciprocal space, arguing for two-dimensional (see, however, Sec. III.D.1.d) fluctuations in real space, which then makes the measured log-$T$ dependence of the specific heat and the linear in $T$ resistivity (see Table II) consistent with the Millis-Hertz theory predictions shown in Table I(a) for antiferromagnetic spin fluctuations, $z=d=2$. [See also the work by Rosch *et al.* (1997), which discusses the possibility of two-dimensional ferromagnetic fluctuations in $Ce(Cu_{0.983}Au_{0.017})_6$.] Bernal *et al.* (1996) argue from their $\mu$SR measurements, which determine the distribution of the local magnetic susceptibility, that the Kondo disorder model is not appropriate for $Ce(Cu_{0.983}Au_{0.017})_6$. For a recent overview of work on $Ce(Cu_{1-x}Au_x)_6$, see von Löhneysen (1999).

### d. $Ce_{1-x}La_xRu_2Si_2$

Antiferromagnetism is induced in the nearly magnetic $CeRu_2Si_2$ by doping with La at $x=0.08$. At this critical concentration, the specific heat (measured between 1 and 8 K) can be fit to the interacting spin-fluctuation theory of Moriya (with three adjustable parameters) for $x=0.075$ in the limited temperature range from 1 to 5.5 K (Kambe *et al.*, 1996). As discussed for the self-consistent renormalization theory of Moriya and coworkers above in the theory section, the parameter $y_0$ is a measure of how close a system is to a quantum critical point, with $y_0\rightarrow 0$ at the magnetic instability. Kambe *et al.* report $y_0=0.10$ for $x=0.05$ and $y_0=0.05$ for $x=0.075$. $\rho$ data for $x=0.05$ are said to follow the self-consistent renormalization theory between 0.2 and 1.5 K, with scatter in the $\rho$ data below 0.2 K. However, an inspection of the graph in Kambe *et al.* gives an apparent temperature dependence of $\rho=\rho_0+AT^2$ for $x=0.05$, which is Fermi-liquid behavior and inconsistent with the self-consistent renormalization theory.

### e. $YbCu_{3.5}Al_{1.5}$

Antiferromagnetism is found in $YbCu_{5-x}Al_x$ for $x=1.6$–$2.0$. At $x_{crit}=1.5$, $C/T$ is $\sim -\log T$ between 0.2 and 1.2 K, but clearly follows the temperature dependence of the self-consistent renormalization theory over the whole temperature range of measurement, 0.1–3 K (Seuring *et al.*, 2001). The resultant $y_0$ fit parameter (which should be zero at a quantum critical point) is 0.05, indicating that the $x=1.5$ sample is not exactly the optimal concentration. The specific-heat data in field scale onto one universal curve for $T>0.24$ K with $\beta=1.5$ (i.e., indicating that collective excitations are responsible for the non-Fermi-liquid behavior), but scaling fails in the low-temperature, $C/T=\gamma_0-aT^{0.5}$ regime.

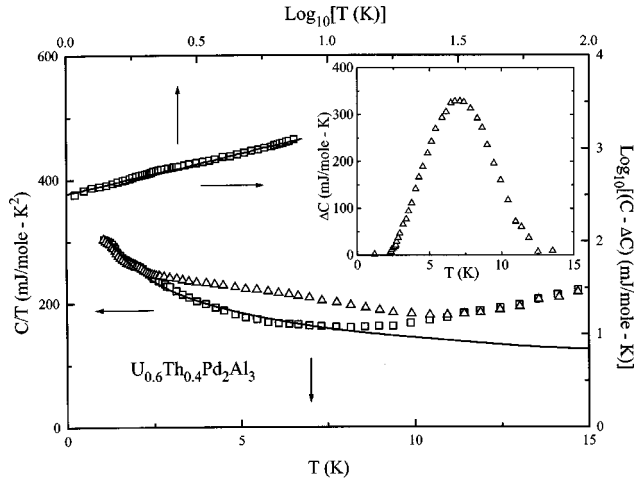


FIG. 19. $C/T$ vs $T$ for $U_{0.6}Th_{0.4}Pd_2Al_3$, after Kim *et al.* (1993): △, data as measured (in the main figure). Using fitted extrapolations of the data above 11 K and below 2 K, the magnetic anomaly $\Delta C$ centered at ~7 K is subtracted from the data, leaving the adjusted data $(C-\Delta C)$ denoted by the squares. As discussed in the text, these data with the magnetic anomaly (shown separately in the inset) subtracted obey $C/T \sim T^{-1+\lambda}$, as shown by the plot in the upper left part of the figure of $\log(C-\Delta C)$ vs $\log T$.

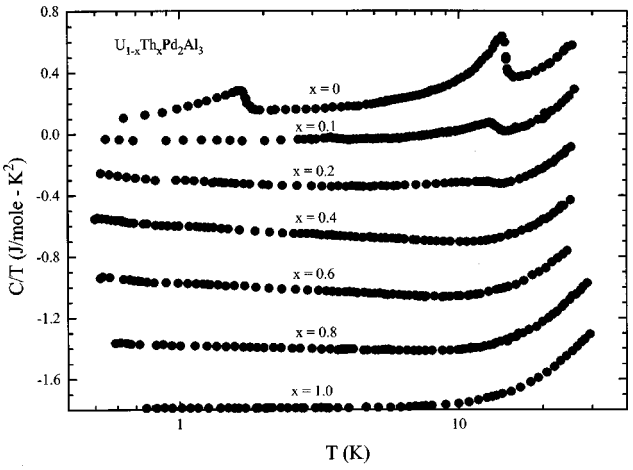


FIG. 20. $C/T$ vs $\log T$ for $U_{1-x}Th_xPd_2Al_3$, after Maple *et al.* (1995). The antiferromagnetic transition at 14 K is clearly visible in the data for $x=0$; this anomaly is suppressed with increasing Th doping. The anomaly seen for $x=0.4$ at $T\sim 7$ K in Fig. 19 is not resolved within the scatter for the $x=0.4$ data shown here. The plot shown here was used in the work of Maple *et al.* (1995) to show $C/T \sim -\log T$ behavior for these samples for $0.4 \leqslant x \leqslant 0.8$.

This was interpreted as perhaps indicating that this is a weak-coupling behavior. (See also the discussion in Sec. III.D below for field-induced non-Fermi-liquid behavior in $CeCu_{5.2}Ag_{0.8}$.) Consistent with the agreement of the specific heat with the self-consistent renormalization theory, $\rho=\rho_0+AT^{1.3}$ between 0.03 and 0.25 K, with linear, temperature behavior above 0.25 K up to 0.6 K.

### *f. $Ce(Ru_{1-x}Rh_x)_2Si_2$*

The tetragonal antiferromagnet $CeRh_2Si_2$, $T_N=35$ K, has its antiferromagnetism suppressed with Ru doping on the Rh site, with $x_c\sim 0.53$, i.e., still slightly Rh rich. Graf *et al.* (1997) reported non-Fermi-liquid behavior in $Ce(Ru_{0.5}Rh_{0.5})_2Si_2$ in $C/T$ and $\chi$, which they fit to the phenomenological Kondo disorder model of Bernal *et al.* (1995). Liu, MacLaughlin, Castro Neto, *et al.* (2000), with measurements of the bulk $\chi$ and NMR linewidth, also find evidence for disorder in $Ce(Ru_{0.5}Rh_{0.5})_2Si_2$. $\chi$ varies approximately as $\log T$ between 2 and 30 K, while $C/T$ shows saturation (Fermi-liquid behavior) to a constant value below about 0.5 K; Graf *et al.* also report Fermi-liquid behavior in $\rho$ (i.e., $\rho=\rho_0+AT^2$) between 0.04 and 0.2 K. Taniguchi *et al.* (1998) investigated the more Ru-rich part of the phase diagram and found what they described as a spin-density-wave transition at 2 K in $Ce(Ru_{0.7}Rh_{0.3})_2Si_2$, with $C/T \sim -\log T$ from 2 to 10 K (i.e., non-Fermi-liquid behavior in the presence of long-range magnetic order; see the following section). For $Ce(Ru_{0.6}Rh_{0.4})_2Si_2$, Taniguchi *et al.* report $C/T \sim -\log T$ between their lowest temperature of measurement, 0.15 K, and 10 K—a very broad temperature range. Their result for $\chi$ for $Ce(Ru_{0.6}Rh_{0.4})_2Si_2$ is reminiscent of the result of Graf *et al.* for $Ce(Rh_{0.5}Ru_{0.5})_2Si_2$, with $\chi$ behaving approximately as $\log T$ between 5 and 50 K, with a bendover below 5 K. As has been done for a number of systems in this review, in order to check whether the $\chi$ data for both $Ce(Ru_{0.5}Rh_{0.5})_2Si_2$ and $Ce(Ru_{0.6}Rh_{0.4})_2Si_2$ would obey a pure power-law dependence down to the lowest temperature of measurement if plotted as $1/\chi-1/\chi_0$, we have scanned and replotted the two sets of data. The

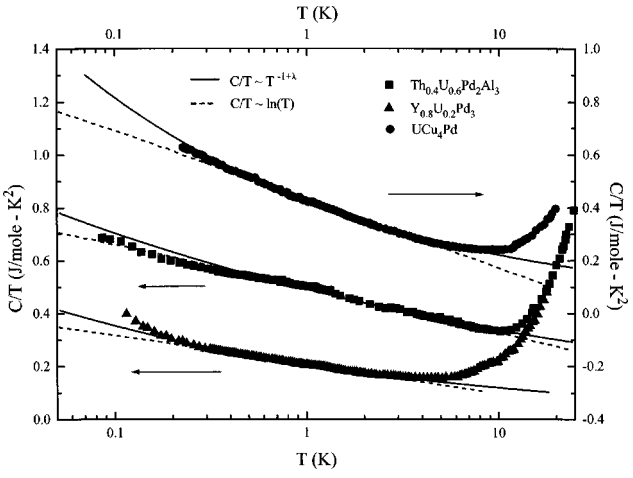


FIG. 21. $C/T$ vs $\log T$ for $Th_{0.4}U_{0.6}Pd_2Al_3$, $Y_{0.8}U_{0.2}Pd_3$, and $UCu_4Pd$, after deAndrade *et al.* (1998): dashed lines, $C/T \sim -\log T$; solid lines, fits of the data to $C/T \sim T^{-1+\lambda}$. The data shown down to 0.08 K for $Th_{0.4}U_{0.6}Pd_2Al_3$ agree slightly better with the $\log T$ dependence at lowest temperatures, while the power-law dependence slightly better fits the data shown in this figure for $Y_{0.8}U_{0.2}Pd_3$ and $UCu_4Pd$. As discussed earlier in the text for $UCu_4Pd$, data to lower temperatures on an annealed sample (Weber *et al.*, 2001) of $UCu_4Pd$ show $\log T$ behavior down to 0.07 K.

result (see Table II) is that both systems show good agreement with this functional form, $\chi^{-1}-\chi_0^{-1}=aT^{\alpha}$, with $\alpha=0.63$ for $Ce(Ru_{0.5}Rh_{0.5})_2Si_2$ (which from the specific-heat and resistivity data is away from the composition for the quantum critical point) and $\alpha=1.00$ for $Ce(Ru_{0.6}Rh_{0.4})_2Si_2$. Thus, for the latter system, in which the specific heat obeys $C/T\sim-\log T$ down to the lowest temperature of measurement (i.e., appears to be at a quantum critical point), the susceptibility data follow fairly well the Curie-Weiss law [$\chi=C/(T+\Theta)$, $\Theta<0$] for local antiferromagnetically coupled moments down to the lowest temperature and up to 100 K. Nakano *et al.* (2000) report $\rho=\rho_0+AT^{1.4}$ for $Ce(Ru_{0.65}Rh_{0.35})_2Si_2$ (according to Nakano *et al.*, this sample displays no spin-density-wave transition) between approximately 0.3 and 3 K, with $\rho$ linear in temperature above 3 K and up to 8 K. Also for this $x=0.35$ sample, they find $\chi\sim T^{0.5}$ between 1.8 and 20 K. For $Ce(Ru_{0.6}Rh_{0.4})_2Si_2$, Nakano *et al.* quote, but do not show data for, the result that $\rho=\rho_0+AT^{1.5}$ at low temperatures.

### g. $CePtSi_{0.9}Ge_{0.1}$

Horn *et al.* (1992) discovered that doping the orthorhombic heavy-fermion system CePtSi with Ge induced antiferromagnetism for $x\geqslant 0.2$. Steglich *et al.* (1994) reported $C/T\sim-\log T$ in $CePtSi_{0.9}Ge_{0.1}$ between 0.8 and 5 K, with a bendover in $C/T$ below 0.8 K down to their lowest temperature of measurement, 0.4 K. Whether $C/T$ trends towards $\gamma_0-A\sqrt{T}$ or towards Fermi liquid, $C/T\rightarrow$const below 0.8 K in $CePtSi_{0.9}Ge_{0.1}$ awaits further measurements at lower temperatures. Scaling of the specific heat and magnetization with magnetic field as discussed above in the theory section (Kolb, 1994) leads to a scaling exponent $\beta=0.8$, i.e., either single-ion or correlated behavior may be responsible for the non-Fermi-liquid properties. Resistivity data on $CePtSi_{0.85}Ge_{0.15}$ show (Weilnhammer, 1997) Fermi-liquid behavior ($\rho\sim T^2$) between 0.07 and 0.5 K, with $\rho=\rho_0+AT$ between 0.5 and 1.8 K, followed by $\rho=\rho_0+AT^{\alpha}$, $\alpha<1$ for higher temperatures due to a shoulder in $\rho$ starting at 6.7 K. Absolute values for $\rho$ were unphysically high ($\rho_0\sim 3100\,\mu\Omega$ cm), possibly due to microcracks. Microscopic resonance measurements are under way to try to determine the role of disorder in this system.

### h. $UCu_{5.6}Al_{6.4}$

Tetragonal $UCu_4Al_8$ is antiferromagnetic, $T_N=40$ K, and changing the Cu/Al ratio has been found to suppress $T_N\rightarrow 0$ at the $UCu_{5.6}Al_{6.4}$ composition (Steglich *et al.*, 1994). Steglich *et al.* (1994) found that $C/T\sim-\log T$ between 0.4 and 4 K in $UCu_{5.6}Al_{6.4}$.

### i. $CePd_{1.6}Ni_{0.4}Al_3$

As stated in the discussion on $Ce_{0.1}La_{0.9}Pd_2Al_3$ in Sec. III.A.1.r, $CePd_2Al_3$ is an antiferromagnet with $T_N=2.8$ K. Galatanu *et al.* (2000) report that, close to where Ni doping suppresses $T_N\rightarrow 0$, $C/T$ obeys $\sim-\log T$ from 1.5 to 6 K for $CePd_{1.6}Ni_{0.4}Al_3$ while $\rho=\rho_0+AT$ between 0.8 and 5 K for $CePd_{1.5}Ni_{0.5}Al_3$,

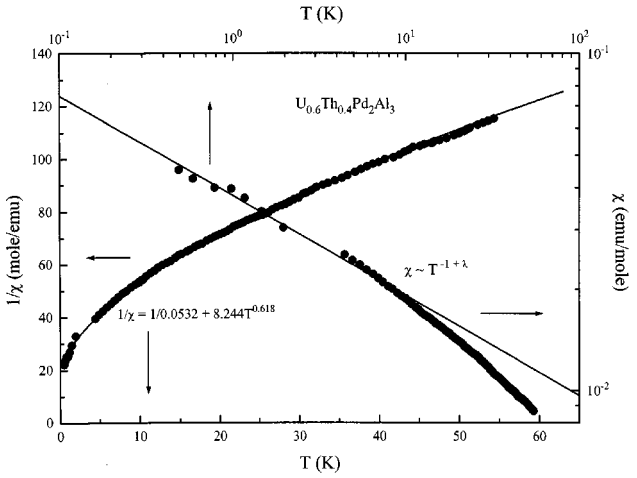


FIG. 22. log$\chi$ vs log $T$ of $U_{0.6}Th_{0.4}Pd_2Al_3$ (upper and right-hand axes), after deAndrade *et al.* (1998), showing a limited temperature range where $\chi\sim T^{-1+\lambda}$. If these data are replotted, it is found that $\chi^{-1}$ is fit by a constant term plus $aT^{\alpha}$ over a very large temperature range, as shown here with the same data plotted as $1/\chi$ vs $T$ (left-hand and lower axes).

where 1.5 and 0.8 K were, respectively, the lowest temperatures of measurement. (The specific heat was not reported for the $Ni_{0.5}$ composition, nor was the resistivity reported for the $Ni_{0.4}$ composition.) Samples were annealed at 900 °C for two weeks, but the effect of annealing was not discussed.

### j. $CeCoGe_{3-x}Si_x$

Tetragonal $CeCoGe_3$ is an antiferromagnet, $T_N=21$ K. Upon exchanging Si for Ge, Eom *et al.* (2000) discovered that $T_N\rightarrow 0$ for $x>1.25$. At $x=1.5$ [reported by Krishnamurthy *et al.* (2000) to display no magnetic order via $\mu$SR measurements down to 0.034 K], Eom *et al.* report $C/T\sim-\log T$ between 0.3 and 2 K, with a downturn in $C/T$ below 0.3 K, and $\rho=\rho_0+AT$ between 0.03 and 6 K. Krishnamurthy *et al.* report that the spin-lattice relaxation rate in their $\mu$SR measurements behaves as $-\log T$ between 0.03 and 1.5 K, which was predicted by Continentino (1994) for a quantum critical point.

### k. $CeCo_{1.2}Cu_{0.8}Ge_2$

$CeCu_2Ge_2$ (see also the pressure-induced section below) is an antiferromagnet with $T_N=4.15$ K. Maeda *et al.* (1999) reported that doping with Co on the Cu sites suppressed the antiferromagnetism in $Ce(Co_{1-x}Cu_x)_2Ge_2$ at $x_c\sim 0.4$, or at a replacement of 60% of the Cu by Co. They find $C/T\sim-\log T$ between 0.35 and 7 K, with increasing divergence in $C/T$ at lower temperatures—similar to that seen in $U_{0.2}Y_{0.8}Pd_3$ and other systems discussed in this review. The resistivity of $CeCo_{1.2}Cu_{0.8}Ge_2$ is not analyzed for a particular temperature dependence, but is stated to be still increasing with decreasing temperature down to 0.5 K. Scanning and analyzing of these $\rho$ data reveals that $\rho=\rho_0-aT^{0.6}$

between 0.5 and 15 K, or close to the $T^{0.5}$ temperature dependence predicted by the multichannel Kondo model.

#### *l. $U(Pt_{0.993}Pd_{0.007})_3$ (III)*

Graf *et al.* (2000) have measured the resistivity of hexagonal $U(Pt_{1-x}Pd_x)_3$ as the Pd concentration is increased towards where the system becomes antiferromagnetic at $x_c \sim 0.007$. They find that in the whole region between pure $UPt_3$ and $U(Pt_{1-x}Pd_x)_3$, $x = x_c$, the exponent $\alpha$ in $\rho = \rho_0 + A T^{\alpha}$ monotonically decreases with increasing $x$, but is always (even for pure $UPt_3$) below $\alpha = 2$, i.e., they find non-Fermi-liquid behavior in the whole regime up to $x_c$. At $x_c$ they find $\alpha \approx 1.6$, consistent with three-dimensional ferromagnetic fluctuations (see also deVisser *et al.*, 2000), as shown in Table I in the theory section.

### 3. Non-Fermi-liquid behavior coexistent with long-range magnetic order

As discussed above, $UCu_3Al_2$ (Nakotte *et al.*, 1996), $U_{0.6}Th_{0.4}Pd_2Al_3$ (Kim *et al.*, 1993; Maple *et al.*, 1995), $U_{0.4}Y_{0.6}Pd_2Al_3$ (Freeman *et al.*, 1998), and $Ce(Ru_{0.7}Rh_{0.3})_2Si_2$ (Taniguchi *et al.*, 1998) show magnetic anomalies in specific heat, susceptibility, and resistivity while at the same time displaying clear non-Fermi-liquid behavior in the specific heat ($C/T \sim \log T$ or $T^{-1+\lambda}$). Single-crystal $UCu_3Al_2$ may "show traces" of non-Fermi-liquid behavior (Nakotte *et al.*, 1996) in $\chi$, while the temperature dependence of $\rho$ in $U_{0.6}Th_{0.4}Pd_2Al_3$ is obscured by the peak at ~7 K due to the antiferromagnetism. Another system, discussed in the next paragraph, has also been investigated which shows evidence of long-range magnetic order coexistent with non-Fermi-liquid behavior in $C/T$, i.e., $C/T \sim \log T$. Such systems do not fit the picture of the quantum critical point (Fig. 2 above), in which one expects antiferromagnetic ordering to the left of the quantum critical point in phase space and below in temperature a region where non-Fermi-liquid behavior occurs. The systems mentioned above and the system discussed in this section all show magnetic behavior in the middle or even above the temperature range where $C/T \sim \log T$.

As early as 1986 it was noticed (Stewart *et al.*, 1986) that $U(Pt_{0.94}Pd_{0.06})_3$ doped with either Pd on the Pt site or with Th on the U site, showed an anomalous upturn in $C/T$ below the antiferromagnetic transition at 5.6 K induced by the doping. This upturn at the time was analyzed as obeying $\Delta C/T$ (where $\Delta C$ is the measured specific heat corrected for the magnetic contribution below $T_N$) $\sim T^{-0.75}$ over a limited (0.6–1.2 K) temperature range. Upon reexamination and remeasurement in light of the discoveries of non-Fermi-liquid behavior in $U_{0.2}Y_{0.8}Pd_3$, Kim *et al.* (1992) found that $\Delta C/T$ in $U(Pt_{0.94}Pd_{0.06})_3$ behaved as $\log T$ between 0.3 and 4.3 K (i.e., over more than a decade of temperature) as shown in Fig. 23. Due to the antiferromagnetic transition, which is contiguous in temperature, strong masking effects in the temperature dependences of $\chi$ and $\rho$ hamper attempts to investigate these quantities for non-Fermi-liquid behavior. Further doping ($Pd_{0.1}$) suppresses $T_N$ (Stewart *et al.*, 1986), allowing $\rho$ and $\chi$ to be checked; $C/T$ remains proportional to $\log T$, although less divergent ($T_0$ is larger by a factor of 4) while $\rho$ is only slightly temperature dependent and $\chi \sim \sqrt{T}$ from 1.8 to 4 K. In a quantum critical point scenario, the long-range interactions at low temperatures responsible for the non-Fermi-liquid behavior in $U(Pt_{0.94}Pd_{0.06})_3$ clearly do not come from the dynamic antiferromagnetism at 5 K studied by Aeppli *et al.* (1988)—which is stabilized at ~6 K by either Pd or Th doping rather than suppressed to $T \to 0$. Instead, the interactions may stem from the antiferromagnetic correlations at 18 K in pure $UPt_3$—just as was speculated for $U_{0.7}Zr_{0.3}Pt_3$ above—since the peak in $\chi$ at 18 K in pure $UPt_3$ is suppressed to lower temperatures by Pd doping (deVisser, 1986).

### 4. Ferromagnetic $T_c$ just suppressed to 0 or just about to be induced via doping

#### *a. $U_xTh_{1-x}Cu_2Si_2$*

Unusually among non-Fermi-liquid systems found to date, $U_xTh_{1-x}Cu_2Si_2$ shows (Lenkewitz *et al.*, 1997) non-Fermi-liquid behavior near a ferromagnetic instability. $UCu_2Si_2$ is ferromagnetic at 101 K, and doping with Th still leaves $T_{\text{Curie}} = 12$ K at $x = 0.15$. Non-Fermi-liquid behavior occurs in the whole composition range, however, beyond where ferromagnetism is suppressed: $C/T$ behaves as $\sim -\log T$, $\chi \sim T^{-1+\lambda}$, and $\rho = \rho_0 + A T^{\sim 1}$ for $x = 0.03$, 0.07, and 0.10 (see Table II), where $C/T$ deviates above a $\log T$ behavior below 1 K for $x = 0.03$. Scaling with magnetic-field experiments of both the magnetization and the specific heat results in a scaling exponent $\beta$ of 1.6, implying that the electron interactions responsible for the non-Fermi-liquid behavior are not single ion in nature.

#### *b. $Ni_xPd_{1-x}$*

Recently, in the continuing search for new non-Fermi-liquid systems, Nicklas *et al.* (1999)—based on the thorough study in the literature of the critical concentration of Ni in Pd for the onset of ferromagnetism (see, for example, Murani, Tari, and Coles, 1974)—performed low-temperature measurements of $\rho$, $\chi$, and $C$ in $Ni_xPd_{1-x}$ alloys. Although several dopant choices were available, they chose Ni in Pd as being metallurgically the best behaved (homogeneous) as well as requiring the least amount of doping (and therefore induced disorder) to reach the ferromagnetic quantum critical point. According to the early work on PdNi (Murani, Tari, and Coles, 1974; Kato and Mathon, 1976), some clustering of Ni at concentrations near the critical concentration for ferromagnetism is metallurgically unavoidable. Using the theory of Lonzarich (see the theory section above) for the temperature dependences of $C/T (\sim \log T)$, $\chi (\sim \chi_0 - a T^{3/4})$, and $\rho (\sim T^{5/3})$ as well as for the behavior of $T_c$ with dopant concentration $[\sim (x - x_c)^{3/4}]$ to analyze their data, Nicklas *et al.* found good agreement between theory and experiment for

$C/T$ (down to 0.4 K, with a positive deviation above $\log T$ beginning to appear for lower temperature) and $\rho$ (down to the lowest temperature of measurement 0.05 K) near the critical doping concentration, $x_c$, of $\approx 0.026$. However, they found Fermi-liquid behavior in the resistivity ($\rho = \rho_0 + AT^2$) at $x = 0.01$, arguing for a quantum critical point scenario. Recently, however, the specific heat at $x = 0.026$ has been measured to lower temperatures, down to 0.09 K, and it has been found (Nicklas, 2000; Scheidt, 2000), contrary to the original statement of a positive deviation above $C/T \sim -\log T$ behavior below 0.4 K, that $C/T$ starts to saturate below 0.7 K and is essentially constant below 0.4 K—arguing that $x_c \neq 0.026$ and that the quantum critical point, if present, lies elsewhere in the phase diagram.

The magnetic susceptibility was measured down to only 1.8 K and showed a tendency towards saturation below 5.5 K, with $\chi \sim T^{3/4}$ then up to ~20 K. As discussed above in the theory section (see Coleman, 1999 and Si *et al.*, 1999) and as found in a number of systems already discussed, including $UCu_{3.5}Pd_{1.5}$, $U_{1-x}M_xPt_3$, and $CeCu_{6-x}(Au, Ag)_x$ (see Table II), if there is a fundamental local deviation from Fermi-liquid behavior, then the susceptibility follows $\chi^{-1} - \chi_0^{-1} \sim T^{\alpha}$, $\alpha \neq 1$. When we replot the $\chi$ data of Nicklas *et al.* (Fig. 24), such a local deviation form fits the data for $x = 0.026$ over the whole temperature range of 1.8–20 K, with $\alpha \sim 1.8$, significantly better than the fit of $\chi \sim T^{3/4}$, the theoretical prediction, to the data. Even in the region where the $T^{3/4}$ dependence fits best, there is a slight waviness in the data that does not follow $T^{3/4}$.

#### c. $CePd_{0.05}Ni_{0.95}$

CePd is a ferromagnet, with $T_c = 6.5$ K. Substituting Ni on the Pd site suppresses $T_c \rightarrow 0$ for 95% Ni substitution. $C/T \sim -\log T$ for $CePd_{0.05}Ni_{0.95}$ between 0.9 and 4 K, while $C/T$ becomes less divergent down to 0.5 K (Kappler *et al.*, 1997). Although Kappler *et al.* claim that these lowest-temperature data fit $\gamma_0 - AT^{0.5}$, data to lower temperatures are required to distinguish between this behavior and simple saturation to Fermi-liquid behavior. $\rho = \rho_0 + AT^{1.1}$ between 3 and 30 K, tending towards $T^{1.3}$ for temperatures between 0.1 and 3 K.

#### d. $URh_{1/3}Ni_{2/3}Al$ (I)

In the same hexagonal structure, URhAl is a ferromagnet ($T_c = 27$ K) and UNiAl is an antiferromagnet ($T_N = 19$ K). At the composition $URh_{1/3}Ni_{2/3}Al$, Prokes *et al.* (2000) discovered a suppression of both kinds of magnetic order and non-Fermi-liquid behavior: $C/T$ behaves as $\sim -\log T$ between 0.5 and 5 K (Prokes *et al.* note that $C/T \sim T^{-1+\lambda}$, $\lambda = 0.94$, fits the data equally well) and $\rho = \rho_0 - AT^{0.96}$ between 0.3 and 7 K, with a superconducting anomaly in $\rho$ at 0.3 K thought to be due to a second phase. The magnetic susceptibility shows spin-glass behavior, with $\chi_{FC}$ diverging from $\chi_{ZFC}$ at 9 K. This system could also be assigned to Sec. III.A.2 above, where $T_N$ was suppressed to 0. Although the sample was annealed at 700 °C for one week, no study of the dependence of the non-Fermi-liquid properties on annealing was undertaken.

### B. Undoped systems at (or close to) a quantum critical point

Only a few systems have been found in which non-Fermi-liquid behavior appears to occur naturally at the quantum critical point without need of doping, pressure, or field. Such an occurrence should of course be statistically very unlikely. Indeed, some (or all) of these systems may in fact, upon measurement to lower temperatures, display either

(a) Fermi-liquid behavior as has been seen in some samples of $CeNi_2Ge_2$, or
(b) magnetic anomalies, as occurred, for example, in $YbRh_2Si_2$ with the discovery of antiferromagnetism at 0.065 K (Trovarelli, Geibel, Mederle, *et al.*, 2000) after an initial discovery paper with $C$ data only down to 0.4 K proposed $YbRh_2Si_2$ to be an undoped system with non-Fermi-liquid behavior at the quantum critical point (Trovarelli, Geibel, Langhammer, *et al.*, 2000).

As discussed for Fig. 2 and the Millis phase diagram, a low-lying antiferromagnetic anomaly can induce non-Fermi-liquid behavior over a broad temperature range. Rather than focusing on what lower-temperature data might reveal, we consider here the current systems that display non-Fermi-liquid behavior with no doping and $P = B = 0$ down to the lowest temperatures of measurement, with the caveat that a number of them may not be exactly at the quantum critical point in the phase diagram and display non-Fermi-liquid behavior due to low-lying, as yet unobserved, antiferromagnetic ordering. $YbRh_2Si_2$ and $U_2Co_2Sn$, which are known to be near rather than at a quantum critical point are included in this section as being best compared to this class of systems.

*A priori*, one would expect an undoped system to display a small, negligible amount of disorder—thus favoring either the quantum critical point or the multichannel Kondo models as theoretical explanations. Where magnetization as a function of field has been reported for these $x = P = B = 0$ non-Fermi-liquid systems, the data have indeed been approximately linear to the highest field of measurement, at least arguing against a distribution of the Kondo temperature disorder model. However, the disorder theory of Rosch for the resistivity—with its wide range of possible exponents for the temperature dependence of $\rho$ depending on the amount of disorder—has been invoked a number of times to explain $\rho$ data of such undoped systems. Since all the "natural" non-Fermi-liquid systems discovered to date are ternaries, some site-switching disorder cannot be ruled out, and indeed strong sample dependences of the residual resistivity $\rho_0$ (proportional to disorder) have been reported.

### 1. $U_2Pt_2In$ (II)

$U_2Pt_2In$, which occurs in the $U_3Si_2$ tetragonal structure with a nearest U-U separation of 3.72 Å (Nakotte, 1994), was reported by Havela *et al.* (1994) to have a pronounced upturn in $C/T$ at low temperatures, with a $\gamma = 415$ mJ/mol U K$^2$. Strydom and Du Plessis (1996) discovered that $\rho$ for $U_2Pt_2In$ was linear in temperature between 1.5 and 10 K (see Table II), which caused them to replot the polycrystalline $C$ data of Havela *et al.* to look for non-Fermi-liquid behavior in those data as well. The data were found to follow $C/T \sim -\log T$ between 1.2 and 5.5 K—thus giving a strong indication that $U_2Pt_2In$ was an undoped non-Fermi-liquid compound.

Estrela *et al.* (1998) measured $\rho$ and $\chi$, and then studied $C$ (Estrela *et al.*, 1999), on a single crystal (see Table II) of $U_2Pt_2In$, where the single crystal was found to form in the $Zr_3Al_2$ structure (with $d_{U\text{-}U} = 3.58$ Å)—a doubling of the $U_3Si_2$ structure in which polycrystalline samples form. The magnetization was found to be linear with field in both the *a*- and *c*-axis directions up to the highest field measured, 35 T. The sample was checked for spin-glass behavior ($\chi_{FC}$ compared to $\chi_{ZFC}$) down to 2 K, and none was found. $\chi$ for $B \| c$ has a peak vs temperature at 7.9 K and is greater than $\chi$ for $B \| a$ (see Table II). $\chi$ was not investigated for temperature dependence in the *c*-axis direction, due to the low-lying peak; for $B \| a$, $\chi \sim \chi_0 - b T^{0.7}$. The resistivity (see Table II) follows $\rho = \rho_0 + A T^{1.1}$ for $I \| a$ between 0.3 and 2.6 K and $\rho = \rho_0 + A T^{0.3}$ for $I \| c$ between 0.3 and 2.3 K. The specific-heat data on the single crystal follow $C/T \sim -\log T$ between 0.1 and 5 K. Specific-heat data to 27 T on a polycrystalline sample were scaled (Kim and Stewart, 2000) to give a scaling exponent of ~0.5. As discussed above in the theory section, the interactions responsible for the non-Fermi-liquid behavior can be either single-ion or correlated in nature based on a scaling exponent, $\beta < 1.0$.

In summary, based on $\rho$ data down to 0.3 K and $C$ data down to 0.1 K, $U_2Pt_2In$—without doping—is a good candidate for a non-Fermi-liquid system caused by a quantum critical point at $T = 0$—as good a candidate as any of the doped systems discussed above in Sec. III.A. As will be seen when, for example, $CeNi_2Ge_2$ is discussed below, $U_2Pt_2In$ has quite high residual resistivity values when compared with other undoped non-Fermi-liquid systems—(Table II). However, the linear $M$ vs $H$ data up to 35 T[3] at least rule out the disorder model involving a distribution of Kondo temperatures that include $T_K \to 0$. More work needs to be done on this system to investigate the temperature dependence of the resistivity as a function of sample quality as well as the temperature dependence to lower temperatures. If the exponent $\alpha$ in $\rho = \rho_0 + A T^{\alpha}$ remains ~1.1 to lower temperatures for $I \| a$, then according to the theory of Rosch (1999) $U_2Pt_2In$ would be classed as a highly ordered system. [Estrela *et al.* (1998) state that a single-crystal structural refinement on their sample indicates a high crystalline quality, in contrast to the large $\rho_0$ measured.] This would leave microcracks in the sample, which have been invoked (Pinto *et al.*, 1995) to explain the large $\rho_0$ in the related $U_2Co_2Sn$ system as a possible explanation for the large $\rho_0$, normally associated with poor microscopic order.

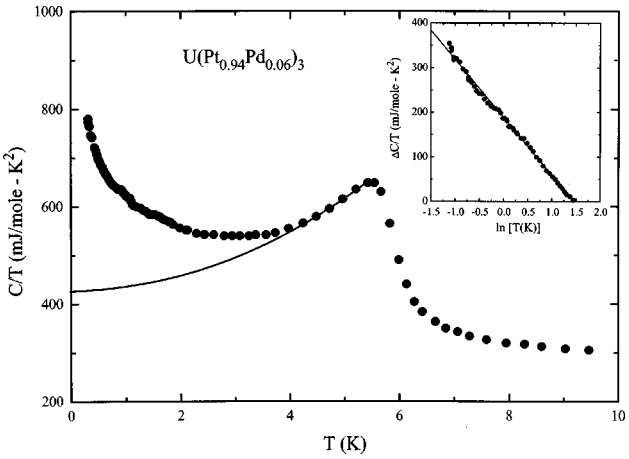


FIG. 23. $C/T$ vs $T$ for antiferromagnetic $U(Pt_{0.94}Pd_{0.06})_3$, $T_N \sim 5.6$ K, after Kim *et al.* (1992). If a fit to the data directly below the peak in $C/T$, shown by the solid line, is subtracted from the data below $T_N$, the difference, $\Delta C$, divided by temperature—shown in the inset—behaves as $-\log T$.

### 2. $CeNi_2Ge_2$

This tetragonal compound is the most widely studied undoped system, with a monotonic improvement with time of $\rho_0$ from its initial value of ~3→0.17 $\mu\Omega$ cm at present. Two groups reported simultaneously that $\rho$ for $CeNi_2Ge_2$ deviated from the expected Fermi-liquid $T^2$ behavior at low temperatures, with $\rho_0$ between 2 and 3 $\mu\Omega$ cm and $\alpha$ in $\rho = \rho_0 + A T^{\alpha}$ approximately 1.5 over a decade of temperature (see Table II). The work of Julian *et al.* (1996) indicated Fermi-liquid $T^2$ behavior in $\rho$ below ~0.2 K, while the work of Steglich *et al.* (1996) reported no deviations from the $\rho = \rho_0 + A T^{1.5}$ power law down to 0.020 K with, however, the $\rho$ data reported in a 1-T applied field (presumably to suppress superconductivity, as discussed below). Steglich *et al.* (1996) further reported specific-heat data down to 0.4 K, with $\sqrt{T}$ behavior below 1 K and $\log T$ behavior between 1 and 3 K (see Table II). An earlier report on the specific heat of $CeNi_2Ge_2$ (Knopp *et al.*, 1988) down to 0.07 K reported a peak in $C/T$ at ~0.3 K, with only ~6% decrease in $C/T$ from the maximum value down to 0.07 K. Recent work (Koerner *et al.*, 2000) on $\rho$ and $C$ of a polycrystalline sample of $CeNi_2Ge_2$, $\rho_0 = 0.8$ $\mu\Omega$ cm, annealed (five days at 700 °C), showed a leveling off (i.e., Fermi-liquid behavior) in $C/T$ (rather than the peak of Knopp *et al.*) below 0.3 K down to 0.06 K, with $\Delta C/T \sim -\log T$ between 0.4 and 10 K, i.e., with no $\sqrt{T}$ region. In addition, Koerner *et al.* report $\rho = \rho_0 + A T^2$, i.e., Fermi-liquid be-

[3]57 T for polycrystalline material, although with a slight nonlinearity thought to be due to 2% second phase of magnetic UPt (Fukushima *et al.*, 1995).

havior, below ~0.2 K, as did Julian *et al.* Thermal expansion results (Gegenwart *et al.*, 1999) also show Fermi-liquid behavior below 0.2 K.

Adding to the conflicting results on $C$, Gegenwart *et al.* (1999) also report $C/T \sim -\log T$ down to 0.4 K (in contrast to the $\sqrt{T}$ between 0.4 and 1 K of Steglich *et al.*, 1996), while Aoki *et al.* (1997) plot their $C/T$ data as $\gamma_0 - a\sqrt{T}$ with good agreement between 0.6 and 7 K for a single crystalline specimen. Further, Steglich *et al.* (2001) have recently reported a sample-dependent upturn in the $C/T$ of polycrystalline samples of $CeNi_2Ge_2$ below 0.3 K, rather than a leveling off.

There have been conflicting results about whether $CeNi_2Ge_2$ has a superconducting transition in the resistivity. Julian *et al.* report no $T_c$ down to 0.020 K, while Gegenwart *et al.* (1999) report $\rho \to 0$ at about 0.1 K. In addition, Gegenwart *et al.* report a significant variation of $\alpha$ in $\rho = \rho_0 + AT^{\alpha}$ that correlates with $\rho_0$, with $\alpha = 1.5$ for $\rho_0 = 2.7\,\mu\Omega$ cm and $\alpha = 1.37$ for $\rho_0 = 0.34\,\mu\Omega$ cm (see Table II). Recently, work by Steglich *et al.* (2000) and Gegenwart *et al.* (2000) in the ternary phase diagram of $CeNi_2Ge_2$ has shown that ~2% Ni excess causes $T_c \sim 0.1$ K. Geibel *et al.* (Geibel, 2000) report that the highest-quality (lowest-$\rho_0$) samples have $\alpha \sim 1.4$ and do not superconduct, contradicting the conclusion of Gegenwart *et al.* (2000), who found their lowest-$\rho_0$ samples to be superconducting.

While the questions of the resistive superconducting transition and the temperature exponent $\alpha$ as a function of $\rho_0$ appear to be settled, after significant materials improvement efforts, the "intrinsic" or "best sample" behavior of $C/T$ below 0.3 K and the resistivity temperature dependence exponent $\alpha$ below 0.2 K still remain unclear. It may in fact be the case that $CeNi_2Ge_2$, in its ternary phase diagram, is close to an actual $T = 0$ quantum critical point such that minor, as yet uncontrolled, stoichiometry changes can have two possible effects: (a) a sample will lie to the right of the quantum critical point (cf. Fig. 2) in the Millis phase diagram and exhibit Fermi-liquid behavior in $C/T$ and $\rho$ below a finite temperature (e.g., the sample of Koerner *et al.*) or (b) a sample will lie sufficiently close to the quantum critical point that $\rho$ exhibits non-Fermi-liquid behavior ($\rho = \rho_0 + AT^{\sim 1.4}$) down to 0.020 K, at least in a small, 0.1-T field needed to suppress superconductivity (e.g., the sample of Gegenwart *et al.*, 1999) and $C/T$ does not show Fermi-liquid behavior but rather a sample-dependent *increase* down to 0.07 K (e.g., the sample of Steglich *et al.*, 2001). $CeNi_2Ge_2$ remains an important system for further study to even lower temperatures (work is in progress to study $\rho$ down to 0.001 K in the $\mu$Kelvin laboratory at the University of Florida), and—with a better understanding of the ternary phase diagram (work under way at MPI/CPfS Dresden)—may prove able to be studied at the quantum critical point.

### 3. $U_2Co_2Sn$

This compound occurs in the same $U_3Si_2$ tetragonal structure as $U_2Pt_2In$ with, however, a smaller nearest U-U separation of only 3.5 Å. Initial interest was focused on $U_2Co_2Sn$ because of this small separation, which is exactly at the Hill limit. As pointed out by Hill (1970), for $d_{U\text{-}U} < 3.5$ Å uranium *f*-electron orbitals in a lattice overlap with those of the neighboring U ions and produce itinerant *f*-electron behavior (i.e., not magnetic order), whereas for $d_{U\text{-}U} > 3.5$ Å uranium *f* electrons are localized and magnetic unless there is significant *f*-electron hybridization with, for example, *d*-electron orbitals. At $d_{U\text{-}U} = 3.5$ Å, uranium systems—being on the edge of becoming magnetic—exhibit strong spin fluctuations, as seen, for example, in $UAl_2$ (Trainor *et al.*, 1975). Initially, based on $\rho$ data for $T > 4$ K, $U_2Co_2Sn$ was thought to display spin-fluctuation behavior (Pinto *et al.*, 1995). In addition, the initial report on the upturn at low temperatures in the specific heat divided by temperature [measured down to 1.3 K (Nakotte, 1994)] was that it was four times less pronounced than that observed in $U_2Pt_2In$, i.e., more consistent with gradual spin-fluctuation behavior ($C/T \sim T^2 \log T$) than divergent, strongly coupled behavior ($C/T \sim -\log T$) as observed in $U_2Pt_2In$.

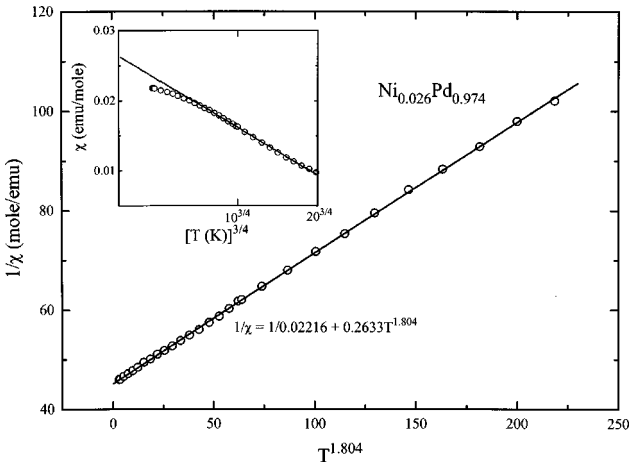


FIG. 24. The magnetic susceptibility of $Ni_{0.026}Pd_{0.974}$ is shown in the inset vs $T^{3/4}$, as in the original work of Nicklas *et al.* (1999), and fit $\chi \sim T^{3/4}$ between 5.5 and 20 K, deviating below the $\chi \sim T^{3/4}$ line in the inset below 5.5 K. If these data are replotted as $\chi^{-1} = \chi_0^{-1} + AT^{\alpha}$, as shown in the main part of the figure, the data follow this relation with $\alpha = 1.80$ over the entire temperature range.

Kim, Alwood, *et al.* (2000) reported resistivity down to 0.1 K and specific heat down to 0.3 K. Surprisingly, $C_e/T = \gamma - A\sqrt{T}$ over the whole temperature range of measurement, 0.3–10 K, where $C_e$ is the measured specific heat corrected for the lattice contribution. As discussed above in the theory section, Tables I(a) and I(b) this is just the weak-coupling behavior predicted by Millis-Hertz/Moriya for a three-dimensional system with antiferromagnetic correlations. Such a broad range of $\sqrt{T}$ behavior in $C/T$ is seen in no other system [cf. the results of Steglich *et al.* (1996) between 0.4 and 1 K in $CeNi_2Ge_2$], and appears in fact inconsistent with the theory of Moriya, which predicts a crossover to $C/T \sim -\log T$ behavior (due to an increase of mode-mode

coupling) well before a decade of temperature is covered with the pure $\sqrt{T}$ dependence. Somewhat surprisingly, scaling of the specific heat with field works quite well ($\beta=1.6$), even though strong coupling ("hyperscaling") of the electron interactions was at one time believed to be necessary to observe scaling in $C$ or $M$ (Heuser *et al.*, 1998b).

The measured $\rho_0$ (see Table II) is too large to be physical and as discussed above may be due to microcracks. With the temperature dependence of $\rho$ not the predicted $\alpha=1.5$ but rather $\alpha\sim1.8$, as well as the observation of Kim *et al.* of a slight *minimum* in $\rho$ around 0.2 K, $U_2Co_2Sn$ was clearly a system needing further characterization. Recently Kim, Alwood, and Stewart (2001) have found a processing technique that avoids microcracks and significantly lowers the residual resistivity; see Table II. Magnetoresistance measurements near the minimum in $\rho$ and measurements of $\rho$ down to 0.008 K are in progress. Also useful would be efforts similar to those carried out in the ternary phase diagram of $CeNi_2Ge_2$ to look for possible different behavior in $C/T$ below 0.3 K in samples with slightly different Co/Sn ratios. In any case, the rather unique $C/T\sim\gamma_0-A\sqrt{T}$ behavior over such a wide temperature range in $U_2Co_2Sn$ exactly when $d_{\text{U-U}}$ is at the Hill limit may be a clue as to where to look for weakly coupled/Millis-Hertz/Moriya behavior in future U systems.

#### 4. $YbRh_2Si_2$

As discussed above in the introduction to this section, tetragonal $YbRh_2Si_2$ was first reported to be a non-Fermi-liquid system (Trovarelli, Geibel, Langhammer, *et al.*, 2000) down to the lowest temperature of measurement, with $\rho=\rho_0+AT$ ($0.02\leqslant T\leqslant10$ K) and $C/T\sim-\log T$ ($0.4\leqslant T\leqslant10$ K). (However, a weak antiferromagnetic transition may leave very little signature in $\rho$.) There is a large anisotropy in $\chi$, with $\chi_{\text{basal plane}}\sim20\chi_{c\text{ axis}}$.

Further work (Trovarelli, Geibel, Mederle, *et al.*, 2000) discovered a weak antiferromagnetic transition at 0.065 K using both $\chi_{\text{ac}}$, where only 450 G was sufficient to suppress $T_N$ below 0.020 K, and extrapolation to zero pressure of $\rho$ vs $T$ anomalies measured in pressures up to 3 GPa. (Unlike in Ce compounds, where pressure suppresses antiferromagnetism, pressure induces/enhances antiferromagnetism in Yb compounds.) This work also extended the measurement of $C$ down to 0.08 K and found an upturn in $C/T$ below 0.35 K, described as either being similar to such upturns observed in, for example, $U_{0.2}Y_{0.8}Pd_3$ or perhaps connected to the low-temperature magnetic anomaly although the size and breadth of the upturn argue against this latter interpretation. The specific heat was measured in fields to 6 T and, for $T>0.35$ K, was found to scale onto one universal curve with a scaling exponent of $1.05\pm0.05$, i.e., the same as for $CeNi_2Ge_2$ (see Table II).

Recently, Custers and Gegenwart (2001) have shown in high precision $\rho$ data that the antiferromagnetic transition at 0.065 K does indeed interrupt the non-Fermi-liquid $\rho=\rho_0+AT$ behavior below about 0.100 K.

The possibility needs to be explored that, with a better knowledge of the phase diagram, $YbRb_2Si_2$ could be made with no antiferromagnetic transition, i.e., directly at the quantum critical point, by varying the relative stoichiometry between Rh and Si.

#### 5. $Yb_2Ni_2Al$ and $CeRu_4Sb_{12}$

These systems were each reported once, and both have uncertainties in the data to date that make their identification as undoped non-Fermi-liquid systems only tentative.

$Yb_2Ni_2Al$ was reported (Geibel *et al.*, 1996) to have $C/T\sim-\log T$ (with some "waviness," or periodic deviations from straight-line behavior on a $C/T$ vs $\log T$ plot of the data) between 0.5 and 4 K. Between 2 and 12 K, $\chi$ almost follows the high-temperature Curie-Weiss behavior ($\chi\sim1/T$), while $\rho$ below 20 K decreases strongly but with neither a clear power law nor a $\log T$ behavior.

$CeRu_4Sb_{12}$ was reported (Takeda and Ishikawa, 1999) to have $\rho=\rho_0+AT^{1.6}$ between 0.1 and 5 K, while $C/T$ was described as fitting either a $\sqrt{T}$ dependence (0.25–1.2 K) or a $\log T$ dependence (0.25–0.7 K), with a large unexplained nuclear level splitting (Schottky anomaly, $C\sim T^2$) below 0.25 K.

#### 6. $CeCu_2Si_2$

Steglich *et al.* (1996) reported that a superconducting sample of $CeCu_2Si_2$ in a magnetic field sufficient to suppress the superconductivity ($\geqslant$ 2 T), but less than 6 T, exhibited non-Fermi-liquid behavior in the resistivity ($\rho=\rho_0+AT^{1.5}$) for $0.02\leqslant T\leqslant1.7$ K, while the specific heat showed $\gamma-a\sqrt{T}$ between 0.7 and 3 K with a tendency for $C/T\rightarrow$const between 0.25 and 0.7 K. For $B\geqslant6$ T, the resistivity returned to Fermi-liquid, $T^2$ behavior.

#### 7. $UBe_{13}$

Although in the original discovery of superconductivity in heavy-fermion $UBe_{13}$ $C/T$ was assumed to be constant below the superconducting transition temperature $T_c$ of 0.9 K (Ott *et al.*, 1983), work shortly thereafter (Ott *et al.*, 1985) observed that $C/T$ had to be, based on entropy arguments, still increasing below 1 K in $U_{1-x}Th_xBe_{13}$, $x\leqslant0.05$.

A measurement of $C/T$ in an applied field to suppress $T_c$ of $U_{0.97}Th_{0.03}Be_{13}$ down to 0.42 K (Kim *et al.*, 1991) found that, in order to match the entropy of the superconducting state at $T_c$ with that of the normal state, $C/T$ (measured in the normal state at 0.42 K) $=1400$ mJ/mol K$^2$ had to grow to 2300 mJ/mol K$^2$ as $T\rightarrow0$, which—according to the basic definition of a Fermi liquid that $C/T\rightarrow$const at low temperatures—may be taken as a definite indication of non-Fermi-liquid behavior in $U_{0.97}Th_{0.03}Be_{13}$. This later work, using the same entropy argument, put the growth in $C/T$ between $T_c^+=0.96$ and 0 K in pure $UBe_{13}$ at ~28% (800 mJ/mol K$^2$

at 0.96 K→1020 mJ/mol K$^2$ at 0 K), i.e., the pure compound also displays non-Fermi-liquid behavior in $C/T$ at low temperatures. It has also been observed that $\rho \neq \rho_0 + AT^2$ in pure $UBe_{13}$ down to $T_c$. Upon suppression of $T_c$ with a 9-T field (Willis, 1988) Fermi-liquid, $T^2$ behavior is first observed between 0.15 and 1 K. Thus, based on the Millis-Hertz phase diagram (Fig. 2) and previous discussion, $UBe_{13}$ appears to be close to a quantum critical point but, based on the $T^2$ behavior in the low-temperature $\rho$ when $T_c$ is suppressed, not at a quantum critical point.

This situation has been further explored by Steglich *et al.* (1997), who point out that $C/T$ follows $\sim -\log T$ (with, however, some "waviness" in the data around a straight line of $C/T$ plotted vs $\log T$) between 0.2 and 3 K in a 12-T field to suppress $T_c$. (Since $C/T$ for $T > T_c$ is essentially unaffected by such a field in $UBe_{13}$, this work is discussed here rather than in the section below on non-Fermi-liquid behavior induced by applied field. In this case the field is incidental rather than required.) Further, $\rho = \rho_0 + AT^{1.5}$ in 8 T for $UBe_{13}$ between $T_c = 0.4$ and 1 K. Thus $UBe_{13}$ has long been recognized as not having Fermi-liquid, $C/T \rightarrow$ const and $\rho = \rho_0 + AT^2$, behavior at low temperatures, and the more recent work of Steglich *et al.* indicates that the non-Fermi-liquid behavior may be comparable to the that of other systems in which non-Fermi-liquid behavior has been discovered, starting in 1991 with $U_{0.2}Y_{0.8}Pd_3$.

### 8. Ce*T*In$_5$, *T*=Ir, Co, Rh

Very recently Sarrao *et al.* (2000; see also Thompson *et al.*, 2000) reported superconductivity in a new class of Ce compounds analogous in their properties to $UBe_{13}$, with a large enhancement in the low-temperature $C/T$ as $T \rightarrow 0 (\equiv \gamma)$. This analogy holds not only in the comparison of the large $\gamma$'s and superconductivity, but also as regards non-Fermi-liquid behavior. Thus applying a field to suppress superconductivity in $CeIrIn_5$ (Petrovic, Movshovich, *et al.*, 2001) results in $\rho = \rho_0 + AT^{1.3}$ from 0.06 to 5 K. Zero-field data in $CeCoIn_5$ (Petrovic, Pagliuso, *et al.*, 2001) give $\rho = \rho_0 + AT^{\sim 1}$ between $T_c$ (=2.3 K) and 20 K, and data in 21 kbar to induce superconductivity in $CeRhIn_5$ (Hegger *et al.*, 2000) give $\rho = \rho_0 + AT^{\sim 1}$ above $T_c = 2.3$ K up to 6 K. Without field suppression of $T_c$ to measure the temperature dependence of $\rho$ to lower temperatures, inclusion of the Co and Rh compounds here relies on the Ir result, but this is a rapidly developing field with experiments under way to clarify this point. Identifying non-Fermi-liquid behavior in the specific heat is hampered by structure (a shoulder in $C/T$ just above $T_c$) in both the Ir and Rh (under pressure) compounds; however, $C/T$ measured down to 0.15 K in 5 T to suppress the superconductivity in $CeCoIn_5$ shows (Petrovic, Pagliuso, *et al.*, 2001), just as in $UBe_{13}$ and $U_{1-x}Th_xBe_{13}$, a strong temperature dependence in $C/T$—more than a factor-of-3 increase in $C/T$ upon cooling from 2.3 K ($T_c^+$) to 0.15 K. Recently, Kim, Alwood, Stewart, *et al.* (2001) have investigated the specific heat and susceptibility in $CeIrIn_5$ and $CeCoIn_5$ for non-Fermi-liquid behavior and found (see Table II) that $C/T$ behaves as $\sim -\log T$ between 0.3 and 8 K in $CeCoIn_5$, while $\chi$ in $CeIrIn_5$ gives evidence for local deviations from Fermi-liquid behavior.

The possibility that the spin fluctuations responsible for the non-Fermi-liquid behavior in $CeTIn_5$ and $UBe_{13}$ are linked to the mechanism for the superconductivity (i.e., not a BCS, phonon-mediated, *s*-wave electron pairing interaction) is under strong discussion. This subject will also appear in Sec. III.C.1, where we consider pressure-induced non-Fermi-liquid behavior that is accompanied by superconductivity at the quantum critical point.

### 9. UCoAl

Hexagonal UCoAl undergoes a metamagnetic transition at the low field of 0.6 T in the single-crystal sample studied by Havela *et al.* (2000a).[4] Thus UCoAl may be considered to be near, in a phase-diagram sense, a magnetic instability and was studied for non-Fermi-liquid behavior by Havela *et al.* They found $\rho = \rho_0 + AT^{5/3}$, as predicted by the self-consistent renormalization theory—see Table I(b)—for a three-dimensional ferromagnet between their lowest temperature of measurement, 1.8 K, and 17 K for current along the *c* axis and between 1.8 and 12 K for current along the *a* axis (see Table II). Work to lower temperatures would be of interest.

### 10. $CaRuO_3$

Measurements of the resistivity of thin films of the pseudocubic perovskite $CaRuO_3$ (Klein *et al.*, 1999) show $\rho = \rho_0 + aT^{1.5}$ between 1.8 and 10 K, and $\rho = \rho_0 + aT^{0.5}$ between 35 and 300 K. The observed low-temperature non-Fermi-liquid temperature dependence would be consistent with antiferromagnetic spin fluctuations (see Table I in the theory section), whereas band-structure calculations (Santi and Jarlborg, 1997) indicate that $CaRuO_3$ is close to a *ferromagnetic* instability. Measurements to lower temperatures of $\rho$, as well as of $\chi$ and $C/T$, would be of interest.

### 11. $U_3Ni_3Sn_4$

Susceptibility measurements on $U_3Ni_3Sn_4$ give $\chi \sim T^{-0.3}$ between 1.8 and 10 K (Shlyk *et al.*, 1999), while recent specific-heat measurements (Shlyk *et al.*, 2000) indicate a rising, non-Fermi-liquid-like $C/T$ below 2 K down to 0.4 K, which can be fit approximately equally well using four parameters to either a $\sqrt{T}$ or a $T^{-1+\lambda}$ dependence. $C/T$ data below 0.4 K indicate saturation, or Fermi-liquid behavior.

[4]See also Sec. III.D, on field-induced non-Fermi-liquid behavior at a metamagnetic transition.

### C. Pressure-induced non-Fermi-liquid behavior

In Ce compounds that are antiferromagnetic, in ferromagnetic MnSi and $ZrZn_2$, and in ferromagnetic $UGe_2$, pressure can be utilized to suppress the magnetic order and investigate whether non-Fermi-liquid behavior occurs at or near the critical pressure $P_c$ for $T_{\text{order}} \rightarrow 0$ as would occur in the quantum critical point scenario. The advantages of using pressure to tune through the phase diagram (see Fig. 2) are (a) the tuning takes place without any change in the disorder (vs tuning using doping), (b) in well-chosen systems the level of disorder can be quite low, and (c) in contrast to undoped systems, which may not be exactly at the quantum critical point, tuning using pressure should be able to reach the precise point in the phase diagram where the quantum critical point occurs at $T=0$.

As is the case with doping (discussed in Sec. III.A above), with pressure it is also not always the case that non-Fermi-liquid behavior occurs upon suppression of $T_N$. For example, in $CeRh_2Si_2$ ($T_N=36$ K) a pressure of $\sim$9 kbar suppresses magnetism but results in Fermi-liquid behavior in both $\rho$ (Grosche *et al.*, 1997) and $C$ (Graf *et al.*, 1997) measurements at $P_c$.

Due to the difficulties of measurement, only a few of the systems studied for pressure-induced non-Fermi-liquid behavior have been studied using specific heat. Far more common are studies in which only the resistivity under pressure is reported, with accompanying $\chi_{\text{ac}}$ in a few cases. Several systems display conflicting results from different groups; this may be due to differences in the application of pressure techniques (piston vs Bridgman anvil) and differences engendered by liquid ($\rightarrow$ quasihydrostatic) vs solid (not hydrostatic) pressure media. Since the previous section ended with the possibility, for $CeTIn_5$ and $UBe_{13}$, that the spin fluctuations responsible for the non-Fermi-liquid behavior also mediate the superconducting interaction, and since a number of the resistive studies searching for pressure-induced non-Fermi-liquid behavior report that superconductivity is also induced near $P_c$ where $T_{\text{order}} \rightarrow 0$, we consider these cases first. Interestingly, even though Fermi-liquid behavior is observed when pressure suppresses antiferromagnetism in $CeRh_2Si_2$, this system also shows induced superconductivity (at $\sim$0.3 K) at $P_c$ (Movshovich *et al.*, 1996).

#### 1. Systems superconducting under pressure

##### *a. $CePd_2Si_2$*

An early study of $\rho$ as a function of pressure (Thompson *et al.*, 1986) indicated that significantly more than 17 kbar would be required to suppress $T_N$, which, at $P=0$, is approximately 10 K. Later studied at and above the critical pressure for suppression of antiferromagnetism by two groups using resistivity measurements, $T_N$ was found to go to 0 at approximately 28 kbar. While one group first reported $\rho=\rho_0+AT^{1.2}$ above a superconducting transition at 0.43 K up to 40 K (two decades of temperature!) at 28 kbar (Grosche *et al.*, 1996) using a piston technique, the second group—using an anvil method—reported simultaneously no superconductivity down to 0.03 K and $\rho=\rho_0+AT^{1.5}$ up to 1 K at $P_c$ (Link, Jaccard, and Lejay, 1996; see Table II). The phase diagram for the suppression of antiferromagnetism and inducement of superconductivity by the first group is shown in Fig. 25 (Julian *et al.*, 1998). The difference in $\rho_0$ values (4 $\mu\Omega$ cm vs 22/33 $\mu\Omega$ cm, respectively) in the two groups' single crystals was later identified (Mathur *et al.*, 1998) as a determining factor as to whether or not superconductivity would occur. However, even with $\rho_0=2.8\,\mu\Omega$ cm, the most recent work by the second group (Raymond and Jaccard, 2000)—which uses an anvil pressure application technique—displays only a sharp drop in $\rho$ at "$T_c$," with $\rho\approx 1\,\mu\Omega$ cm at lower temperatures. Further inconsistencies (Raymond and Jaccard, 2000) include a different phase diagram than that shown in Fig. 25 in that (1) the maximum in "$T_c$" is at pressures significantly higher than $P_c$. If this is not due simply to nonhydrostatic pressure effects, it may affect the applicability of the magnetic-spin-fluctuation-induced superconductivity theory (for a discussion thereof, see Mathur *et al.* and references therein); and (2) $P_c$ is 34 instead of 28 kbar. In addition, Raymond and Jaccard observe different resistivity behavior in their $CePd_2Si_2$, with Fermi-liquid, $T^2$, behavior in $\rho$ between 0.03 and 3 K at $P_c$ and non-Fermi-liquid, $\rho=\rho_0+AT^{1.2}$ behavior first found at $1.15\,P_c$. (A note added in proof to Raymond and Jaccard stated that another group had found $\rho\rightarrow 0$ at 24 kbar in a crystal from the same batch as theirs.)

This sample dependence of superconductivity is reminiscent of early results in the prototypical heavy-fermion superconductor $CeCu_2Si_2$ (Steglich *et al.*, 1979), where significant investigation of the ternary phase diagram was necessary to establish bulk superconductivity as measured by the specific heat and by the Meissner effect in $\chi_{\text{dc}}$. It is worth noting that a similar sample dependence of the resistivity at the superconducting transition under pressure was also reported in $CeRh_2Si_2$, where $\chi_{\text{ac}}$ measurements of the sample that showed $\rho\rightarrow 0$ indicated only 1% of full superconducting shielding (Movshovich *et al.*, 1996).

##### *b. $CeCu_2Si_2$*

In the complicated ternary phase diagram of the prototypical heavy-fermion superconductor $CeCu_2Si_2$, either a slight Ce or Cu deficiency results in antiferromagnetism at 0.7 K instead of superconductivity (Steglich *et al.*, 1997). Aliev *et al.* (1983) showed that 7.7 kbar induced superconductivity, as determined by resistivity measurements, in a nonsuperconducting polycrystalline sample. Later studies on well-characterized samples (Steglich *et al.*, 1996) showed that the application of $P_c=6.7$ kbar suppresses antiferromagnetism and induces superconductivity at 0.65 K, similar to the superconductivity observed in $CeCu_2Si_2$ without the Ce or Cu deficiency. The application of a magnetic field of 2 T destroys the superconductivity and allows measurement of the specific heat to look for non-Fermi-liquid behavior. The data (Steglich *et al.*, 1996) are shown in Fig. 26 and

show crossover behavior consistent with the theory of Moriya and Takimoto (1995): $C/T$ behaves as $\sim\sqrt{T}$ at lower temperatures (0.4–1.2 K) and crosses over to $\sim\log T$ behavior at higher temperatures (1.2–5 K). Resistivity data on this sample are unfortunately not available.

#### c. $CeCu_2Ge_2$

This was the second system investigated in which pressure was found to cause superconductivity in a highly correlated electron system [cf. the work of Aliev *et al.* (1983) on $CeCu_2Si_2$ cited above]. Jaccard *et al.* (1992), based on trends observed in thermopower measurements, predicted that $CeCu_2Ge_2$ ($T_N=4.1$ K) would become a heavy-fermion superconductor just like $CeCu_2Si_2$ upon the application of high pressure. At $P_c \approx 75$ kbar, $T_N \to 0$ and superconductivity appears at $T_c = 0.6$ K, with $T_c$ remaining approximately constant—in contrast to $CePd_2Si_2$—up to the highest pressure of measurement 101 kbar. The resistivity in 101 kbar, measured up to ~6 K, obeys approximately $\rho=\rho_0+AT^1$ from $T_c$ up to 4 K. Later work (Jaccard *et al.*, 1999) found that $T_c$ remains constant up to 135 kbar, after which $T_c$ increases to ~2 K by 166 kbar. The behavior of the exponent $\alpha$ in $\rho=\rho_0+AT^\alpha$ was also further investigated in the later work; $\alpha$ starts off at $P=P_c$ equal to 2 and sinks monotonically with increasing pressure to $\alpha\approx 1$ for 130–140 kbar, followed by an increase back to ~2 around 160 kbar.

#### d. $CeIn_3$

In this binary, cubic compound with $T_N=10.1$ K, 26 kbar suppresses antiferromagnetism and induces superconductivity at 0.2 K (Walker *et al.*, 1997). The ambient-pressure residual resistivity is "less than 1 $\mu\Omega$ cm"; $\rho_0 = 0.6\,\mu\Omega$ cm at 24.1 kbar. Contrary to results in $CePd_2Si_2$, Fermi-liquid, $T^2$ behavior is recovered at pressure slightly higher than $P_c$ (e.g., at 30 kbar), and at 29 kbar the exponent $\alpha$ in $\rho=\rho_0+AT^\alpha$ varies between $\alpha=1.6$ at 3 K (lowest temperature of measurement) and $\alpha=0.8$ at 25 K, i.e., it is nowhere temperature independent.

#### e. $UGe_2$

Oomi *et al.* (1998) found that the ferromagnetism, $T_C=52$ K, in $UGe_2$ is suppressed at a critical pressure $P_c \sim 15$–$16$ kbar via resistivity measurements that extended down to only 4.2 K. Further, Oomi *et al.* found that the $A$ coefficient in $\rho=\rho_0+AT^2$ goes through a maximum at $\sim 0.8P_c$, while the temperature range in which the $T^2$ behavior describes the resistivity shrinks (see Sec. III.C.2.c for a discussion of $Ce_7Ni_3$) in this pressure range to, e.g., 4.2–5.5 K at 0.5 $P_c$ vs at least 4.2–10 K at $P_c$. Saxena *et al.* (2000) recently reported superconductivity (similar to what was found for $CePd_2Si_2$ under pressure; see Fig. 25) in high quality single crystals of $UGe_2$ at pressures from 10 to 16 kbar, i.e., primarily *below* $P_c$, coexistent with the magnetism. The maximum superconducting transition temperature, ~0.7 K, as a function of pressure in $UGe_2$ is found at the same pressure for which Oomi *et al.* reported the maximum magnitude in $A$/smallest temperature range of $T^2$ behavior, i.e., at $\sim 0.8P_c$. Unlike the behavior of the resistivity in $CePd_2Si_2$ above the superconducting transition in this compound Saxena *et al.* report $\rho=\rho_0+AT^2$ above the superconducting transition up to at least ~6 K in the data shown for $P=13.5$ kbar. However, the data of Saxena *et al.* nearer 0.8 $P_c$ behave as $\rho=\rho+AT^\alpha$, with $\alpha$ well below $\alpha=2$.

Thus these five systems ($CePd_2Si_2$, $A$-type Ce/Cu deficient $CeCu_2Si_2$, $CeCu_2Ge_2$, $CeIn_3$, and $UGe_2$) all show at least non-Fermi-liquid behavior in the resistivity and induced superconductivity at the critical pressure where $T_{\rm order}\to 0$. The possibility of magnetically mediated, non-BCS superconductivity has been discussed in the cited references for each system (see especially Mathur *et al.*, 1998 and Saxena *et al.*, 2000). The slope of the critical field near $T_c(H=0)$, $H'_{c2}$, is given in Table II for these systems and is proportional to the electron effective mass $m^*$ and the specific heat $\gamma$ ($=C/T$ as $T\to 0$, Orlando *et al.*, 1979). Thus the size of the measured critical-field slopes is indicative of strongly correlated, high-effective-mass behavior at $P_c$. For comparison, $H'_{c2}$ values for ambient-pressure superconducting $CeCu_2Si_2$ and $UBe_{13}$ are $\sim -20$ T/K and $-44$ T/K, respectively (Stewart, 1984).

### 2. Nonsuperconducting systems under pressure

#### a. $CeRu_2Ge_2$

In the same tetragonal structure as $CePd_2Si_2$, $CeRh_2Si_2$, $CeCu_2Si_2$, and $CeCu_2Ge_2$, $CeRu_2Ge_2$ has a more complex magnetic phase diagram (Wilhelm and Jaccard, 1999), with antiferromagnetism at 8.55 K and ferromagnetism at 7.4 K. After a complicated process of suppression of magnetism with pressure (e.g., $T_N$ first increases with pressure), $P_c$ is determined to be ~84 kbar and, at this pressure, $\rho=\rho_0+AT^{1.58\pm 0.08}$ between 0.03 and 1.5 K with no sign of induced superconductivity. Scanning data at 91.5 kbar from an earlier study (Wilhelm and Jaccard, 1998) gives $\rho=\rho_0+AT^{1.26}$ between 0.03 and 11 K. Alternating-current measurements of specific heat have been performed (Bouquet *et al.*, 2000) and, in arbitrary units, show $C/T$ looking rather Fermi liquid like down to 1.5 K at $P_c$. Although the temperature ranges of these measured $\rho$ and $C$ data do not quite overlap, the temperature range of non-Fermi-liquid behavior in $C/T$ data as a function of field or pressure is almost always smaller than the corresponding temperature range for non-Fermi-liquid in the resistivity. For example, in $CeNi_2Ge_2$, a pressure of either 12.5 or 16.4 kbar was found to give $C/T=$ const between 0.4 and 5 K (Sparn *et al.*, 1998), while resistivity at 17 kbar (Grosche *et al.*, 2000) still shows (qualitatively) approximately the same non-Fermi-liquid behavior ($\rho=\rho_0+AT^{1.2}$) observed at ambient pressures between 0.4 and 4 K, although the $A$ coefficient falls rapidly with increasing pressure.

*b. $CeCu_{6-x}Au_x$*

As discussed above in the doping section, $CeCu_6$ is an orthorhombic heavy-fermion system that becomes antiferromagnetic when doped with $x \sim 0.2$ of either Au or Ag. Upon reducing the amount of Au or Ag doping, non-Fermi-liquid behavior is found when $T_N \rightarrow 0$ at $x \sim 0.1$. Another way to induce non-Fermi-liquid behavior, using applied pressures up to 9 kbar to suppress antiferromagnetism in either $CeCu_{5.8}Au_{0.2}$ ($T_N = 0.25$ K) or $CeCu_{5.7}Au_{0.3}$ ($T_N = 0.5$ K, see Fig. 27), has been thoroughly investigated by the group of von Löhneysen. As revealed by measurements of the specific heat rather than resistivity, non-Fermi-liquid behavior ($C/T \sim -\log T$) is found at a $P_c$ of 4.1 kbar for $x = 0.2$ and $0.07 \leqslant T \leqslant 3$ K (Sieck *et al.*, 1997) and 8.2 kbar for $x = 0.3$ and $0.1 \leqslant T \leqslant 2$ K (Bogenberger and von Löhneysen, 1995; see Fig. 27). It is worth noting that the characteristic temperatures, $T_0$ (see Table II), found for both critical pressures and for the tuning-via-doping case of $CeCu_{5.9}Au_{0.1}$, agree with one another.

Just as magnetic field suppresses the long-range magnetic fluctuations necessary for non-Fermi-liquid behavior, thus recovering Fermi-liquid behavior, sufficient pressure above $P_c$ (6.9 vs 4.1 kbar) for $CeCu_{5.8}Au_{0.2}$ also has produced a beginning of saturation in $C/T$ at low temperatures (Sieck *et al.*, 1997).

*c. $Ce_7Ni_3$*

$Ce_7Ni_3$ occurs in an hexagonal structure with three distinct Ce lattice sites. The compound exhibits antiferromagnetism at 1.8 K, which Umeo and co-workers (1996a, 1996b) suppressed using pressure, $P_c \sim 3.1$ kbar, in a study of the specific heat, ac susceptibility, and resistivity. The susceptibility behaves as $\chi_0 - a\sqrt{T}$ between 0.3 and 5 K at 4.7 kbar while $\chi \sim$ const at 6 kbar. Consistent with these results, specific heat varies as $C/T \sim -\log T$ between 0.45 and 6 K at 3.7 and 5.2 kbar, while $C/T \sim$ const at 6 kbar. Unfortunately, the resistivity at 3.8 kbar, or just above $P_c$—although definitely not $T^2$—does not present a pure temperature dependence over a significant temperature range. At pressures at and above 6.4 kbar, $\rho = \rho_0 + A T^2$ over a broader and broader temperature range, as pressure increases. There is a monotonic falloff in the size of "$A$" with increasing pressure above the critical pressure where $T_N \rightarrow 0$ (see Fig. 28). Later measurements of $C$ and $\chi$ to lower temperatures found a crossover to Fermi-liquid behavior in $C$ at pressures $P_c$ near 3.8 kbar (3.5–4.1 kbar) below 0.5 K, indicating that—at least in the specific heat—$Ce_7Ni_3$ is not exactly at a quantum critical point when pressure suppresses antiferromagnetism. On the other hand, $\chi_{ac}$ (Umeo *et al.*, 1999) as well as $\chi_{dc}$ (Umeo *et al.*, 1998) continued to increase (i.e., to exhibit non-Fermi-liquid behavior) down to 0.09 K around $P_c$. Umeo *et al.* (1998) reported that $\chi_{dc} \sim T^{-0.2}$, $B \| a$ (see Table II) for both 3.9 and 5.8 kbar over their whole temperature range of measurement (0.5–4 K). For $B \| c$ (see Fig. 29 for a $\log \chi$ vs $\log T$ plot) they found that $\chi_{dc}$ at 3.4 and 3.9 kbar do not follow a simple power law, while for 4.8 and 5.8 kbar they observed that $\chi_{dc}$ tends towards a constant, or possibly towards Fermi-liquid behavior. When we replot all four sets of data (see Fig. 30 for the 3.4- and 3.9-kbar data) as $(\chi^{-1} - \chi_0^{-1})$ vs $T^{\alpha}$—just as we discovered for several non-Fermi-liquid systems already discussed in this review—a good fit over the whole temperature range (0.5–4 K) is found. What is unusual is that, for the 3.9-kbar (i.e., $\approx P_c$) data, $\alpha = 1.0$ ($\alpha = 0.9$, 1.1, and 1.27 for 3.4, 4.8, and 5.8 kbar, respectively). Thus, just at the critical pressure in $Ce_7Ni_3$ where $T_N \rightarrow 0$, rather than $\alpha \neq 1$—which would imply a local deviation from Fermi-liquid behavior as was discussed above in the theory section—we find that the susceptibility of $Ce_7Ni_3$ follows a simple Curie-Weiss behavior down to the lowest temperature of measurement. Although the temperature range over which the data are reported is not large, it is interesting that the simple Curie-Weiss law applies just at $P_c$ (and only there), where pressure brings the system to a quantum critical point. The same thing happened over a very large temperature range (1.8–100 K) in $Ce(Ru_{0.6}Rh_{0.4})_2Si_2$, which was also, via doping to $x_c$, at a quantum critical point. The effective moment calculated from the slope of the inverse susceptibility vs temperature plot is only $1.7\mu_B$, or significantly less than the effective moment found (Umeo *et al.* 1996b) for $Ce_7Ni_3$ at zero pressure from the higher-temperature (100–300 K) Curie-Weiss behavior, $2.5\mu_B$ ($\sim$ that of a local, $f^1$ state). However, what is of potential interest is not just the size of the effective moment. The simple, $\chi^{-1} - \chi_0^{-1} \sim T$, Curie-Weiss temperature dependence at a quantum critical point at low temperatures (in the surrounding phase diagram $\chi^{-1} - \chi_0^{-1}$ definitely does not behave linearly with $T$), together with a doped system at $x_c$ with the same behavior, may indicate a trend worthy of further investigation.

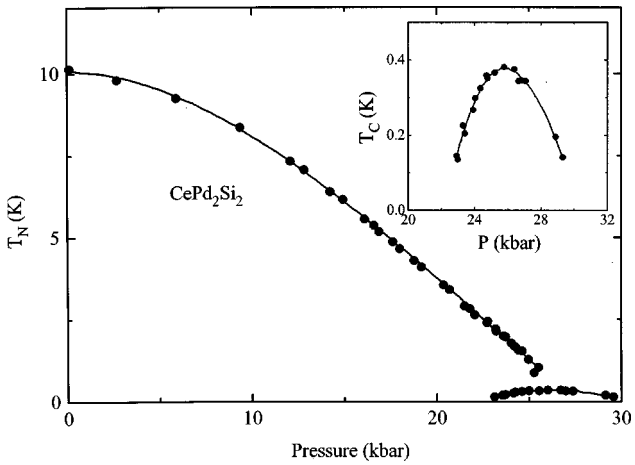


FIG. 25. Phase diagram for the antiferromagnet $CePd_2Si_2$ as a function of pressure, after Julian *et al.* (1998). The superconducting transition induced by pressure at low temperatures and pressures between 23 and 29 kbar shown in the main figure is expanded in the inset.

*d. MnSi*

This cubic system exhibits helical ferromagnetic order below 30 K, which is suppressed by ~15 kbar. Up to 17.2

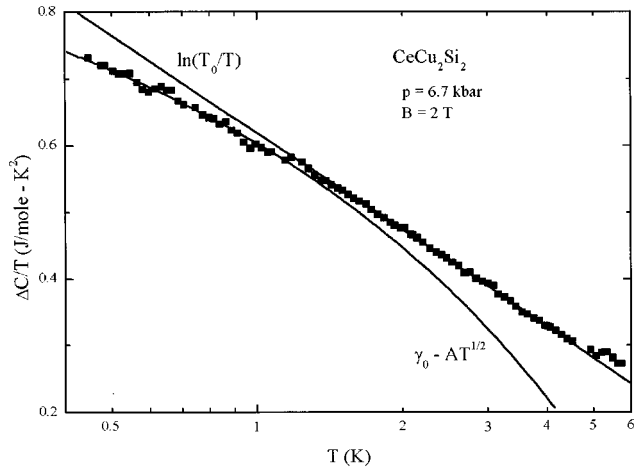


FIG. 26. The electronic specific heat $\Delta C$, divided by temperature vs $\log T$ for $CeCu_2Si_2$ in 6.7 kbar in a sufficiently large magnetic field (2 T) to suppress the pressure-induced superconductivity transition to allow inspection of the non-Fermi-liquid behavior in the specific heat: Lower, curved solid line, a fit of the lowest temperature $\Delta C/T$ data to $\gamma_0 - AT^{0.5}$; upper straight line, a fit through the higher-temperature $\Delta C/T$ data to $\log T$.

kbar, $\rho = \rho_0 + AT^{1.6-1.8}$ (Julian *et al.*, 1998) between 0.02 and 10 K. In contrast to the non-Fermi-liquid behavior exhibited by the resistivity, ac susceptibility data down to ~1 K exhibit Fermi-liquid behavior ($\chi \rightarrow$ const independent of temperature) for pressures at and just above $P_c$, with the highest pressure of measurement being 16.1 kbar (Pfleiderer *et al.*, 1997). Thessieu *et al.* (1997) report a large increase in the magnetization as a function of field, or a metamagnetic transition, at $P_c$. As $P \rightarrow P_c$, the ferromagnetic transition becomes weakly first order (Pfliederer *et al.*, 1997), a behavior that has been discussed theoretically by Belitz, Kirkpatrick, and Vojta (1999). This changeover to a first-order phase transition before $P_c$ is reached complicates the investigation of non-Fermi behavior as $P \rightarrow P_c$.

#### *e. $ZrZn_2$*

$ZrZn_2$ is a cubic ferromagnet at ~17 K; in it, the magnetism is suppressed to $T=0$ by about 7.5 kbar (Grosche *et al.*, 1995; Julian *et al.*, 1998). At $P_c$, $\rho$ is $\sim \rho_0 + AT^{\alpha}$ between 1 and 20 K, with, however, some temperature dependence of $\alpha$ ($\approx$1.67 between 10 and 20 K, with $\alpha$ less below 10 K.)

#### *f. $CeNiGa_2$*

Orthorhombic $CeNiGa_2$ is an antiferromagnet, $T_N = 4$ K. Hauser *et al.* (1998) reported that $T_N \rightarrow 0$ at a $P_c \sim 4$ kbar. At $P_c$ (see Table II), $\rho = \rho_0 + AT^{1.5}$ over a temperature range that grows with increasing pressure such that at 9.5 kbar the $T^{1.5}$ temperature dependence is observed up to 4 K, or over double the temperature range observed at $P_c$. At 12.5 kbar, $\rho$ still has a non-Fermi-liquid temperature dependence, $\rho = \rho_0 + AT^{1.7}$ (also up to 4 K), and recovers Fermi-liquid, $\rho \sim T^2$, behavior by 23 kbar. This broad range of non-Fermi-liquid behavior above $P_c$ contrasts with that observed for the other systems discussed in this pressure-induced section.

### D. Field-induced non-Fermi-liquid behavior

#### 1. Field suppression of $T_N \rightarrow 0$

As discussed above, pressure has been used since 1995 (Grosche *et al.*, 1995, in ferromagnetic $ZrZn_2$; Bogenberger and von Löhneysen, 1995, in antiferromagnetic $CeCu_{5.7}Au_{0.3}$) to suppress magnetism and search for remanent long-range magnetic correlations that prevent entry into the Fermi-liquid ground state. At least one system, antiferromagnetic $CeRh_2Si_2$, showed no such non-Fermi-liquid behavior when $T_N$ was suppressed with pressure (Movshovich *et al.*, 1996). The difficulties of measurement under pressure, particularly of the specific heat, have limited the number of systems studied for non-Fermi-liquid behavior to approximately the same number as are found among pure compounds, which, as discussed, should be quite rare. Due to the large number of low-temperature antiferromagnets, and inspired by the success of doping studies finding a rich behavior of non-Fermi-liquid properties when approaching the point in the phase diagram where $T_{\text{mag order}} \approx 0$, Heuser *et al.* in 1998 began publishing a series of articles looking into the possibility of suppressing $T_N \rightarrow 0$ with magnetic field. They found field-induced non-Fermi-liquid behavior, first on polycrystalline $CeCu_{6-x}Ag_x$ material down to 0.3 K (Heuser *et al.*, 1998a) and later on single crystals down to 0.07 K (Heuser *et al.*, 1998b). (See the doping section above for a discussion of non-Fermi-liquid behavior at ambient pressure and field in $CeCu_{5.8}Ag_{0.2}$.) Although field measurements are possible in a much larger number of laboratories than are pressure measurements, to date only limited further work has been carried out on this new method of studying non-Fermi-liquid behavior. Although several systems showing such non-Fermi-liquid behavior at $B_{\text{crit}}$ ($T_N \rightarrow 0$) have recently been discovered, several systems (e.g., $CePtSi_{0.4}Ge_{0.6}$, $T_N = 2$ K) showing Fermi-liquid behavior upon field suppression of $T_N \rightarrow 0$ (Heuser *et al.*, 1999) have also been reported. Work is continuing, but these early results show that magnetic-field suppression of antiferromagnetism does not, in every system, necessarily suppress all long-range magnetic correlations at $B_{\text{crit}}$ where $T_N \rightarrow 0$ and leave only Fermi-liquid behavior, contrary to earlier arguments (von Löhneysen *et al.*, 1996). Field suppression of antiferromagnetism, like pressure, does not induce any disorder and, like pressure, opens up an entire new dimension in the phase diagram for study. However, the usually assumed advantage of field over pressure, that is, field should not change the interatomic spacing (an unavoidable side effect of pressure-induced non-Fermi-liquid behavior), is not always in fact the case, as shown by the strong coupling between the metamagnetic transition and the volume (Flouquet *et al.*, 1995) in $CeRu_2Si_2$ at the metamagnetic transition.

*a. $CeCu_{6-x}Ag_x$*

The first report (Heuser *et al.*, 1998a) of Heuser on field-induced non-Fermi-liquid behavior in $CeCu_{6-x}Ag_x$ reported on the resistivity down to 0.08 K, $C/T$ down to 0.3 K, and $\chi$ down to 1.8 K for $x=0.48$ and 1.2, where $T_N=0.5$ and 0.8 K, respectively. Since the magnetic susceptibility is known to be directionally dependent ($\chi_c/\chi_b\sim 3$) in orthorhombic $CeCu_6$, the field suppression of $T_N$ in antiferromagnetic, doped $CeCu_6$ should also be directionally dependent. Thus the results of this first work (see also Heuser, 1999)—$\rho=\rho_0+AT$ (0.1–0.4 K), $C/T\sim-\log T$ (0.3–3 K), $(1/\chi-1/\chi_0)\sim aT^{0.9}$—needed to be extended to single crystals.

Heuser's second study (Heuser *et al.*, 1998) was on a single crystal of $CeCu_{5.2}Ag_{0.8}$, $T_N=0.74$ K, to which a field was applied. At $B_{crit}=2.3$ T, $B$ parallel to the $c$ (easy) axis, where $T_N\rightarrow 0$ it was found that:

(1) $\rho=\rho_0+AT^{1.4\pm0.1}$ between 0.03 and 0.17 K (see also Scheit *et al.*, 1999), followed by $\rho=\rho_0+AT$ up to 0.3 K,
(2) $C/T\sim\gamma_0-aT^{0.5}$ between 0.07 and 0.20 K, followed by $C/T\sim-\log T$ behavior up to 1.2 K (see Fig. 31),

i.e., specific-heat work to temperatures below 0.3 K revealed a change in the higher-temperature, $\log T$ behavior. At $B_{crit}=5$ T, $B\|a$ and separately at $B_{crit}=5.7$ T, $B\|b$, Heuser reported (1999) that the specific heat of $CeCu_{5.2}Ag_{0.8}$ follows $C/T\sim-\log T$ between 0.3 and 2 K, but that at lower temperatures the $C/T$ data bend over into apparent Fermi-liquid behavior, i.e., the data cannot be fit to $\gamma_0-aT^{0.5}$. Thus only in the easy-axis direction in $CeCu_{5.2}Ag_{0.8}$ are sufficient long-range magnetic interactions remanent in $B_{crit}$ to cause non-Fermi-liquid behavior.

These easy-axis, $B\|c$, $\rho$ and $C/T$ results (see Fig. 32 for a phase diagram) are consistent with the self-consistent renormalization theory of Moriya and coworkers [see Table I(b)] even though the effect of field is not considered in their published theories. However, Moriya has communicated that the results of the self-consistent renormalization theory should remain unchanged if the field applied is not too high, which applies to the few Tesla used in Heuser's work (Moriya and Takimoto, 1998). Using the self-consistent renormalization theory to calculate $y_0$ (as discussed above in the theory section, $y_0=0$ at a quantum critical point), Heuser (1999) finds that $y_0=0.02$ at 2.3 T, $B\|c$ from the data (Fig. 31) for single-crystal $CeCu_{5.2}Ag_{0.8}$. Increasing field—as found also in non-Fermi-liquid systems achieved with other methods (doping, pressure, or as-prepared)—suppresses the long-range magnetic correlations, and Fermi-liquid behavior is recovered (see Fig. 31) at low temperatures in both the specific heat and the resistivity. In addition, as seen just above $P_{crit}(T_N\rightarrow 0)$ by Umeo *et al.* in their pressure-induced non-Fermi-liquid behavior study of $Ce_7Ni_3$, the coefficient $A$ in $\rho=\rho_0+AT^2$ just above $B_{crit}$ is very large and decreases with increasing field very rapidly (Scheidt *et al.*, 1999).

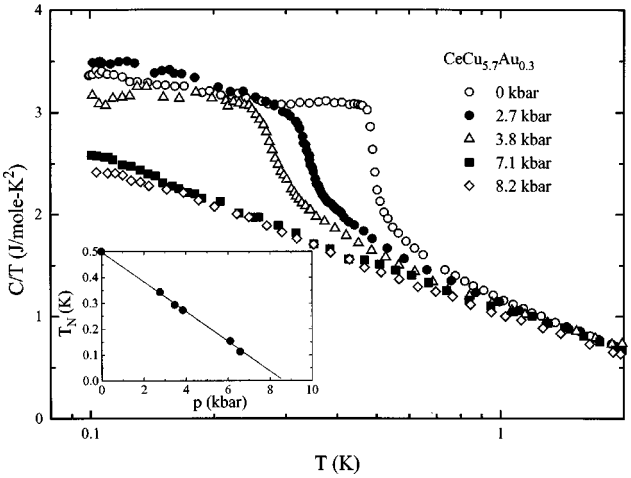


FIG. 27. $C/T$ vs $\log T$ of the antiferromagnet $CeCu_{5.7}Au_{0.3}$ as a function of pressure, after Bogenberger and von Löhneysen (1995). From the extrapolation of $T_N$ to $T=0$ with increasing pressure shown in the inset, there may be an antiferromagnetic transition slightly below the lowest temperature of measurement, 0.1 K at 7.1 kbar, where the $C/T$ data show more than a decade in temperature agreement with $C/T\sim-\log T$. If this is the case, then this would correspond—in Fig. 2—to being to the left of the quantum critical point as a function of pressure at 7.1 kbar.

Interestingly, Heuser reports at $B_{crit}=2.3$ T, $B\|c$ for $CeCu_{5.2}Ag_{0.8}$ that $1/\chi-1/\chi_0=aT$, i.e., just the Curie-Weiss law, over the broad temperature range of 1.8 and 40 K (Heuser, 1999) with a calculated effective moment of $2.4\mu_B$, or rather close to the effective moment ($2.54\mu_B$), $\mu_{eff}$, of a local $f^1$ state. This simple Curie-Weiss power law compares to $1/\chi-1/\chi_0=aT^{0.8}$ for $CeCu_{5.8}Ag_{0.2}$ in $B=0$ (see Table II). For work on another single crystal $CeCu_{5.7}Ag_{0.3}$, with $T_N=0.22$ K, Heuser (1999) finds the same Curie-Weiss behavior (and same $\mu_{eff}$) at $B_{crit}=0.7$ T, $B\|c$, from 1.8 to 30 K, i.e., this large temperature range and agreement in the temperature dependence between two systems with widely varying $T_N$ values at their respective $B_{crit}$ values argues for a common underlying reason. Further, another system discussed above in Sec. III.C.2.c in this review, $Ce_7Ni_3$ at $P_c\sim 3.9$ kbar, which is at the critical parameter for $T_N\rightarrow 0$, also showed a simple Curie-Weiss behavior for the susceptibility, with $\mu_{eff}=1.7\mu_B$. At the very least, this coincidence deserves further investigation.

For the resistivity and specific heat in the field-induced non-Fermi-liquid system $CeCu_{5.7}Ag_{0.3}$ at $B_{crit}=0.7$ T, $B\|c$, the behavior is also similar to that found for single-crystal $CeCu_{5.2}Ag_{0.8}$ (see Table II). The noteworthy difference is that the deviation from the higher-temperature $\log T$ behavior in $C/T$ first occurs below 0.13 K, with $y_0$ derived from the data equal to 0.015. Apparently, as the doping is decreased towards the critical doping where $T_N\rightarrow 0$ in zero field, the $\log T$ behavior extends to lower and lower temperature in a monotonic fashion, trending toward the disappearance of the $\gamma_0-aT^{0.5}$ and instead $C/T\sim-\log T$ to the lowest temperatures measured at $x_{crit}=0.2$, as reported above in the doping section.

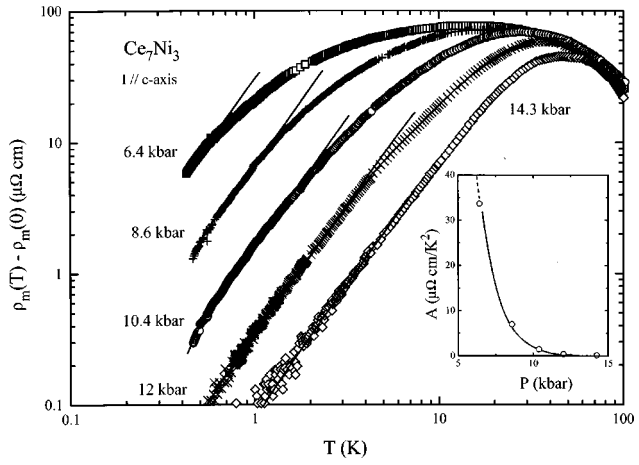


FIG. 28. $\log(\rho-\rho_0)$ vs $\log T$ for a single crystal of $Ce_7Ni_3$ as a function of pressure above the critical pressure where $T_N \to 0$, after Umeo *et al.* (1996a, 1996b): straight lines, $\rho=\rho_0+AT^2$ behavior, which grows in its temperature range of extent while the coefficient $A$ falls monotonically with increasing $P>P_c$, as shown in the inset.

Scaling of the specific heat and magnetization of both single-crystal $CeCu_{5.7}Ag_{0.3}$ and $CeCu_{5.2}Ag_{0.8}$ with magnetic field has been performed—the resultant scaling exponents are 0.9 and 1.6 for the two compounds, respectively, and for each compound $C$ and $\chi$ give the same result, as expected. Interestingly, at low temperatures where $C/T$ deviates from the $\log T$ behavior in $CeCu_{5.2}Ag_{0.8}$ (i.e., below 0.20 K), the scaling fails to bring the various sets of data, $B>B_{\rm crit}$, onto a common curve (Heuser *et al.*, 1998b), as discussed above in the theory section. Since the self-consistent renormalization theory is for weakly interacting spin fluctuations, and scaling should work in strongly coupled systems, this was

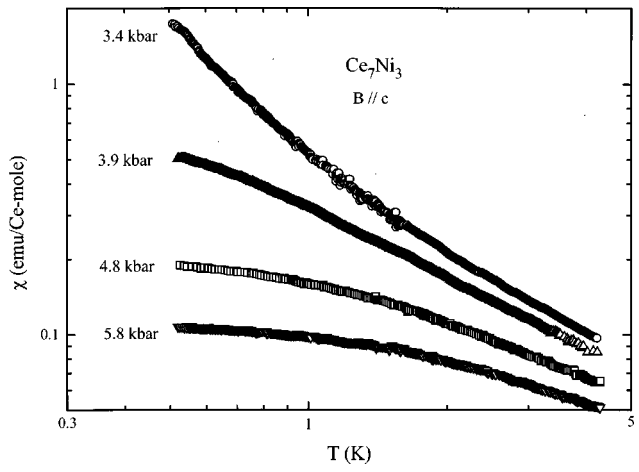


FIG. 29. $\log\chi$ vs $\log T$ for a single crystal of $Ce_7Ni_3$, $B\|c$, as a function of pressure, after Umeo *et al.* (1998). For $P=3.4$ and 3.9 kbar the $\chi$ data do not follow a straight line, i.e., $\chi$ does not obey $T^{\alpha}$, whereas for $P=4.8$ and 5.8 kbar, Umeo *et al.* remark that their $\chi$ data show a tendency at low temperature to saturate towards a constant, or apparent Fermi-liquid behavior.

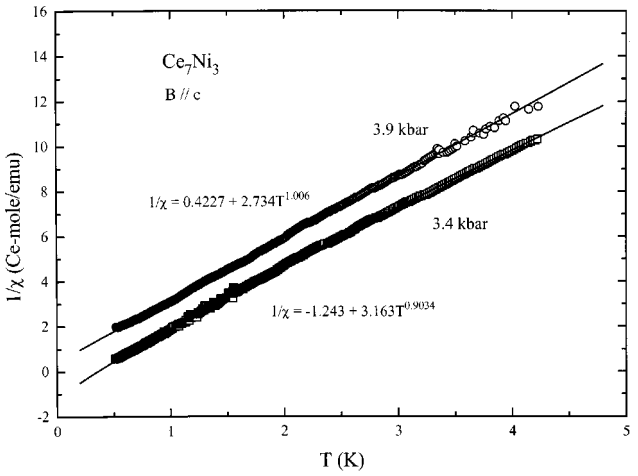


FIG. 30. The $\chi$ data from Fig. 29 for $Ce_7Ni_3$, $B\|c$, for 3.4 and 3.9 kbar, replotted to show that the data follow $\chi^{-1}=\chi_0^{-1}+aT^{\alpha}$, with $\alpha=0.9$ and 1.0, respectively, over the whole temperature range of measurement.

considered to be as expected. However, more recent work on $U_2Co_2Sn$, in which $C/T=\gamma_0-aT^{0.5}$ between 0.3 and 10 K as discussed above in the undoped section, found scaling to function. Perhaps the solution to this apparent discrepancy lies in the observation that such a broad temperature range for finding $C/T=\gamma_0-aT^{0.5}$ is in fact inconsistent with the self-consistent renormalization theory, and thus perhaps $U_2Co_2Sn$ is not a weak-coupling system despite the apparent weak-coupling temperature dependence.

### *b. $YbCu_{5-x}Al_x$*

Polycrystalline samples of both $x=1.6$ ($T_N=0.25$ K) and $x=1.7$ ($T_N=0.55$ K) have been studied for field-induced non-Fermi-liquid behavior (Bauer, Galatanu, *et al.*, 2000; Seuring *et al.*, 2000). $C/T$ followed $\sim-\log T$ between 0.3 and 3 K and 0.3 and 5 K for the two compositions, with $B_{\rm crit}=2.0$ and 2.5 T, respectively. At the respective $B_{\rm crit}$, the resistivity followed $\rho=\rho_0+AT^{1.5}$ for both compositions between 0.03 and 0.32 K, followed by a regime that was linear in temperature up to ~0.5 K. This argues that measurements of the specific heat to lower temperatures[5] would show deviations at $B_{\rm crit}$ from $C/T\sim-\log T$ consistent with the self-consistent renormalization theory. The magnetic susceptibility for $x=1.7$ in $B_{\rm crit}=2.5$ T follows a $1-a\sqrt{T}$ behavior between 1.8 and 6 K. With increasing field above the respective $B_{\rm crit}$ values, both compositions have scaling of the specific heat with field, with $\beta=1.5$. Increasing field above $B_{\rm crit}$ causes $\rho=\rho_0+AT^2$ over a temperature regime that grows monotonically with field, with the co-

[5]Such measurements would need to be on single crystals due to directional dependence effects—as seen above for field-induced non-Fermi-liquid behavior in $CeCu_{6-x}Ag_x$—which are important in $C/T$ below 0.3 K.

efficient $A$ very large just at $B_{\rm crit}$ and then rapidly decreasing with increasing field.

#### c. $YbRh_2Si_2$

As discussed above in Sec. III.B.4, $YbRh_2Si_2$ ($T_N$=0.065 K) shows non-Fermi-liquid behavior above ~0.100 K in the resistivity and, above 0.4 K, in the specific heat. Custers and Gegenwart (2001) discovered that the non-Fermi-liquid behavior in the resistivity, $\rho=\rho_0+AT$, could be extended downwards in their high precision resistivity data by the application of a sufficient field (0.05 T for $B\|a$, 0.7 T for $B\|c$) to suppress the antiferromagnetism. For $B\|a$, the linear behavior in $\rho$ extended down to the lowest temperature of measurement, 0.020 K, while for $B\|c$ there were deviations below 0.030 K.

#### d. $CeCu_{5.8}Au_{0.2}$

In addition to the field-induced non-Fermi-liquid behavior for $CeCu_{6-x}Ag_x$ discussed just above in Sec. III.D.1.a, the search for field-induced non-Fermi-liquid behavior has now been extended (von Löhneysen *et al.*, 2001) to $CeCu_{5.8}Au_{0.2}$. Interestingly, although the resistivity results agree with the Ag-doped results, the specific heat of $CeCu_{5.8}Au_{0.2}$ in a sufficient field (0.5 T) in the $c$-axis direction to suppress the antiferromagnetism obeys $C=\gamma_0-AT^{0.5}$, or weak coupling Millis-Hertz/Moriya behavior for a three-dimensional system with antiferromagnetic correlations (see Table I). This is in contrast to the $C/T\sim-\log T$ behavior found in $CeCu_{6-x}Ag_x$ in field, as well as the $C/T\sim-\log T$ behavior found for pressure suppression of $T_N$ in $CeCu_{6-x}Au_x$ itself. This difference in the magnetic fluctuations remaining after field or pressure has suppressed $T_N$ is worthy of further investigation.

### 2. Metamagnetic systems

Just as doping can either suppress or induce magnetism in a phase diagram, field can either suppress antiferromagnetism or induce "metamagnetism," the signature of which is usually taken to be a sharp rise in the magnetization $M$ vs $B$ at $B_{\rm metamag}$ for field in a particular crystalline direction. Current theoretical understanding of metamagnetism is incomplete (Held *et al.*, 1997), and there are certainly systems in which a sharp rise in $M$ vs $B$ is observed at $B_{\rm metamag}$ without there being strong, long-range magnetic interactions persisting to low temperatures also at $B_{\rm metamag}$ to cause non-Fermi-liquid behavior at that field—for example, as found recently at $B_{\rm metamag}$=18.5 T in $UPd_2Al_3$ (Kim, Alwood, and Steward, 2001). However, three heavy-fermion systems have been found in which non-Fermi-liquid behavior is observed in field near $B_{\rm metamag}$.

#### a. $CeRu_2Si_2$ ($B_{metamag}$=8 T)

In work focused on other properties, Aoki *et al.* (1998) found that $C/T(B_{\rm metamag})\sim a-bT$ in $CeRu_2Si_2$ between 0.2 and 0.9 K. Heuser *et al.* (2000) have since focused on the non-Fermi-liquid behavior in $CeRu_2Si_2$ at $B_{\rm metamag}$ and found that $C/T(B_{\rm metamag})\sim a-bT$ between 0.06 and 1.8 K (see Table II) for $B\|c$, while $C/T\sim$const for fields only 1 T away from $B_{\rm metamag}$. However, as stated above, a large volume change takes place at $B_{\rm metamag}$ (Flouquet *et al.*, 1995), and how the specific heat at constant volume $C_V$ (instead of the measured specific heat at constant pressure $C_P$), behaves at $B_{\rm metamag}$ should be investigated.

#### b. $UPt_3$ ($B_{metamag}$=20.5 T)

Inspired by the findings in $CeRu_2Si_2$, Kim, Hall, *et al.* (2000) investigated the resistivity, magnetization, and specific heat as a function of field at and around $B_{\rm metamag}$ in hexagonal $UPt_3$, where the crystalline direction at which the sharp rise in $M$ vs $H$ occurs is perpendicular to the $c$ axis, or in the $a$-$b$ plane. Data for $C/T$, $\chi$ ($=M/B$), and $\rho$ indicated Fermi-liquid behavior at 18 T, as did data for $C/T$ and $\rho$ at 24 T, with $\chi$ displaying apparent weak ferromagnetism above $B_{\rm metamag}$. However, at (or near) $B_{\rm metamag}$ in $UPt_3$, $B\perp c$, clear non-Fermi-liquid behavior over more than a decade in temperature was found: $C/T$ followed $\sim-\log T$ from 0.5 to 10 K and $\chi=\chi_0-aT$ between 0.5 and 20 K at $B_{\rm metamag}$, while $\rho=\rho_0+AT^{1.2}$ between 0.5 and 3 K at 22 T.

#### c. $Sr_3Ru_2O_7$ ($B_{metamag}$=5.5 T)

The magnetization of single crystal $Sr_3Ru_2O_7$, $B$ in the $ab$ plane shows (Perry *et al.*, 2001) a jump of $\sim0.15\mu_B$ at $B_{\rm metamag}$=5.5 T. Near $B_{\rm metamag}$, Perry *et al.* report that the resistivity is given by $\rho=\rho_0+AT$ at low temperatures, where 2.5 K was the lowest temperature of measurement. They further report (see Table II) that $C/T\sim-\log T$ near (7.7 T), but not at, $B_{\rm metamag}$.

Work on other metamagnetic heavy-fermion systems is continuing to look for non-Fermi-liquid behavior caused by long-range magnetic interactions that occur just below the field-induced (or "meta") magnetism at $B_{\rm metamag}$. The systems discussed here, in which non-Fermi-liquid behavior is induced when $B\rightarrow B_{\rm metamag}$, may be similar to the findings discussed above of (a) non-Fermi-liquid behavior in $\rho$ in zero field (with a lowest temperature, however, of only 1.8 K) for UCoAl, where $B_{\rm metamag}$=0.6 T, and (b) pressure-induced metamagnetism in MnSi at the critical pressure where $T_{\rm Curie}\rightarrow0$ and non-Fermi-liquid behavior is observed in $\rho$.

## IV. DISCUSSION AND CONCLUSIONS

At present, it seems clear that there is a class of materials that show remarkable, even divergent, behavior in their physical properties at low temperatures. This group of over 50 non-Fermi-liquid materials seems to have sufficient consistency in its properties, which are sufficiently reproducible, that it poses a serious exception to the previously accepted Landau Fermi-liquid description of the metallic state at low temperatures. Disorder and sample quality have begun to be recognized as important in at least many of these systems. It is now

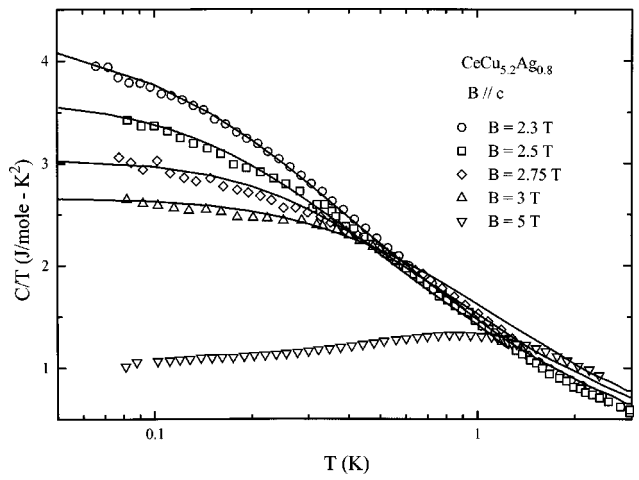


FIG. 31. $C/T$ vs $\log T$ for a single crystal of $CeCu_{5.2}Ag_{0.8}$ as a function of magnetic field, $B \| c$, $B \geq B_c$, where $T_N \rightarrow 0$, after Heuser *et al.* (1998b): solid lines, fits to data at each field to the self-consistent renormalization theory of Moriya and coworkers, for the specific heat as discussed in the text. For $B = B_c$ (2.3 T), the fit parameter $y_0 = 0.02$, i.e., the data are—according to the self-consistent renormalization theory—close to but not exactly at a quantum critical point.

incumbent on researchers involved in this study to perform precise measurements on well-characterized samples so as not to lose sight of the ultimate goal—understanding the intrinsic physics in these fascinating alloys and compounds.

Having presented both the theory and current experimental status of non-Fermi-liquid behavior, with Table I summarizing the various theoretical predictions and Table II summarizing the resistivity, susceptibility, specific-heat, and entropy measurements of each non-Fermi-liquid system, let us now try to find some common thread of understanding in this quite varied and extensive body of work. After a discussion of the characteristic temperature $T_0$, each measured parameter will be discussed in turn, followed by brief concluding remarks.

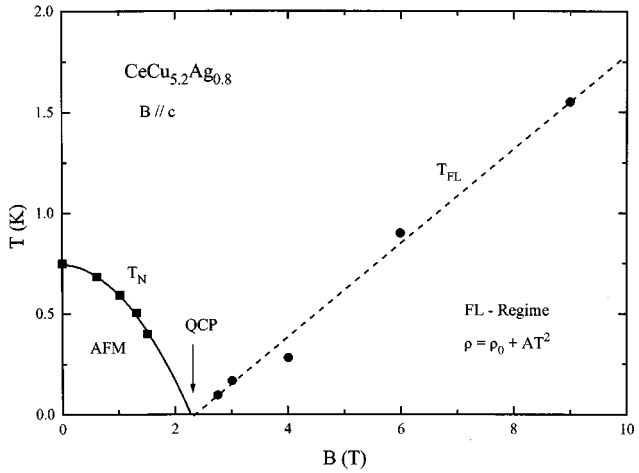


FIG. 32. The phase diagram for field-induced non-Fermi-liquid behavior in $CeCu_{5.2}Ag_{0.8}$ after Heuser (1999) and Heuser *et al.* (1998b), in analogy to the schematic diagram of Millis, Fig. 2. Increasing field suppresses antiferromagnetism until, at approximately 2.3 T, a quantum critical point is reached. At this field, non-Fermi-liquid behavior should be observed down to $T=0$. With further increase of the field, a crossover behavior with decreasing temperature is observed, with non-Fermi-liquid behavior observed in the resistivity above the dashed crossover line and Fermi-liquid (FL) behavior observed in the resistivity below this line.

### A. Characteristic temperature, $T_0$

Called $T_K$, or the Kondo temperature, in works that stress the multichannel Kondo model, this characteristic temperature has been calculated from both resistivity and specific-heat data, as discussed and displayed in Table II for all the non-Fermi-liquid systems reviewed herein. Due to the variety of temperature dependences found for $\chi$, Table II does not report $T_0$ derived from $\chi$, since intercomparisons of $T_0$ between systems with different temperature dependences would be less valid.

$T_0$ gives an idea of the energy scale for the electron-electron interactions causing the non-Fermi-liquid behavior or, in the Kondo picture, $T_K$ is the temperature below which the local moment is compensated by the conduction electrons, with $A$ in $\rho = \rho_0 + AT^{\alpha}$ proportional to $T_0^{-\alpha}$ and $C/T$ at 1 K roughly proportional to $T_0^{-1}$. It is noticeable immediately that $T_0$ derived from $\rho$ data and $T_0$ derived from $C/T$ data, although roughly tracking each other, are quite different in magnitude, indicating limits on the utility of this parameter. In addition, the assignment of $T_0$ is not unique, and a number of methods exist for arriving at this value. For example, in Table II, $T_0$ has been found by setting the slope of the $C/T$ vs $\ln T$ plot equal to $-R(0.25/T_0)$, where $R = 8.314$ J is the gas constant. One can also find $T_0$ by setting the temperature where the (extrapolated) $C/T$ vs $-\ln T$ line intercepts the temperature axis equal to $0.41T_0$. This gives a different numerical value; e.g., for the data for $U_{0.2}Y_{0.8}Pd_3$ of Seaman *et al.* (1991), this intercept method gives $T_0 = 135$ K instead of the result of the slope method for the specific heat, which gives the $T_0 = 42$ K value for the data of Seaman *et al.* listed in Table II. Thus, rather than focusing on the absolute values of $T_0$ shown in Table II, the usefulness of this parameter—derived from either the $\rho$ or the $C/T$ data—is to identify trends and to help intercompare systems semiquantitatively.

As an example of such a trend, consider the efforts to obtain higher-quality $CeNi_2Ge_2$ in order to identify the "intrinsic" value of $\alpha$ in $\rho = \rho_0 + AT^{\alpha}$ for comparison to the theory of Rosch. The current best value of $\alpha$ (Geibel, 2000) is approximately 1.4, where the "best" sample is defined as having the minimum residual resistivity $\rho_0$. This minimum-disorder sample also shows the lowest value of $T_0$ as derived from the resistivity, thus establishing $T_0$ as a possible parameter additional to $\rho_0$ for tracking sample quality. (Note that the specific heat of the various $CeNi_2Ge_2$ samples is similar enough that the $T_0$

values derived from the specific heat are, well within the ±5% error bar, all the same.)

Where specific-heat data are lacking, e.g., in many of the high-pressure-induced non-Fermi-liquid systems, $T_0$ derived from the resistivity may be used to estimate the size of the specific heat, with lower $T_0$ values indicating larger specific-heat values (see, for example, $UBe_{13}$ in Table II). Of particular note is the lowest $T_0$ in Table II, 0.2 K for $CeCu_2Ge_2$ at 101 kbar.

These useful aspects of $T_0$ having been mentioned, it should be noted that $T_0$ values derived from $\rho$ data where there is a negative $A$ coefficient—based on the experience with annealed $UCu_4Pd$—may not be representative of the intrinsic nature of the sample, i.e., $T_0$ based on the specific heat may be more indicative of the intrinsic behavior of the material.

### B. Resistivity

It would normally be attractive to separate non-Fermi-liquid systems that show non-Fermi-liquid temperature dependence with a positive slope ($\rho=\rho_0+AT^\alpha$, $\alpha\neq 2$) from those with a negative slope ($\rho=\rho_0-AT^\alpha$), with the statement that a rising resistivity in a metal with decreasing temperature is certainly a qualitatively different behavior than the normal, metallic, falling resistivity with decreasing temperature. A discussion of the exponent in light of various theories, including Rosch's (1999) theory on the influence of disorder on the temperature dependence of $\rho$, would then follow. Unfortunately, the recent work of Weber *et al.* (2001) shows that—at least in $UCu_4Pd$—annealing drastically reduces the negative slope seen in unannealed material and also changes the temperature dependence. Thus this review can do no more than note the systems with negative slope with temperature listed at the top of Table II (all unannealed), together with the obviously important effect of annealing pointed out by Weber *et al.*, and appeal for further annealing studies—particularly in the prototype system $U_{0.2}Y_{0.8}Pd_3$.

Another parameter in the resistivity besides the slope that mirrors order in the lattice is the residual resistivity, $\rho_0$, which for the non-Fermi-liquid systems shown in Table II is—as expected—the smallest for an undoped non-Fermi-liquid system, $CeNi_2Ge_2$. This system, with the smallest $\rho_0$ ($0.34\,\mu\Omega$) of any known non-Fermi-liquid system, and a residual resistivity ratio of 200, is also one of the most thoroughly studied, with $\rho=\rho_0+AT^\alpha$, $\alpha=1.4$, between 0.02 and 2.5 K. In the theory of Rosch (1999; see Fig. 3), such a residual resistivity ratio would correspond to a fairly well-ordered system, with the parameter $x$ in Fig. 3 around $10^{-2}$ or $10^{-3}$. The theoretical curves shown in Fig. 3 would then suggest that, at temperatures lower than 0.02 K, the exponent $\alpha$ in $CeNi_2Ge_2$ should fall to 1.2—or measurably smaller than 1.4. The residual resistivity, $\rho_0$, is notoriously sample dependent as verified by the data in Table II: various samples of $CeNi_2Ge_2$ have $\rho_0$ values differing by a factor of 8, while annealing $UCu_4Pd$ lowers $\rho_0$ by a similar factor, and a different preparation of $U_2Co_2Sn$—perhaps due to cracks—has $\rho_0$ lower by a factor of 13. Before any attempt is made to experimentally check Rosch's theory (Fig. 3) for the temperature dependence of the exponent $\alpha$ to milliKelvin temperatures, the degree of the disorder—preferably in a series of samples with differing thermal histories—should be well characterized.

An additional resistivity parameter in Table II with unusual values for certain systems is also worth comment: the large positive slope observed in $CeCu_{5.9}Au_{0.1}$, $CeCu_2Si_2$, $UBe_{13}$, and field-induced $CeCu_{6-x}Ag_x$. The coefficient $A$ in $\rho=\rho_0+AT^\alpha$ varies between 14.9 and 69 $\mu\Omega\,\mathrm{cm/K}^\alpha$ for these four systems; a much more typical number would be $\sim 0.3\ \mu\Omega\,\mathrm{cm/K}^\alpha$ with $U_2Pt_2In$ intermediate at $A=8.5\ \mu\Omega\,\mathrm{cm/K}^\alpha$. These four systems have two other commonalities: the resistivity follows $\rho_0+AT^\alpha$ over a more limited temperature range than observed in most other systems and, consistent with the expected smaller than typical characteristic temperature $T_0$ [expected since $T_0\equiv(\rho_0/A)^{1/\alpha}$], the specific heat divided by temperature at 1 K is larger than observed in most other systems. Such a large slope of the resistivity vs temperature implies a higher density of electron-scattering excitations at low energies that then, with increasing temperature above $T=0$, become populated and increase the resistivity with increasing temperature more rapidly. This would imply an associated difficulty in observing dHvA oscillations in these four systems, which is at least consistent with the present inability to observe dHvA oscillations in $UBe_{13}$ (Goodrich, 2000).

To compare with the theories of Table I, the expectation that, as $T\to 0$, $\alpha=1.5$ for a three-dimensional antiferromagnet and 1.0 for a two-dimensional antiferromagnet finds good agreement with a number of systems listed in Table II. Of course, in these *a priori* three-dimensional systems, $\alpha=1.0$ then requires some argument about the two-dimensional nature of the spin excitations. Although one such system ($CeCu_{5.9}Au_{0.1}$) has neutron-scattering evidence of such two-dimensionality (Schröder *et al.*, 1998; Stockert *et al.*, 1998), such verification is lacking for the other $\alpha=1$ systems and would be a worthwhile goal for future neutron-scattering investigations. For the four systems in Sec. III.A.4 that are near to a ferromagnetic instability, one system ($U_xTh_{1-x}Cu_2Si_2$) has a specific heat ($C/T\sim-\log T$) and a resistivity ($\sim T$) that agree with the noninteracting fluctuation theory of Millis, while one system ($Ni_xPd_{1-x}$) has $C/T\sim-\log T$ and $\rho\sim T^{5/3}$, which agree with the theories of Moriya *et al.* and of Lonzarich.

Finally, it is worth noting that the resistivity often shows a pure temperature law non-Fermi-liquid behavior to much lower temperatures (e.g., down to 0.02 K in $U_{0.2}Y_{0.8}Pd_3$) than observed in the specific heat, where deviations below 0.2 or 0.3 K from a pure $C/T\sim-\log T$ behavior are quite common. See Coleman's (1999) discussion of the theories of non-Fermi-liquid behavior for a discussion of why the resistivity may not recover Fermi-liquid behavior at low temperatures.

### C. Susceptibility

The measurement of the magnetic susceptibility as a function of temperature and field gives important infor-

mation about the behavior of the magnetic moments, their screening, and interactions in a material. Thus such data are central to trying to understand non-Fermi-liquid behavior and are the basis for, e.g., the determination of the distribution $P(T_K)$ of Kondo temperatures in the Kondo disorder model. If the magnetization as a function of field for a system is linear (as in, e.g., $U_{1-x}Y_xAl_2$), then generally there is not a large number of uncompensated spins present, arguing against the Kondo disorder model. Information on spin-glass behavior gathered through measurement of the frequency dependence of $\chi_{ac}$ and through measurement of irreversible behavior in $\chi_{\text{field cooled}}$ vs $\chi_{\text{zero-field cooled}}$ can be a useful indicator for whether the Griffiths-phase model for non-Fermi-liquid behavior is applicable in a given system, although possible quantum effects at low temperatures may cloud the issue. Despite the obvious utility of magnetic susceptibility data, the measurement of $\chi_{dc}$ below 1.8 K is quite rare, leaving an intercomparison of temperature dependencies (required, for example, in a test of the Griffiths-phase model prediction of $C/T \sim \chi \sim T^{-1+\lambda}$) in a common low-temperature regime between $\rho$, $\chi$, and $C/T$ results lacking in the large majority of non-Fermi-liquid systems, as may be seen in Table II. Clearly, the variety of observed temperature dependencies in $\chi$ is much larger than for either $\rho$ or $C/T$, making the lack of low-temperature data, where one might hope to find a pure temperature dependence instead of possibly some crossover behavior, particularly important. Another experimental difficulty is the occasional strong directional dependence of $\chi$ for the various crystalline lattice directions (e.g., in $Ce_7Ni_3$), making determination of temperature dependencies from polycrystalline material—which most of the samples studied are—somewhat problematic.

However, when low-temperature $\chi$ data are available, they help substantially in understanding the non-Fermi-liquid behavior. The work of deAndrade *et al.* (1998) compared low-temperature $\chi_{dc}$ data (down to 0.5 K) and $C/T$ data (down to 0.1 K) to the $T^{-1+\lambda}$ Griffiths-phase model with relatively good agreement between $\lambda_C$ and $\lambda_\chi$. A replotting in the present review of the $\chi_{dc}$ data for one of the samples considered by deAndrade *et al.*, $U_{0.6}Th_{0.4}Pd_2Al_3$, as $\chi^{-1}-\chi_0^{-1}$ vs $T^\alpha$ found agreement over a much broader temperature range, with an altered $\lambda_\chi$. Such a replotting of the $\chi$ data as $\chi^{-1}-\chi_0^{-1}$ vs $T^\alpha$ found the broadest temperature range of agreement for this form for $UCu_{3.5}Pd_{1.5}$—up to 200 K. If experimental investigations on the possibility of local deviations (Si *et al.*, 1999, 2000; Coleman, 1999) from Fermi-liquid behavior are to be carried out, this would be a possible candidate system to study. Interestingly, a doped system in which successive efforts have precisely determined $x_c$ for non-Fermi-liquid behavior in $C/T$ down to 0.15 K [$Ce(Ru_{0.6}Rh_{0.4})_2Si_2$], a system at the critical pressure for suppression of $T_N \to 0$ ($Ce_7Ni_3$) and both systems for which single crystals are available at the critical magnetic field for suppression of $T_N \to 0$ ($CeCu_{5.2}Ag_{0.8}$ and $CeCu_{5.7}Ag_{0.3}$) show $\chi^{-1}-\chi_0^{-1} \sim T^\alpha$, $\alpha = 1$—or simple Curie-Weiss behavior of local moments.

Systems with other temperature dependencies over large ranges of temperature are $(U_{1-x}La_x)_2Zn_{17}$ ($\chi = \chi_0 - a\sqrt{T}$ between 1.8 and 40 K) and $Ce_{0.1}La_{0.9}Cu_2Si_2$ ($\chi = \chi_0 - a \log T$ between 1.8 and 20 K). In general, however, the observed temperature dependencies were found only over limited (less than a decade in temperature) ranges. This is certainly consistent with possible crossover behavior being observed in the rather high-temperature regime commonly measured (starting at 1.8 K), and underlines the need for further work to lower temperatures.

The class of doped systems far from a magnetic instability (e.g., where $T_N \to 0$) but with spin-glass behavior possibly or certainly present remains a fertile field of interest for disorder-induced non-Fermi-liquid theories, and is certainly worthy of concerted effort to characterize the non-Fermi-liquid properties—including the spin-glass behavior—as a function of annealing. The disappearance of the frequency dependence of the peak in $\chi_{ac}$ (i.e., apparent disappearance of spin-glass behavior) in annealed $UCu_4Pd$ (Weber *et al.*, 2001), coupled with the still-present-after-annealing non-Fermi-liquid behavior of the specific heat ($C/T \sim -\log T$), certainly supports the need for further annealing studies. The prototype non-Fermi-liquid system, $U_{0.2}Y_{0.8}Pd_3$, on which so much spin-glass characterization has been done (Gajewski *et al.*, 1996) is certainly one candidate for such work. A check to see if there is spin-glass behavior at temperatures lower than 1.8 K in $UCu_{5-x}Pt_x$ would be interesting.

Finally, more theoretical input on the expected temperature dependence of $\chi$ with disorder, as well as work about crossover, higher-temperature, temperature dependencies, would help in understanding non-Fermi-liquid behavior.

### D. Specific heat

This review has mostly dealt with systems that have a specific heat that shows a pure temperature dependence (primarily $C/T \sim -\log T$), or can be fit to a theory [e.g., the two-channel Kondo model ($U_{1-x}Th_xRu_2Si_2$) or the self-consistent renormalization theory ($Ce_{1-x}La_xRu_2Si_2$)], over at least a decade in temperature. As has been stressed here, the decision to identify a material as exhibiting non-Fermi-liquid behavior is based on a consideration of more than just one measured parameter. However, since the specific heat for a number of materials displays, for example, $C/T \sim -\log T$ up to 10 K or sometimes even 20 K (if the subtraction of the lattice contribution can be reliably made), and since the specific heat is fairly routinely measured down to 0.3 K, considering a system as belonging to the non-Fermi-liquid class of materials without this broad temperature range of observed non-Fermi-liquid temperature dependence in $C/T$ should be done only if there is convincing evidence in both the $\rho$ and $\chi$ data for non-Fermi-liquid behavior. That said, several systems have been listed in this review, e.g., $CeCu_2Si_2$, whose non-Fermi-liquid behavior does not meet this broad

temperature range stricture. This has been done in order to give the reader some idea about the properties of systems "on the edge" of non-Fermi-liquid behavior, to provide a link to the much broader class of Fermi-liquid materials. The properties of such systems, as was shown via the discussion about early work on $Ce(Ru_{0.5}Rh_{0.5})_2Si_2$ that led to finding the quantum critical point precisely at $Ce(Ru_{0.6}Rh_{0.4})_2Si_2$, may also indicate the presence of a quantum critical point nearby in their phase diagram. In addition, as more is learned about this class of systems, the focus of what is interesting and important for furthering understanding will change, and too narrow a focus in this early review might prevent making important correlations later that are visible only after further theoretical and experimental work.

One of the puzzles apparent when considering the specific-heat data for over 50 systems together is that a few systems showed a more divergent behavior than $\log T$ (i.e., an upturn on a $C/T$ vs log-$T$ plot) at the lowest temperatures. These systems are $U_{0.2}Y_{0.8}Pd_3$, $UCu_{3.5}Al_{1.5}$, $U_2Cu_{12}Al_5$, $U_{0.9}Th_{0.1}Ni_2Al_3$, $CeCo_{1.2}Cu_{0.8}Ge_2$, $U_{0.03}Th_{0.97}Cu_2Si_2$, $YbRh_2Si_2$, and at least some samples of $CeNi_2Ge_2$. Since sample dependence was also seen in the only other sample in which more than one measurement exists ($U_{0.2}Y_{0.8}Pd_3$), this unusual behavior should be investigated on carefully annealed samples and preferably down to at least 0.001 K to see if this behavior is some sort of crossover behavior that leads to another pure temperature dependence at even lower temperature. Even if the upturns are only the high-temperature starts of some magnetic ordering transition below 0.1 K, this would be useful to know.

At the other extremum, a few systems show pure, $C/T \sim -\log T$ temperature dependence down to ~0.1 K and over more than one decade of temperature. These systems are $CeCu_{5.9}Au_{0.1}$, annealed $UCu_4Pd$, $U_{1-x}M_xPt_3$, $CePt_{0.96}Si_{1.04}$, $Ce(Ru_{0.6}Rh_{0.4})_2Si_2$, and $CeCu_{5.8}Au_{0.2}$ at $P_{crit}(T_N \to 0)$.

A number of systems were fit to the self-consistent renormalization theory, including $CeNi_2Ge_2$, $CeCu_2Si_2$, $Ce_{1-x}La_xRu_2Si_2$, $U_{1-x}Th_xPt_2Si_2$, and $CeCu_{6-x}Ag_x$ at $B_{crit}(T_N \to 0)$. Often such fits are to the low-temperature-limiting behavior ($C/T = \gamma_0 - A\sqrt{T}$) and not to the full functional form that yields the parameter $y_0$, which, when equal to zero, signifies a system directly at a quantum critical point. Although some values of $y_0$ were close to zero, all the derived values were in fact finite and thus indicative of the system not being directly at the quantum critical point. It is interesting to note the very broad temperature range (0.3–10 K) of $C/T = \gamma_0 - A\sqrt{T}$ dependence in pure $U_2Co_2Sn$; the extent of this temperature dependence is inconsistent with the self-consistent renormalization theory.

This review has extended the work of deAndrade *et al.* (1998) in comparing $\chi$ and $C/T$ data with the functional form $T^{-1+\lambda}$, finding less agreement than did deAndrade *et al.* between $\lambda$ determined from $C/T$ and $\lambda$ determined from $\chi$ in $U_{1-x}Th_xPd_2Al_3$ using the functional form $(\chi^{-1} - \chi_0^{-1}) \sim T^{\alpha}$. Also, with the recent work on annealing $UCu_4Pd$, whereupon $C/T \sim -\log T$ down to 0.07 K, presumably this will remove this system from deAndrade *et al.*'s list of materials that better obey the functional form $T^{-1+\lambda}$. However, this review has, via replotting of published data, found two new systems, neither of which obeys $C/T \sim -\log T$—thus ruling out the problem of distinguishing between two similarly good temperature dependencies—where $C/T \sim T^{-1+\lambda}$: $U_{1-x}Th_xRu_2Si_2$ and $Ce_{1-x}Th_xRhSb$ for various values of $x$. Although lower-temperature data are needed for these systems, they offer new possibilities for investigating the Griffiths-phase scenario for non-Fermi-liquid behavior.

Listed in Table II is the entropy calculated up to 10 K for most of the measured non-Fermi-liquid systems, in an attempt to find a further parameter to help organize such a diverse set of results. A number of systems have $S(10\,\mathrm{K})$ in the $0.6$–$0.9R\ln 2$ range, while a few systems (e.g., $U_{0.07}Th_{0.93}Ru_2Si_2$) have $S(10\,\mathrm{K})$ values below $0.2R\ln 2$. (It should be stressed that these entropy values are expressed per mole of Ce or U; thus a dilute doped system is compared on an equal footing with a concentrated lattice system.) This is an indication that, in the low-entropy systems, only a fraction of the moment-bearing electrons are participating in the non-Fermi-liquid behavior. This may well have significance for understanding the microscopic nature of non-Fermi-liquid behavior, and may indicate that differing regions of the Fermi surface—as in the "hot lines" picture for the resistivity (Hlubilina and Rice, 1995; Coleman, 1999)—have either Fermi-liquid or non-Fermi-liquid nature, with a different proportion for different systems. Since $U_{0.07}Th_{0.93}Ru_2Si_2$, with $S(10\,\mathrm{K}) \sim 0.08R\ln 2$, has a $C/T$ value at 1 K comparable with other systems that have $S(10\,\mathrm{K}) \sim 0.5R\ln 2$, this difference in entropies seems to be indicating a fundamental difference.

This review was started with the hope that assembling together what has become an unmanageable mass of data since the discovery work of Seaman *et al.* in 1991 would help bring some order and insight to the investigation of non-Fermi-liquid behavior; it has perhaps at least raised some useful questions. For example, does the pure Curie-Weiss behavior of the magnetic susceptibility of $Ce_7Ni_3$ at $P_{crit}(T_N \to 0)$, $Ce(Ru_{0.6}Rh_{0.4})_2Si_2$ at $x_c(T_N \to 0)$, and $CeCu_{6-x}Ag_x$ at $B_{crit}(T_N \to 0)$ reveal a heretofore unremarked insight into the behavior of systems at a quantum critical point? Would $\chi$ data under pressure for $CeCu_{5.8}Au_{0.2}$ reveal the same behavior at $P_{crit}$? Why do certain systems show $C/T \sim -\log T$ over more than two decades of temperature down to a lowest temperature of measurement of 0.1 K, while others show more divergent behavior in $C/T$ at lowest temperatures? Are all non-Fermi-liquid systems with a negative temperature coefficient in the resistivity ($\rho = \rho_0 - AT$) going to lose or radically change this behavior upon annealing, as does $UCu_4Pd$?

Clearly, the study of non-Fermi-liquid behavior in *d*- and *f*-electron metals would benefit from further annealing studies and from more work on $\rho$, $C/T$, and especially $\chi$ to lower temperatures. Additional theoretical

guidance as to the behavior of $\chi$ in non-Fermi-liquid systems—which seems experimentally the most diverse of the parameters discussed herein—would be welcome. As to the search after order and insight in the study of non-Fermi-liquid behavior, perhaps this compilation will provide workers in the field a useful tool to that end.

## ACKNOWLEDGMENTS

Just as some interesting systems have no doubt escaped my attempt to make this review as complete as possible in the finite time allotted, the list of people who have aided my efforts to understand non-Fermi-liquid behavior may, as well, have unintentional gaps. For helpful discussions and for the occasional preprint I would like to thank warmly B. Andraka, E. D. Bauer, A. Castro Neto, P. Coleman, D. Cox, C. Geibel, K. Heuser, K. Ingersent, D. MacLaughlin, B. Maple, A. Millis, A. Rosch, E.-W. Scheidt, Q. Si, F. Steglich, J. Thompson, and A. Tsvelik. J. Kim helped do the many figures, and K. Heuser helped with the theory section in the early stages of writing this review. Finally, I would like to thank D. MacLaughlin, E.-W. Scheidt, Q. Si, J. Thompson, and A. Tsvelik for a critical reading of the manuscript. Work at Florida was performed under the auspices of the U.S. Department of Energy, Contract No. DE-FG05-86ER45268.

## REFERENCES

Aeppli, G., E. Bucher, A. I. Goldman, G. Shirane, C. Broholm, and J. K. Kjems, 1988, J. Magn. Magn. Mater. **76-77**, 385.
Affleck, I., and A. W. W. Ludwig, 1991, Nucl. Phys. B **352**, 849.
Aliev, F. G., N. B. Brandt, V. V. Moschalkov, and S. M. Chudinov, 1983, Solid State Commun. **45**, 215.
Altshuler, B. L., L. B. Ioffe, and A. J. Millis, 1995, Phys. Rev. B **52**, 5563.
Amara, M., D. Finsterbusch, B. Luy, B. Lüthi, F. Hulliger, and H. R. Ott, 1995, Phys. Rev. B **51**, 16 407.
Amitsuka, H., T. Hidano, T. Honma, H. Mitamura, and T. Sakakibara, 1993, Physica B **186**, 337.
Amitsuka, H., T. Hidano, T. Sakakibara, T. Suzuki, T. Akazawa, and T. Fujita, 1995, J. Magn. Magn. Mater. **140-144**, 1403.
Amitsuka, H., K. Kuwahara, M. Yokoyama, K. Tenya, T. Sakakibara, M. Mihalik, and A. A. Menovsky, 2000, Physica B **281&282**, 326.
Amitsuka, H., and T. Sakakibara, 1994, J. Phys. Soc. Jpn. **63**, 736.
Amitsuka, H., T. Sakakibara, A. de Visser, F. E. Kayzel, and J. J. M. Franse, 1997, Physica B **230-232**, 613.
Amitsuka, H., T. Shimamoto, T. Honma, and T. Sakakibara, 1995, Physica B **206&207**, 461.
Andraka, B., 1994a, Phys. Rev. B **49**, 3589.
Andraka, B., 1994b, Phys. Rev. B **49**, 348.
Andraka, B., 1994c, J. Alloys Compd. **209**, 43.
Andraka, B., and G. R. Stewart, 1993, Phys. Rev. B **47**, 3208.
Andraka, B., and A. Tsvelik, 1991, Phys. Rev. Lett. **67**, 2886.
Andrei, N., and C. Destri, 1984, Phys. Rev. Lett. **52**, 364.
Andres, K., J. E. Graebner, and H. R. Ott, 1975, Phys. Rev. Lett. **35**, 1779.
Aoki, Y., T. D. Matsuda, H. Sugawara, H. Sato, H. Ohkumi, R. Settai, Y. Onuki, E. Yamamoto, Y. Haga, A. V. Andreev, V. Sechovsky, L. Havela, H. Ikeda, and K. Miyake, 1998, J. Magn. Magn. Mater. **177-181**, 271.
Aoki, Y., K. Terayama, H. Sato, K. Maeda, and Y. Onuki, 1995, Physica B **206-207**, 451.
Aoki, Y., J. Urakawa, H. Sugawara, H. Sato, T. Fukuhara, and K. Maezawa, 1997, J. Phys. Soc. Jpn. **66**, 2993.
Aronson, M., R. Osborn, R. A. Robinson, J. W. Lynn, R. Chau, C. L. Seaman, and M. B. Maple, 1995, Phys. Rev. Lett. **75**, 725.
Bauer, E., A. Galatanu, L. Naber, M. Galli, F. Marabelli, C. Seuring, K. Heuser, E.-W. Scheidt, T. Schreiner, and G. R. Stewart, 2000, Physica B **281-282**, 319.
Bauer, E. D., E. J. Freeman, C. Sirvent, and M. B. Maple, 2000, unpublished.
Belitz, D., T. R. Kirkpatrick, and T. Vojta, 1999, Phys. Rev. Lett. **82**, 4707.
Bernal, O. O., D. E. MacLaughlin, A. Amato, R. Feyerherm, F. N. Gygax, A. Schenck, R. H. Heffner, L. P. Le, G. J. Nieuwenhuys, B. Andraka, H. von Löhneysen, O. Stockert, and H. R. Ott, 1996, Phys. Rev. B **54**, 13 000.
Bernal, O. O., D. E. MacLaughlin, H. G. Lukefahr, and B. Andraka, 1995, Phys. Rev. Lett. **75**, 2023.
Bhatt, R. N., and D. S. Fisher, 1992, Phys. Rev. Lett. **68**, 3072.
Bogenberger, B., and H. von Löhneysen, 1995, Phys. Rev. Lett. **74**, 1016.
Booth, C. H., D. E. MacLaughlin, R. H. Heffner, R. Chau, M. B. Maple, and G. H. Kwei, 1998, Phys. Rev. Lett. **81**, 3960.
Bouquet, F., Y. Wang, H. Wilhelm, D. Jaccard, and A. Junod, 2000, Solid State Commun. **113**, 367.
Boyanovsky, D., and J. L. Cardy, 1983, Phys. Rev. B **27**, 5557.
Brezin, E., 1982, J. Phys. (France) **43**, 15.
Bucher, E., J. P. Maita, G. W. Hull, R. C. Fulton, and A. S. Cooper, 1975, Phys. Rev. B **11**, 440.
Castro Neto, A. H., G. Castilla, and B. A. Jones, 1998, Phys. Rev. Lett. **81**, 3531.
Chau, R., E. J. Freeman, and M. B. Maple, 2001, preprint, University of California, Department of Physics.
Chau, R., and M. B. Maple, 1996, J. Phys.: Condens. Matter **8**, 9939.
Chau, R., M. B. Maple, and R. A. Robinson, 1998, Phys. Rev. B **58**, 139.
Coleman, P., 1999, Physica B **259-261**, 353.
Coleman, P., A. Tsvelik, N. Andrei, and H. Y. Kee, 1998, J. Phys.: Condens. Matter **10**, L239.
Continentino, M. A., 1993, Phys. Rev. B **47**, 11 587.
Continentino, M. A., 1994, Phys. Rep. **239**, 179.
Continentino, M. A., 1996, Z. Phys. B: Condens. Matter **101**, 197.
Continentino, M. A., G. M. Japiassu, and A. Troper, 1989, Phys. Rev. B **39**, 9734.
Cox, D. L., 1987, Phys. Rev. Lett. **59**, 1240.
Cox, D. L., 1993, Physica B **186-188**, 312.
Cox, D. L., and M. Jarrell, 1996, J. Phys.: Condens. Matter **8**, 9825.
Cox, D. L., and A. Zawadowski, 1998, Adv. Phys. **47**, 599.
Custers, J., and P. Gegenwart, 2001, unpublished.
Dai, P., H. A. Mook, C. L. Seaman, M. B. Maple, and J. P. Koster, 1995, Phys. Rev. Lett. **75**, 1202.
Dalichaouch, Y., and M. B. Maple, 1994, Physica B **199-200**, 176.

deAndrade, M. C., R. Chau, R. P. Dickey, N. R. Dilley, E. J. Freeman, D. A. Gajewski, M. B. Maple, R. Movshovich, A. H. Castro Neto, G. Castilla, and B. A. Jones, 1998, Phys. Rev. Lett. **81**, 5620.

Degiorgi, L., 1999, Rev. Mod. Phys. **71**, 687.

deVisser, A., 1986, Ph.D. thesis (University of Amsterdam).

deVisser, A., M. J. Graf, P. Estrela, A. Amato, C. Baines, C. Andreica, F. N. Gygax, and A. Schenk, 2000, Phys. Rev. Lett. **85**, 3005.

Dobrosavljevic, V., T. R. Kirkpatrick, and G. Kotliar, 1992, Phys. Rev. Lett. **69**, 1113.

Eom, D. H., M. Ishikawa, and N. Takeda, 2000, Physica B **281-282**, 369.

Estrela, P., A. deVisser, F. R. deBoer, G. J. Nieuwenhuys, L. C. J. Pereira, and M. Almeida, 1999, Physica B **259-261**, 409.

Estrela, P., L. C. Pereira, A. deVisser, F. R. deBoer, M. Almeida, M. Godinho, J. Rebizant, and J. C. Spirlet, 1998, J. Phys.: Condens. Matter **10**, 9465.

Fisher, M. P. A., P. B. Weichmann, G. Grinstein, and D. S. Fisher, 1989, Phys. Rev. B **40**, 546.

Flouquet, J., S. Kambe, L. P. Regnault, P. Haen, J. P. Brison, F. Lapierre, and P. Lejay, 1995, Physica B **215**, 77.

Freeman, E. J., M. C. de Andrade, R. P. Dickey, N. R. Dilley, and M. B. Maple, 1998, Phys. Rev. B **58**, 16 027.

Fukushima, T., S. Matsuyama, T. Kumada, K. Kindo, K. Prokes, H. Nakotte, F. R. de Boer, L. Havela, V. Sechovsky, J. M. Winand, J. Rebizant, and J. C. Spirlet, 1995, Physica B **211**, 142.

Gajewski, D. A., N. R. Dilley, R. Chau, and M. B. Maple, 1996, J. Phys.: Condens. Matter **8**, 9793.

Galatanu, A., R. Hauser, G. Gilscher, H. Michor, L. Naber, and E. Bauer, 2000, Physica B **281-282**, 83.

Gangopadhyay, A. K., J. S. Schilling, E. Schuberth, P. Gutsmiedl, F. Gross, and K. Andres, 1988, Phys. Rev. B **38**, 2603.

Gangopadhyay, A. K., J. S. Schilling, H. D. Yang, and R. N. Shelton, 1987, Phys. Rev. B **36**, 4086.

Gegenwart, P., P. Hinze, C. Geibel, M. Lang, and F. Steglich, 2000, Physica B **281-282**, 5.

Gegenwart, P., F. Kromer, M. Lang, G. Sparn, C. Geibel, and F. Steglich, 1999, Phys. Rev. Lett. **82**, 1293.

Geibel, C., 2000, private communication.

Geibel, C., U. Klinger, B. Buschinger, M. Weiden, G. Olesch, F. Thomas, and F. Steglich, 1996, Physica B **223-224**, 370.

Geibel, C., C. Schank, S. Thies, H. Kitazawa, C. D. Bredl, A. Böhm, M. Rau, A. Grauel, R. Caspary, R. Helfrich, U. Ahlheim, G. Weber, and F. Steglich, 1991, Z. Phys. B: Condens. Matter **84**, 1.

Geibel, C., S. Thies, D. Kaczorowski, A. Mehner, A. Grauel, B. Seidel, U. Ahlheim, R. Helfrich, K. Peterson, C. D. Bredl, and F. Steglich, 1991, Z. Phys. B: Condens. Matter **83**, 305.

Germann, A., A. K. Nigam, J. Dutzi, A. Schröder, and H. von Löhneysen, 1988, J. Phys. Colloq. **49**, C8-755.

Germann, A., and H. von Löhneysen, 1989, Europhys. Lett. **9**, 367.

Goldenfeld, N., 1992, *Lectures on Phase Transitions and the Renormalization Group* (Addison-Wesley, New York).

Goodrich, R., 2000, private communication.

Götzfried, T., K. Heuser, S. Kehrein, E.-W. Scheidt, and G. R. Stewart, 2001, unpublished.

Graf, M. J., R. J. Keizer, A. de Visser, and S. T. Hannahs, 2000, Physica B **284-288**, 1281.

Graf, T., J. D. Thompson, M. F. Hundley, R. Movshovich, Z. Fisk, D. Mandrus, R. A. Fisher, and N. E. Phillips, 1997, Phys. Rev. Lett. **78**, 3769.

Griffiths, R. B., 1969, Phys. Rev. Lett. **23**, 17.

Grosche, F. M., P. Agarwal, S. R. Julian, N. J. Wilson, R. K. W. Haselwimmer, S. J. S. Lister, N. D. Mathur, F. V. Carter, S. S. Saxena, and G. G. Lonzarich, 2000, J. Phys.: Condens. Matter **12**, L533.

Grosche, F. M., S. R. Julian, N. D. Mathur, F. V. Carter, and G. G. Lonzarich, 1997, Physica B **237-238**, 197.

Grosche, F. M., S. R. Julian, N. D. Mathur, and G. G. Lonzarich, 1996, Physica B **223-224**, 50.

Grosche, F. M., C. Pfleiderer, G. J. McMullan, G. G. Lonzarich, and N. R. Bernhoeft, 1995, Physica B **206-207**, 20.

Hauser, R., M. Galli, E. Bauer, A. Kottar, G. Hilscher, and D. Kaczorowski, 1998, J. Magn. Magn. Mater. **177-181**, 292.

Havela, L., A. Kolomiets, F. Honda, A. V. Andreev, V. Sechovsky, L. E. DeLong, Y. Shiokawa, T. Kagayama, and G. Oomi, 2000a, Physica B **281-282**, 379.

Havela, L., A. Kolomiets, F. Honda, A. V. Andreev, V. Sechovsky, L. E. DeLong, T. Kagayama, and G. Oomi, 2000b, Physica B **284-288**, 1297.

Havela, L., V. Sechovsky, P. Svoboda, M. Divis, H. Nakotte, K. Prokes, F. R. de Boer, A. Purwanto, R. A. Robinson, A. Seret, J. M. Winand, J. Rebizant, J. C. Spirlet, M. Richter, and H. Eschrig, 1994, J. Appl. Phys. **76**, 6214.

Hegger, H., C. Petrovic, E. G. Moshopoulou, M. F. Hundley, J. L. Sarrao, Z. Fisk, and J. D. Thompson, 2000, Phys. Rev. Lett. **84**, 4986.

Held, K., M. Ulmke, N. Blümer, and D. Vollhardt, 1997, Phys. Rev. B **56**, 14 469.

Hertz, J. A., 1976, Phys. Rev. B **14**, 1165.

Heuser, K., 1999, Ph.D. thesis (Universität Augsburg) (Shaker Verlag, Aachen, ISBN 3-8265-6343-3).

Heuser, K., J. S. Kim, E.-W. Scheidt, T. Schreiner, and G. R. Stewart, 1999, Physica B **259-261**, 392.

Heuser, K., E.-W. Scheidt, T. Schreiner, Z. Fisk, and G. R. Stewart, 2000, J. Low Temp. Phys. **118**, 235.

Heuser, K., E.-W. Scheidt, T. Schreiner, and G. R. Stewart, 1998a, Phys. Rev. B **57**, R4 198.

Heuser, K., E.-W. Scheidt, T. Schreiner, and G. R. Stewart, 1998b, Phys. Rev. B **58**, R15 959.

Hill, H. H., 1970, in *Plutonium 1970 and Other Actinides*, edited by W. N. Miner (American Institute of Mining, Metallurgical, and Petroleum Engineers, New York), p. 2.

Hirsch, O., H. Lumpe, and G. R. Stewart, 2001, unpublished.

Hlubina, R., and T. M. Rice, 1995, Phys. Rev. B **51**, 9253.

Homma, Y., S. Kawai, and Y. Shiokawa, 2000, Physica B **281-282**, 249.

Horn, S., E. Holland-Moritz, M. Loewenhaupt, F. Steglich, H. Scheuer, A. Benoit, and J. Flouquet, 1981, Phys. Rev. B **23**, 3171.

Horn, S., A. Mehner, C. Kämmerer, B. Seidel, C. D. Bredl, C. Geibel, and F. Steglich, 1992, J. Magn. Magn. Mater. **108**, 205.

Ioffe, L. B., and A. J. Millis, 1995, Phys. Rev. B **51**, 16 151.

Ishigaki, A., and T. Moriya, 1998, J. Phys. Soc. Jpn. **67**, 3924.

Jaccard, D., K. Behnia, and J. Sierro, 1992, Phys. Lett. A **163**, 475.

Jaccard, D., H. Wilhelm, K. Alami-Yadri, and E. Vargoz, 1999, Physica B **259-261**, 1.

Jarrell, M., H. B. Pang, and D. L. Cox, 1997, Phys. Rev. Lett. **78**, 1996.

Jarrell, M., H. Pang, D. L. Cox, and K. H. Luk, 1996, Phys. Rev. Lett. **77**, 1612.
Jee, C. S., B. Andraka, J. S. Kim, and G. R. Stewart, 1991, Phys. Rev. B **43**, 2656.
Julian, S. R., F. V. Carter, F. M. Grosche, R. K. W. Haselwimmer, S. J. Lister, N. D. Mathur, G. J. McMullan, C. Pfleiderer, S. S. Saxena, I. R. Walker, N. J. W. Wilson, and G. G. Lonzarich, 1998, J. Magn. Magn. Mater. **177-181**, 265.
Julian, S. R., C. Pfleiderer, F. M. Grosche, N. D. Mathur, G. J. McMullan, A. J. Diver, I. R. Walker, and G. G. Lonzarich, 1996, J. Phys.: Condens. Matter **8**, 9675.
Kadowski, K., and S. B. Woods, 1986, Solid State Commun. **58**, 507.
Kambe, S., S. Raymond, H. Suderow, J. McDonough, B. Fak, L. P. Regnault, R. Calemczuk, and J. Flouquet, 1996, Physica B **223-224**, 135.
Kang, J.-S., J. W. Allen, M. B. Maple, M. S. Torikachvili, W. P. Ellis, B. B. Pate, Z.-X. Shen, J. J. Yeh, and I. Lindau, 1989, Phys. Rev. B **39**, 13 529.
Kappler, J.-P., M. J. Besnus, P. Haen, and J. Sereni, 1997, Physica B **230-232**, 162.
Kato, T. and J. Mathon, 1976, J. Phys. F: Met. Phys. **6**, 221.
Keimer, B., R. J. Birgenau, A. Cassanho, Y. Endoh, R. W. Erwin, M. A. Kastner, and G. Shirane, 1991, Phys. Rev. Lett. **67**, 1930.
Kim, J. S., J. Alwood, S. A. Getty, F. Sharifi, and G. R. Stewart, 2000, Phys. Rev. B **62**, 6986.
Kim, J. S., J. Alwood, and G. R. Stewart, 2001, unpublished.
Kim, J. S., J. Alwood, G. R. Stewart, J. L. Sarrao, and J. D. Thompson, 2001, Phys. Rev. B **64**, 134524.
Kim, J. S., B. Andraka, and G. R. Stewart, 1991, Phys. Rev. B **44**, 6921.
Kim, J. S., B. Andraka, and G. R. Stewart, 1992, Phys. Rev. B **45**, 12 081.
Kim, J. S., D. Hall, K. Heuser, and G. R. Stewart, 2000, Solid State Commun. **114**, 413.
Kim, J. S., N. Sato, and G. R. Stewart, 2001, J. Low Temp. Phys. **124**, 527.
Kim, J. S., and G. R. Stewart, 1999, unpublished.
Kim, J. S., and G. R. Stewart, 2000, unpublished.
Kim, J. S., S. Thomas, D. Hall, and G. R. Stewart, 1999, Phys. Rev. B **60**, 6761.
Kim, W. W., 1995, Ph.D. thesis (University of Florida).
Kim, W. W., J. S. Kim, B. Andraka, and G. R. Stewart, 1993, Phys. Rev. B **47**, 12 403.
Klein, L., L. Antognazza, T. H. Geballe, M. R. Beasley, and A. Kapitulnik, 1999, Physica B **259-261**, 431.
Knopp, G., A. Loidl, R. Caspary, U. Gottwick, C. D. Bredl, H. Spille, F. Steglich, and A. P. Murani, 1988, J. Magn. Magn. Mater. **74**, 341.
Koerner, S., E.-W. Scheidt, T. Schreiner, K. Heuser, and G. R. Stewart, 2000, J. Low Temp. Phys. **119**, 147.
Koerner, S., A. Weber, J. Hemberger, E.-W. Scheidt, and G. R. Stewart, 2001, J. Low Temp. Phys. **121**, 105.
Kolb, R., 1994, Diplom. thesis (Universität Augsburg).
Kondo, J., 1964, Prog. Theor. Phys. **32**, 37.
Krishnamurthy, V. V., K. Nagamine, I. Watanabe, K. Nishiyama, S. Ohira, M. Ishikawa, D. H. Eom, and T. Ishikawa, 2000, Physica B **289-290**, 47.
Lenkewitz, M., S. Corsepius, G.-F. von Blanckenhagen, and G. R. Stewart, 1997, Phys. Rev. B **55**, 6409.
Link, P., D. Jaccard, and P. Lejay, 1996, Physica B **223-224**, 303.
Liu, C.-Y., D. E. MacLaughlin, A. H. Castro Neto, H. G. Lukefahr, J. D. Thompson, J. L. Sarrao, and Z. Fisk, 2000, Phys. Rev. B **61**, 432.
Liu, C.-Y., D. E. MacLaughlin, H. G. Lukefahr, G. Miller, K. Hui, M. B. Maple, M. C. de Andrade, and E. J. Freeman, 2000, Phys. Rev. B **62**, 430.
Lonzarich, G. G., 1997, in *The Electron*, edited by M. Springford (Cambridge University Press, Cambridge/New York), Chap. 6.
Lopez de la Torre, M. A., M. Ellerby, M. Watmough, and K. A. McEwen, 1998, J. Magn. Magn. Mater. **177-181**, 445.
Ludwig, A. W. W., and I. Affleck, 1991, Phys. Rev. Lett. **67**, 3160.
MacLaughlin, D. E., O. O. Bernal, and H. G. Lukefahr, 1996, J. Phys.: Condens. Matter **8**, 9855.
MacLaughlin, D. E., R. H. Heffner, G. J. Nieuwenhuys, G. M. Luke, Y. Fudamoto, Y. J. Uemura, R. Chau, M. B. Maple, and B. Andraka, 1998, Phys. Rev. B **58**, 11 849.
Maeda, K., H. Sugawara, T. D. Matsuda, T. Namiki, Y. Aoki, H. Sato, and K. Hisatake, 1999, Physica B **259-261**, 401.
Maple, M. B., M. C. deAndrade, J. Herrmann, Y. Dalichaouch, D. A. Gajewski, C. L. Seaman, R. Chau, R. Movshovich, M. C. Aronson, and R. Osborn, 1995, J. Low Temp. Phys. **99**, 223.
Maple, M. B., R. P. Dickey, J. Herrmann, M. C. deAndrade, E. J. Freeman, D. A. Gajewski, and R. Chau, 1996, J. Phys.: Condens. Matter **8**, 9773.
Maple, M. B., C. L. Seaman, D. A. Gajewski, Y. Dalichaouch, V. B. Barbetta, M. C. deAndrade, H. A. Mook, H. G. Lukefahr, O. O. Bernal, and D. E. MacLaughlin, 1994, J. Low Temp. Phys. **95**, 225.
Mathur, N. D., F. M. Grosche, S. R. Julian, I. R. Walker, D. M. Freye, R. K. W. Haselwimmer, and G. G. Lonzarich, 1998, Nature (London) **394**, 39.
Mayr, F., 1997, Diplom. thesis (Universität Augsburg).
Mayr, F., G.-F. von Blanckenhagen, and G. R. Stewart, 1997, Phys. Rev. B **55**, 947.
Millis, A. J., 1993, Phys. Rev. B **48**, 7183.
Miranda, E., V. Dobrosavljevic, and G. Kotliar, 1996, J. Phys.: Condens. Matter **8**, 9871.
Miranda, E., V. Dobrosavljevic, and G. Kotliar, 1997a, Phys. Rev. Lett. **78**, 290.
Miranda, E., V. Dobrosavljevic, and G. Kotliar, 1997b, Physica B **230-232**, 569.
Moriya, T., and T. Takimoto, 1995, J. Phys. Soc. Jpn. **64**, 960.
Moriya, T., and T. Takimoto, 1998, private communication.
Motrunich, O., S. C. Mau, D. A. Huse, and D. S. Fischer, 2000, Phys. Rev. B **61**, 1160.
Movshovich, R., T. Graf, D. Mandrus, J. D. Thompson, J. L. Smith, and Z. Fisk, 1996, Phys. Rev. B **53**, 8241.
Murani, A. P., A. Tari, and B. R. Coles, 1974, J. Phys. F: Met. Phys. **4**, 1769.
Mydosh, J. A., and P. J. Ford, 1973, in *Amorphous Magnetism*, edited by H. O. Hooper and A. M. de Graaf (Plenum, New York), p. 237.
Nakano, T., Y. Ohmori, S. Murayama, K. Hoshi, and Y. Onuki, 2000, Physica B **281-282**, 346.
Nakotte, H., 1994, Ph.D. thesis (University of Amsterdam).
Nakotte, H., K. H. J. Buschow, E. Brück, J. C. P. Klaasse, K. Prokes, F. R. de Boer, A. V. Andreev, and A. Lacerda, 1997, Physica B **230-232**, 616.
Nakotte, H., K. Prokes, E. Brück, K. H. J. Buschow, F. R. de Boer, A. V. Andreev, M. C. Aronson, A. Lacerda, M. S.

Torikachvili, R. A. Robinson, M. A. M. Bourke, and A. J. Schultz, 1996, Phys. Rev. B **54**, 12 176.
Neubert, A., T. Pietrus, O. Stockert, H. von Löhneysen, A. Rosch, and P. Wölfle, 1997, Physica B **230-232**, 587.
Nicklas, M., 2000, Ph.D. thesis (Universität Augsburg).
Nicklas, M., M. Brando, G. Knebel, F. Mayr, W. Trinkl, and A. Loidl, 1999, Phys. Rev. Lett. **82**, 4268.
Nishigori, S., K. Fujiwara, and T. Ito, 1999, Physica B **259-261**, 397.
Nishioka, T., K. Mizutani, S. Taniguchi, and M. Kontani, 1998, J. Magn. Magn. Mater. **177-181**, 451.
Nozières, P., and A. Blandin, 1980, J. Phys. (France) **41**, 193.
Oomi, G., T. Kagayama, and Y. Onuki, 1998, J. Alloys Compd. **271-273**, 482.
Orlando, T., E. J. McNiff, S. Foner, and M. R. Beasley, 1979, Phys. Rev. B **19**, 4545.
Ott, H. R., E. Felder, and A. Bernasroni, 1993, Physica B **186-188**, 207.
Ott, H. R., H. Rudigier, Z. Fisk, and J. L. Smith, 1983, Phys. Rev. Lett. **50**, 1595.
Ott, H. R., H. Rudigier, Z. Fisk, and J. L. Smith, 1985, Phys. Rev. B **31**, 1651.
Perry, R. S., L. M. Galvin, S. A. Grigera, L. Capogna, A. J. Schofield, A. P. MacKenzie, M. Chiao, S. R. Julian, S. I. Ikeda, S. Nakatsuji, Y. Maeno, and C. Pfleiderer, 2001, Phys. Rev. Lett. **86**, 2661.
Petrovic, C., R. Movshovich, M. Jaime, P. G. Pagliuso, M. F. Hundley, J. L. Sarrao, Z. Fisk, and J. D. Thompson, 2001, Europhys. Lett. **53**, 354.
Petrovic, C., P. G. Pagliuso, M. F. Hundley, R. Movshovich, J. L. Sarrao, J. D. Thompson, and Z. Fisk, 2001, J. Phys.: Condens. Matter **13**, L337.
Pfleiderer, C., G. J. McMullan, S. R. Julian, and G. G. Lonzarich, 1997, Phys. Rev. B **55**, 8330.
Pfleiderer, C., G. J. McMullan, and G. G. Lonzarich, 1994, Physica B **199-200**, 634.
Pietri, R., B. Andraka, R. Troc, and V. H. Tran, 1997, Phys. Rev. B **56**, 14 505.
Pines, D., 2000, Physica C **341-348**, 59.
Pinto, R. P., M. M. Amado, M. A. Salgueiro, M. E. Braga, J. B. Sousa, B. Chevalier, F. Mirambet, and J. Etourneau, 1995, J. Magn. Magn. Mater. **140-144**, 1371.
Privman, V., and M. E. Fisher, 1983, J. Stat. Phys. **33**, 385.
Prokes, K., I. H. Hagmusa, P. Estrela, J. C. P. Klaasse, A. V. Andreev, V. Sechovsky, E. Brück, and F. R. de Boer, 2000, Physica B **281-282**, 377.
Ramirez, A. P., P. Chandra, P. Coleman, Z. Fisk, J. L. Smith, and H. R. Ott, 1994, Phys. Rev. Lett. **73**, 3018.
Raymond, S., and D. Jaccard, 2000, Phys. Rev. B **61**, 8679.
Rivier, N., and K. Adkins, 1975, J. Phys. F: Met. Phys. **5**, 1745.
Rosch, A., 1999, Phys. Rev. Lett. **82**, 4280.
Rosch, A., 2000, private communication.
Rosch, A., A. Schröder, O. Stockert, and H. von Löhneysen, 1997, Phys. Rev. Lett. **79**, 159.
Sachdev, S., 1999, *Quantum Phase Transitions* (Cambridge University Press, Cambridge, England).
Sachdev, S., and N. Read, 1996, J. Phys.: Condens. Matter **8**, 9723.
Sachdev, S., and J. Ye, 1992, Phys. Rev. Lett. **69**, 2411.
Santi, G., and T. Jarlborg, 1997, J. Phys.: Condens. Matter **9**, 9563.
Sarrao, J. L., H. Hegger, M. Jaime, P. G. Pagliuso, C. Petrovic, Z. Fisk, M. F. Hundley, R. Movshovich, and J. D. Thompson, 2000, unpublished.
Sato, H., J. Urakawa, Y. Aoki, T. Namiki, H. Sugawara, Y. Onuki, H. Amitsuka, and T. Sakakibara, 1999, Physica B **259-261**, 390.
Saxena, S. S., P. Agarwal, K. Ahilan, F. M. Grosche, R. K. W. Haselwimmer, M. J. Steiner, E. Pugh, I. R. Walker, S. R. Julian, P. Monthoux, G. G. Lonzarich, A. Huxley, I. Sheikin, D. Braithwaite, and J. Flouquet, 2000, Nature (London) **406**, 587.
Scheidt, E.-W., 2000, private communication.
Scheidt, E.-W., J. S. Kim, and G. R. Stewart, 2001, unpublished.
Scheidt, E.-W., T. Schreiner, K. Heuser, S. Koerner, and G. R. Stewart, 1998, Phys. Rev. B **58**, R10 104.
Scheidt, E.-W., T. Schreiner, K. Heuser, and G. R. Stewart, 1999, Physica B **259-261**, 388.
Schlabitz, W., J. Baumann, B. Pollit, U. Rauchschwalbe, H. M. Mayer, U. Ahlheim, and C. D. Bredl, 1986, Z. Phys. B: Condens. Matter **62**, 171.
Schlottmann, P., and P. D. Sacramento, 1993, Adv. Phys. **42**, 641.
Schroeder, A., G. Aeppli, E. Bucher, R. Ramazashvili, and P. Coleman, 1998, Phys. Rev. Lett. **80**, 5623.
Seaman, C. L., M. B. Maple, B. W. Lee, S. Ghamaty, M. S. Torikachvili, J.-S. Kang, L. Z. Liu, J. W. Allen, and D. L. Cox, 1991, Phys. Rev. Lett. **67**, 2882.
Sengupta, A. M., and A. Georges, 1995, Phys. Rev. B **52**, 10 295.
Seuring, C., 2000, Ph.D. thesis (Universität Augsburg).
Seuring, C., K. Heuser, E.-W. Schreiner, T. Schreiner, E. Bauer, and G. R. Stewart, 2000, Physica B **281-282**, 374.
Seuring, C., E.-W. Scheidt, E. Bauer, and G. R. Stewart, 2001, J. Low Temp. Phys. **123**, 25.
Shamir, N., M. Melamud, H. Shaked, and M. Weger, 1978, Physica B **94**, 225.
Shapiro, S. M., A. I. Goldman, G. Shirane, D. E. Cox, Z. Fisk, and S. L. Smith, 1985, J. Magn. Magn. Mater. **52**, 418.
Shlyk, L., P. Estrela, J. C. Waerenborgh, L. E. DeLong, A. deVisser, D. P. Rojas, F. Gandra, and M. Almeida, 2000, Physica B **292**, 89.
Shlyk, L., J. C. Waerenborgh, P. Estrela, A. deVisser, L. E. DeLong, A. M. Gurevich, and M. Almeida, 1999, Physica B **259-261**, 423.
Si, Q., S. Rabello, K. Ingersent, and J. L. Smith, 2000, Nature (in press).
Si, Q., J. L. Smith, and K. Ingersent, 1999, Int. J. Mod. Phys. B **13**, 2331.
Sieck, M., F. Huster, and H. von Löhneysen, 1997, Physica B **230-232**, 583.
Sieck, M., C. Speck, M. Waffenschmidt, S. Mock, and H. von Löhneysen, 1996, Physica B **223-224**, 325.
Smith, J. L., and Q. Si, 2000, Phys. Rev. B **61**, 5184.
Sondhi, S. L., S. M. Girvin, J. P. Carini, and D. Shahar, 1997, Rev. Mod. Phys. **69**, 315.
Sparn, G., L. Donnevert, P. Hellman, R. Horn, F. Laube, A. Link, S. Thomas, P. Gegenwart, B. Buschinger, C. Geibel, and F. Steglich, 1998, Rev. High Pressure Sci. Technol. **7**, 431.
Steglich, F., J. Aarts, C. D. Bredl, W. Lieke, D. Meschede, W. Franz, and J. Schäfer, 1979, Phys. Rev. Lett. **43**, 1892.
Steglich, F., B. Buschinger, P. Gegenwart, M. Lohmann, R. Helfrich, C. Langhammer, P. Hellmann, L. Donnevert, S.

Thomas, A. Link, C. Geibel, M. Lang, G. Sparn, and W. Assmus, 1996, J. Phys.: Condens. Matter **8**, 9909.
Steglich, F., P. Gegenwart, C. Geibel, P. Hinze, M. Lang, C. Langhammer, G. Sparn, T. Tayama, O. Trovarelli, N. Sato, T. Dahm, and G. Varelogiannis, 2001, in *More is Different: Fifty Years of Condensed Matter Physics*, edited by N. P. Ong and R. N. Bhatt (Princeton University Press, Princeton), p. 191.
Steglich, F., P. Gegenwart, C. Geibel, P. Hinze, M. Lang, C. Langhammer, G. Sparn, and O. Trovarelli, 2000, Physica B **280**, 349.
Steglich, F., P. Gegenwart, R. Helfrich, C. Langhammer, P. Hellman, L. Donnevert, C. Geibel, M. Lang, G. Sparn, W. Assmus, G. R. Stewart, and A. Ochiai, 1997, Z. Phys. B: Condens. Matter **103**, 235.
Steglich, F., C. Geibel, K. Gloos, G. Olesch, C. Schank, C. Wassilew, A. Loidl, A. Krimmel, and G. R. Stewart, 1994, J. Low Temp. Phys. **95**, 3.
Sternlieb, B. J., G. Shirane, J. M. Tranquada, M. Sato, and S. Shamoto, 1993, Phys. Rev. B **47**, 5320.
Stewart, G. R., 1984, Rev. Mod. Phys. **56**, 755.
Stewart, G. R., Z. Fisk, J. L. Smith, H. R. Ott, and F. M. Mueller, 1984, in *Proceedings of the 17th International Conference on Low Temperature Physics*, edited by U. Eckern, A. Schmid, W. Weber, and H. Wühl (North-Holland, Amsterdam), p. 321.
Stewart, G. R., Z. Fisk, and J. Willis, 1983, Phys. Rev. B **28**, 172.
Stewart, G. R., A. L. Giorgi, J. O. Willis, and J. O'Rourke, 1986, Phys. Rev. B **34**, 4629.
Stockert, O., A. Neubert, and H. von Löhneysen, 1997, Physica B **230-232**, 250.
Stockert, O., H. von Löhneysen, A. Rosch, N. Pyka, and M. Loewenhaupt, 1998, Phys. Rev. Lett. **80**, 5627.
Strydom, A. M., and P. d. V. Du Plessis, 1996, Physica B **223-224**, 222.
Süllow, S., T. J. Gortenmulder, G. J. Niewenhuys, A. A. Menovsky, and J. A. Mydosh, 1994, J. Alloys Compd. **215**, 223.
Takeda, N., and M. Ishikawa, 1999, Physica B **259-261**, 92.
Taniguchi, T., Y. Tabata, H. Tanabe, and Y. Miyako, 1998, J. Magn. Magn. Mater. **177-181**, 419.
Thessieu, C., C. Pfleiderer, and J. Flouquet, 1997, Physica B **239**, 67.
Thompson, J., R. D. Parks, and H. Borges, 1986, J. Magn. Magn. Mater. **54-57**, 377.
Thompson, J. D., R. Movshovich, Z. Fisk, F. Bouquet, N. J. Curro, R. A. Fisher, P. C. Hammel, H. Hegger, M. F. Hundley, M. Jaime, P. G. Pagliuso, C. Petrovic, N. E. Phillips, and J. L. Sarrao, 2001, J. Magn. Magn. Mater. **226-230,** 5.
Trainor, R. J., M. B. Brodsky, and H. V. Culbert, 1975, Phys. Rev. Lett. **34**, 1019.
Trinkl, W., 1996, Diplom. thesis (Universität Augsburg).
Trinkl, W., S. Corsepius, E. Guha, and G. R. Stewart, 1996, Europhys. Lett. **35**, 207.
Trinkl, W., U. Weilnhammer, S. Corsepius, T. Schreiner, E.-W. Scheidt, and G. R. Stewart, 1996, Phys. Rev. B **54**, 1163.
Trovarelli, O., C. Geibel, C. Langhammer, S. Mederle, P. Gegenwart, F. M. Grosche, M. Lang, G. Sparn, and F. Steglich, 2000, Physica B **281-282**, 372.
Trovarelli, O., C. Geibel, S. Mederle, C. Langhammer, F. M. Grosche, P. Gegenwart, M. Lang, G. Sparn, and F. Steglich, 2000, Phys. Rev. Lett. **85**, 626.
Tsvelik, A., 2000, private communication.
Tsvelik, A., and M. Reizer, 1993, Phys. Rev. B **48**, 9887.
Tsvelik, A., and P. B. Wiegmann, 1984, Z. Phys. B: Condens. Matter **54**, 201.
Umeo, K., H. Kadomatsu, and T. Takabatake, 1996a, Phys. Rev. B **54**, 1194.
Umeo, K., H. Kadomatsu, and T. Takabatake, 1996b, J. Phys.: Condens. Matter **8**, 9743.
Umeo, K., T. Pietrus, H. von Löhneysen, and T. Takabatake, 1999, Physica B **259-261**, 407.
Umeo, K., T. Takabatake, H. Ohmoto, T. Pietrus, H. von Löhneysen, K. Koyama, S. Hane, and T. Goto, 1998, Phys. Rev. B **58**, 12 095.
Vollmer, R., S. Mock, T. Pietrus, H. von Löhneysen, R. Chau, and M. B. Maple, 1997, Physica B **230-232**, 603.
von Blanckenhagen, G.-F., E.-W. Scheidt, T. Schreiner, and G. R. Stewart, 2001, Phys. Rev. B **64**, 064413.
von Löhneysen, H., 1996, J. Phys.: Condens. Matter **8**, 9689.
von Löhneysen, H., 1999, J. Magn. Magn. Mater. **200**, 532.
von Löhneysen, H., F. Huster, S. Mock, A. Neubert, T. Pietrus, M. Sieck, O. Stockert, and M. Waffenschmidt, 1997, Physica B **230-232**, 550.
von Löhneysen, H., C. Pfleiderer, T. Pietrus, O. Stockert, and B. Will, 2001, Phys. Rev. B **63**, 134411.
von Löhneysen, H., T. Pietrus, G. Portisch, H. G. Schlager, A. Schröder, M. Sieck, and T. Trappmann, 1994, Phys. Rev. Lett. **72**, 3262.
Walker, I. R., F. M. Grosche, D. M. Freye, and G. G. Lonzarich, 1997, Physica C **282-287**, 303.
Weber, A., S. Koerner, E.-W. Scheidt, S. Kehrein, and G. R. Stewart, 2001, Phys. Rev. B **63**, 205116.
Weilnhammer, U., 1997, Diplom. thesis (Universität Augsburg).
Wilhelm, H., and D. Jaccard, 1998, Solid State Commun. **106**, 239.
Wilhelm, H., and D. Jaccard, 1999, Physica B **259-261**, 79.
Willis, J. O., 1988, J. Appl. Phys. **64**, 5613.
Wu, W. D., A. Keren, L. P. Le, G. M. Luke, B. J. Sternlieb, Y. J. Uemura, C. L. Seaman, Y. Dalichaouch, and M. B. Maple, 1994, Phys. Rev. Lett. **72**, 3722.
Zülicke, U., and A. J. Millis, 1995, Phys. Rev. B **51**, 8996.